NEWCASTLE UNIVERSITY

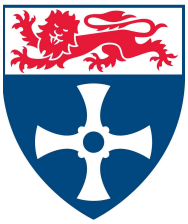

SCHOOL OF ENGINEERING

ELECTRICAL AND ELECTRONIC ENGINEERING

Optimal scheduling of Distributed Energy Resources connected to Electricity Distribution Networks using Robust Mixed-Integer Second-Order Cone Programming

by

Natalia Maria ZOGRAFOU BARREDO

A thesis submitted for the degree of Doctor of Philosophy

July 2021

Abstract

Tackling climate change is a global emergency, driving the electricity sector to go through rapid changes, including the increasing reliance on local generating assets, called distributed energy resources (DER). DER range from onsite energy storage systems, to gas or diesel generators, and renewable generators, but could also include other forms of generation such as electric vehicles with vehicle-to-grid capabilities. This PhD proposes a model to optimally schedule DER connected to radial distribution networks, which can form an active distribution network or a microgrid, aiming at delivering improvements in operational cost, security of supply and environmental sustainability. This is mathematically formulated using robust mixed-integer second-order cone programming. The proposed model takes into account an accurate power flow model for radial networks and a robust approach to deal with uncertainty in the market price, the electricity demand, the renewable generation, and the time and duration of a scheduled interruption from the main grid when DER form part of a microgrid. Computational experiments support the suitability of the proposed model, in a number of case studies informed by real-world data and operational scenarios. This research concludes the following. Firstly, that it is important to account for detailed modelling of network losses in operational decisions of such systems, as they profoundly affect both the cost and the network's operating state and conditions. Secondly, that the robust approach used in this thesis in order to deal with uncertainty allows distribution system and/or microgrid operators to manage trade-offs between the level of the aforementioned uncertainties they are willing to tolerate, and the operational cost of network assets. Benefits of using the proposed model include, reduction of the operational cost, and mitigation of technical constraint violations in actual conditions. The proposed model can be used by a range of stakeholders including, microgrid operators, distribution system operators, and DER owners.

Declaration

I hereby declare that this thesis is a record of work undertaken by myself, that it has not been the subject of any previous application for a degree, and that all sources of information have been duly acknowledged.

Parts of this thesis have been published by the author in IEEE Transactions on Smart Grid and have been cited as follows.

[1] **N. -M. Zografou-Barredo**, C. Patsios, I. Sarantakos, P. Davison, S. L. Walker and P. C. Taylor, "MicroGrid Resilience-Oriented Scheduling: A Robust MISOCP Model," in IEEE Transactions on Smart Grid, vol. 12, no. 3, pp. 1867-1879, May 2021, doi: 10.1109/TSG.2020.3039713.

Acknowledgements

Being able to do my PhD research has been a true privilege and a beautiful journey that provided me with experiences and lessons that I will always carry with me in my life and career.

First, I would like to thank my supervisors, Dr Haris Patsios, Professor Sara Walker, and Dr Peter Davison, for their guidance and advice during my PhD, for their constructive feedback, and for helping me to evolve as a researcher. I would also like to express my sincere gratitude to Newcastle University and the Engineering and Physical Sciences Research Council (EPSRC) for funding my PhD research.

I profoundly thank my colleagues that stood by my side throughout this journey. Professor Philip C. Taylor, for his constructive feedback, advice and for challenging me, Dr Ilias Sarantakos, for his support, feedback and above all for his encouragement, Dr Meltem Peker Sarhan, for her feedback around mathematical optimisation, and Dr Zoya Pourmirza, for her positivity and support. I would also like to thank my colleagues from the power systems group for the happy and peaceful atmosphere in my office space during my PhD research.

Furthermore, I am deeply thankful to my friends for their love and support during my PhD, and my whole family for their positive attitude in everything I have pursued in my life and for their love.

Finally, I would like to thank my parents and my sister for their unconditional love and endless support. I wouldn't have been here without you, and therefore devote this thesis to you.

To my parents and my sister,
for their unconditional love and endless support.

Nomenclature

Abbreviations

AC	Alternating Current
BoU	Budget of Uncertainty
DC	Direct Current
DER	Distributed Energy Resources
DFES	Distribution Future Energy Scenarios
DG	Dispatchable Generator
DNO	Distribution Network Operator
DRO	Distributionally Robust Optimisation
DSO	Distribution System Operator
ESS	Energy Storage System
EV	Electric Vehicle
HILP	High-Impact Low-Probability
IGDT	Information Gap Decision Theory
MG	MicroGrid
MISOCP	Mixed-Integer Second-Order Cone Programming
MPC	Model Predictive Control
OPF	Optimal Power Flow

PLS	Probability of Load Shedding
PoU	Probability of Underperforming
pu	Per unit
PV	Photovoltaic
PWL – PF	Piecewise Linear Power Flow
R – MISOCP	Robust Mixed-Integer Second-Order Cone Programming
RO	Robust Optimisation
SO	Stochastic Optimisation
SOC – PF	Second-Order Cone Power Flow
UK	United Kingdom

Binary Decision Variables

ω_i	Binary decision variables used for the mathematical formulation of the robust approach presented in Chapter 3.
isl_t^L, isl_t^R	Binary variables which show whether the network is connected or disconnected from the main grid. These variables are used for the islanding event uncertainty. (Chapter 4)
SD_{it}	Binary variables which show whether the dispatchable generator of bus i is shut-down or not at time t. (Chapter 4)
SU_{it}	Binary variables which show whether the dispatchable generator of bus i is starting-up or not at time t. (Chapter 4)
u_{it}	On/off state of the dispatchable generator of bus i at time t. (Chapter 4)

u_{it}^{ESS} Binary variables which show the discharging state of the ESS at bus i at time t (Chapter 4). If u_{it}^{ESS} = 1 the ESS at bus i discharges at time t. If u_{it}^{ESS} = 0 the ESS at bus i does not discharge at time t.

u_{it}^{EV} Binary variables which show the charging or discharging state of the EV parking lot at bus i at time t (Chapter 4). If u_{it}^{ESS} = 1 the EV parking lot located at bus i discharges at time t. If $(1-u_{it}^{ESS})$ = 1 the EV parking lot located at bus i charges at time t.

v_{it}^{ESS} Binary variables which show the charging state of the ESS at bus i at time t (Chapter 4). If u_{it}^{ESS} = 1 the ESS at bus i charges at time t. If u_{it}^{ESS} = 0 the ESS at bus i does not charge at time t.

Continuous Decision Variables

$\omega_{ij,t}^{PWL}$ Tangent line for the piecewise linearisation of $\cos(\theta_{it} - \theta_{jt})$ (Appendix B)

ρ Auxiliary decision variable, which represents the value of the objective function of the R-MISOCP model. The objective function of the R-MISOCP model calculates the operational cost. (Chapter 4)

θ_{it} Voltage angle of bus i at time t. (Appendix B)

D_{it}^{P} Real demand of bus i at time t. (Chapter 4)

D_{it}^{Q} Reactive demand of bus i at time t. (Chapter 4)

$D_{it}^{P,shed}$ Real demand not supplied. (Chapter 4)

G_{it}^{P} Real generation of bus i at time t. (Chapter 4)

G_{it}^{Q} Reactive generation of bus i at time t. (Chapter 4)

I_{ijt}^{sq} Squared current magnitude at branch i-j at time t. (Chapters 3 and 4)

$P_{it}^{Ch,ESS}$	Charging power of ESS at time t at bus i. (Chapter 4)
$P_{it}^{Ch,EV}$	Charging power of EV parking lot at time t at bus i. (Chapter 4)
$P_{it}^{Dch,ESS}$	Discharging power of ESS at time t at bus i. (Chapter 4)
$P_{it}^{Dch,EV}$	Discharging power of EV parking lot at time t at bus i. (Chapter 4)
P_{it}^{DG}	Real power generation of the dispatchable generator located at bus i at time t. (Chapter 4)
P_{it}^{EV}	Power of EV parking lot at time t at bus i. (Chapter 4)
P_{it}^{Grid}	Real power imported from the main grid. (Chapter 4)
P_{it}^{Ren}	Real power produced by the renewable generator at time t at bus i. (Chapter 4)
p_{it}^{D}	Auxiliary variables of the robust formulation for the real demand. (Chapter 4)
p_{it}^{M}	Auxiliary variables of the robust formulation for the market price. (Chapter 4)
p_{it}^{Ren}	Auxiliary variables of the robust formulation for the renewable generation. (Chapter 4)
PF_{ijt}^{P}	Real power flow from bus i to bus j at time t. (Chapter 4)
PF_{ijt}^{Q}	Reactive power flow from bus i to bus j at time t. (Chapter 4)
Q_{it}^{DG}	Reactive power generation of dispatchable generator located at bus i at time t. (Chapter 4)
Q_{it}^{Grid}	Reactive power imported from the main grid. (Chapter 4)
$SOC_{i,initial}^{ESS}$	Initial state of change of ESS at bus i. (Chapter 4)
SOC_{it}^{ESS}	State of change of ESS at bus i at time t. (Chapter 4)
SOC_{it}^{EV}	State of change of EV parking lot at bus i at time t. (Chapter 4)

v_{it}^{sq}	Squared voltage magnitude at bus i at time t. (Chapter 4)
x_i, φ_i	Decision variables for the robust formulation.
y_{it}^{D}	Auxiliary variables of the robust formulation for the real demand. (Chapter 4)
y_{it}^{M}	Auxiliary variables of the robust formulation for the market price. (Chapter 4)
y_{it}^{Ren}	Auxiliary variables of the robust formulation for the renewable generation. (Chapter 4)
z^{M}	Auxiliary variable of the robust formulation for the market price. (Chapter 4)
z_i, p_{ij}, y_i	Auxiliary decision variables due to the robust formulation.
z_t^{D}	Auxiliary variables of the robust formulation for the real demand. (Chapter 4)
z_t^{Ren}	Auxiliary variables of the robust formulation for the renewable generation. (Chapter 4)

Integer Decision Variables

$\gamma^{I,Left}, \gamma^{I,Right}$	Auxiliary budgets of uncertainty for the islanding event. • $\gamma^{I,Left}$, represents the number of time periods that the network will operate disconnected from the main grid before the time that the islanding event is expected to start. • $\gamma^{I,Right}$, represents the number of time periods that the network will operate disconnected from the main grid after the time that the islanding event is expected to end.

Indices

i, j, k, n, t	Indexing for parameters and decision variables

Parameters

$\beta_{ij}, \delta_{ij}, \eta_i$	Parameters in the constraints of the robust formulation. (Chapter 3)
Γ^I	Budget of uncertainty for the uncertainty in the time and duration of a scheduled interruption from the main grid (or *islanding event uncertainty*). (Chapter 4)
Γ^M	Budget of uncertainty for the market price uncertainty. (Chapter 4)
Γ_i	Budget of uncertainty for the i^{th} constraint. (Chapter 3)
Γ_t^D	Budget of uncertainty for the demand uncertainty. (Chapter 4)
Γ_t^{Ren}	Budget of uncertainty for the renewable generation (solar PV) uncertainty. (Chapter 4)
λ_{ij}	Uncertain data in the robust approach of Chapter 3.
$\underline{D_i^P}$	Expected real demand at bus i. (Chapters 3 and 4)
$\underline{D_i^Q}$	Expected reactive demand at bus i. (Chapters 3 and 4)
$\varkappa, \vartheta$	Parameters in the second-order cone constraints of the robust formulation. (Chapter 3)
$\widehat{d}$	The maximum deviation of the real demand from its expected value, i.e. the real demand can take values within the interval $[D_{it}^P - \widehat{d}, D_{it}^P + \widehat{d}]$. (Chapter 4)
$\widehat{m_{it}}$	The maximum deviation of the market price from its expected value, i.e. the market price can take values within the interval $[m_{it} - \widehat{m_{it}}, m_{it} + \widehat{m_{it}}]$. (Chapter 4)
$\widehat{p^{Ren}}$	The maximum deviation of the renewable generation (solar PV) from its expected value, i.e. the renewable generation (solar PV) can take values within the interval $[P_{it}^{Ren} - \widehat{p^{Ren}}, P_{it}^{Ren} + \widehat{p^{Ren}}]$. (Chapter 4)

a_i, b_i	Parameters for the cost function of the dispatchable generator at bus i. (Chapter 4)
b_{ij}	Susceptance of line i – j. (Appendix B)
c, d, e	Auxiliary parameters that belong to the objective function of an optimisation problem which shows the mathematical formulation of the employed robust approach. (Chapter 3)
c^{Shed}	Cost for the real load shedding. (Chapter 4)
$C_i^{ESS,Max}$	Maximum capacity of ESS unit at bus i. (Chapter 4)
$C_i^{EV,Max}$	Maximum capacity of EV parking lot at bus i. (Chapter 4)
c_{SD_i}	Shut-down cost of the dispatchable generator at bus i. (Chapter 4)
c_{SU_i}	Start-up cost of the dispatchable generator at bus i. (Chapter 4)
$D\tau$	Fraction of hour that each time period represents. In particular, in this thesis $D\tau$ = 1/6 as there are 144 time periods. (Chapter 4)
d_n	Constants used for the n linear segments of the piecewise linear power flow approximation. (Appendix B)
EV_{it}^{schdl}	Parameter that represents the EV parking lot schedule. If EV_{it}^{schdl} = 1, then there are EVs at the parking lot. If EV_{it}^{schdl} = 0, then there are no EVs at the parking lot. (Chapter 4)
g_{ij}	Conductance of line i – j. (Appendix B)
h_n	Constants used for the n linear segments of the piecewise linear power flow approximation. (Appendix B)
I_t	Parameter that represents the time periods that the network is expected to be disconnected from the main grid. For I_t = 1

	the network is disconnected from the main grid. For $I_t = 0$ the network is connected to the main grid. (Chapter 4)
m	Number of budget of uncertainty combinations that are taken into account by the BoU Algorithm. (Chapter 3)
m_{it}	Market price. This is the cost to import power from the main grid which is connected to bus i at time t. In this thesis, the main grid is connected to bus i = 1. (Chapter 4).
N	Number of Monte Carlo iterations. N = 10 000 in this thesis. (Chapter 3)
PF_{ij}^{P}	The real power flow from bus i to bus j. (Chapters 3 and 4)
PF_{ij}^{Q}	The reactive power flow from bus i to bus j. (Chapters 3 and 4)
PF_{ij}^{loss}	Upper limit of active network losses of branch i-j. (Appendix B)
r_{ij}	Resistance of line i – j. (Chapters 3 and 4)
RD_i	Ramp-down limit for dispatchable generator at bus i. (Chapter 4)
RU_i	Ramp-up limit for dispatchable generator at bus i. (Chapter 4)
$SOC_i^{Sat,EV}$	EV parking lot state of change, associated with the CC to CV charging method for Li-ion batteries according to [2]. (Chapter 4)
$SOC_{arrival}^{EV}$	Arrival EV parking lot state of charge. (Chapter 4)
$SOC_{departure}^{EV}$	Departure EV parking lot state of charge. (Chapter 4)
t_{end}^{isl}	The time period that the network is expected to operate connected to the main grid. (Chapter 4)
t_{Max}^{EV}	The time period that the EVs depart from the EV parking lot. (Chapter 4)

t^{EV}_{Min}	The time period that the EVs arrive at the EV parking lot. (Chapter 4)
t^{isl}_{start}	The time period that the network is expected to disconnect from the main grid. (Chapter 4)
v^{ref}_{it}	Voltage at slack bus.
V^{sq}_{i}	Squared voltage magnitude at bus i at time t. (Chapters 3 and 4)
x_{ij}	Reactance of line i – j. (Chapters 3 and 4)
λ_{ij}	Random value of the expected parameter λ_{ij} that takes values in the interval $[\lambda_{ij} - \hat{\lambda}_{ij}, \lambda_{ij} + \hat{\lambda}_{ij}]$. (Chapter 3)
m_{it}	The expected value of the market price. (Chapter 4)

Sets

$\mathbb{Z}$	The set of all integers.
Ω_G	The set of dispatchable generators.
Ω_N	The set of network nodes.
Ω_{Ren}	The set of renewable generators (which is solar PV in this thesis.)
Ω_T	The set of all time periods within a 24-hour scheduling horizon. In this thesis, there are 144 time periods within a 24-hour scheduling horizon.
E	The set of network branches.
J_i	The set of columns of the i^{th} optimisation problem constraint.

Symbols

$\_$, $\overline{\ }$	Lower, Upper limit symbols.

Contents

List of Figures

List of Tables

Chapter 1. Introduction

Contents

1.1. Chapter summary

This chapter aims to provide a background and motivation behind the research of this PhD thesis. This chapter is structured as follows.

- **Section 1.2** discusses what are considered as DER in this thesis, the benefits of optimising their operation in electricity distribution networks, and the motivation of this research.
- **Section 1.3** presents a brief literature review.
- **Section 1.4** presents the aim and objectives of this PhD research.
- **Section 1.5** lists the main contributions and conclusions of this research.
- **Section 1.6** presents the structure of this thesis.

1.2. Background & Motivation

Climate change is a global emergency, pushing modern societies to bring rapid changes across sectors, including the electricity sector. For example, in the UK[1], the government has set the ambitious goal of net-zero carbon emissions by 2050 [10]. In the electricity sector, the requirement to meet zero CO_2 emissions, the restructuring of the electricity business, and the various technological developments in microgeneration, have set a new paradigm of power systems in modern societies [11, 12, 1]. These technological developments, have brought advances in distributed generation units (microturbines, fuel cells, etc.) and distributed storage devices (energy storage systems, batteries, etc.), forming the broader class of distributed energy resources (DER) [1].

In this thesis, Distributed Energy Resources (DER) are defined following the definition by Ofgem[2] as, electricity generating plants that are connected to the electricity distribution networks [13]. DER include solar panels, combined heat and

[1] *UK* stands for *United Kingdom*

[2] *Ofgem* stands for *Office of Gas and Electricity Markets*. Ofgem is the regulator for Gas and Electricity Markets in the UK. `https://www.ofgem.gov.uk/`

power plants, energy storage systems, gas turbines, microturbines, batteries in electric vehicles, and controllable loads [14, 15, 16, 17, 18].

The penetration of DER is expected to increase over the coming years. According to the report of Ofgem in [13], the National Grid's[3] Future Energy Scenario (2020)[4] estimates that, by 2050 generators connected to electricity distribution networks could hold up to 42% of the total generation capacity. DER can be used to increase the penetration of renewable generation, to improve power system reliability, to provide services in order to avoid expensive planning decisions, and can deliver energy in order to balance the three elements of the so-called *energy trilemma*: energy security, energy equity, and environmental sustainability [13, 19, 20]. However, the proliferation of DER now and in the future, makes it clear that DER generation cannot be treated any more as a negative demand [21], and that in order to achieve whole system benefits with DER, a degree of coordination is required. The connection of DERs at medium or low voltage distribution networks have increased the flexibility of network stakeholders over the past decades, shaping new concepts for their coordination, including the concept of active network management and the concept of microgrids [22].

Active network management aims to coordinate in an economic and sustainable way DER while following the existing distribution network regulations [23]. Distribution networks equipped with automation systems that allow the optimization, operation and control of the network assets are called *smart* or *active distribution networks*, and are operated by *distribution system operators* (DSO) [24, 25]. The outputs of the day-ahead scheduling problem of smart distribution networks can be used as setpoints for the real-time control of distributed energy resources, for the participation in the day-ahead and real-time electricity markets, and for the provision of ancillary services (e.g. frequency regulation [26]) [25].

Microgrids (MG) are medium or low voltage distribution networks with distributed

[3]National Grid is the Electricity System Operator in the UK. `https://www.nationalgrideso.com/`

[4]The UK government has set the goal of net-zero carbon emissions by 2050 [10]. There are various ways to reach this goal. Therefore, a range of scenarios have been developed by the Great Britain Electricity System Operator (GB ESO) and Distribution Network Operators (DNOs). These different scenarios are called, *Future Energy Scenarios (FES)* by the GB ESO (`https://www.nationalgrideso.com/future-energy/future-energy-scenarios`), and *Distribution Future Energy Scenarios (DFES)* by DNOs. For example, the DFES proposed by a DNO operating in the North of England called Northern Powergrid, can be found in `https://odileeds.github.io/northern-powergrid/2020-DFES/`.

generation units, energy storage devices, and flexible loads [17]. A MG can be operated in an autonomous or non-autonomous way, forming two modes of operation: the islanded and the grid-connected mode. MGs apart from environmental and economic benefits, also present a practical solution to enhance power system resilience (which represents the ability of a power system to supply the demand in the face of a high-impact low-probability (HILP) event), by decreasing the probability of load shedding [27]. MG resilience merits are well-acknowledged by the academic community, creating routes for a range of studies, including research on DER coordination for the so-called *resilience-oriented optimal scheduling problem* (e.g. [27, 8, 28, 29, 30, 31]) [32, 33].

The coordination of DER in active distribution networks and microgrids calls for methods that schedule the operation of DER in advance, and that account for two factors. First, technical constraints and parameters regarding the network and the DER, and second, uncertainty, which is created by the difference between the real-time and the forecasted values of some data used by these methods, such as the electricity demand and the renewable generation. Taking into account technical constraints regarding the network and the DER, aims to capture the characteristics of the electricity distribution network, its topology, and the location of the DER across the network. This has economic benefits, as it can reduce the network losses when distributing the power from the point of generation to the point of consumption, but this also provides a secure operation by respecting the constraints of the network. The violation of the network constraints may lead not only to a more expensive operation, but also to electricity customers experiencing power cuts.

Modelling uncertainty when considering optimal coordination of DER is equally important [34, 18]. This thesis, focuses on uncertainty related to the lack of knowledge of the exact value of some data that are used to coordinate the DER, which can occur due to the fact that these values are forecasted. For example, the electricity demand, the market price and the generation produced by renewable energy sources (such as solar PV) [35]. In cases where DER form part of a microgrid and a scheduled interruption from the main grid is expected (e.g. an upstream maintenance or a foreseeable natural disaster like a hurricane [27, 8, 28]), the uncertainty in the time and the duration of this interruption can also be formulated through the *islanding event*

uncertainty (such as in the study [28]). Uncertainty is important to be considered in the coordination of DER, to avoid the risk of renewable DER being curtailed, and therefore use green energy as much as possible in order to supply the demand. Failing to incorporate uncertainty in decision-making problems, can also result in significant changes in the outputs of the problem [36], which when coordinating DER can manifest as an underestimation of the operational cost or violations of technical constraints.

This work presents a model for the optimal scheduling problem of distributed energy resources connected to electricity distribution networks, which addresses the two aforementioned factors. The proposed model can be used for a range of concepts which have been introduced for the coordination of distributed energy resources, such as *active network management* and to schedule DER that form part of a *MicroGrid*. In this PhD thesis, the scheduling time horizon is 24 hours, but the proposed model can also be used for a longer or a shorter scheduling horizon. The outputs of the model presented in this PhD thesis can be used as set points in a control problem (for example, for a hierarchical control scheme [37], and control of active distribution systems [38]). Apart from the direct use of the model outputs, the results of the model proposed in this thesis could inform planning and design decisions of electricity distribution networks with DER (e.g. [39, 40]). Some stakeholders that can benefit from the model and its outputs include, MG operators, system operators, electricity distribution *network* or *system* operators, aggregators, and DER owners.

1.3. Brief literature review

Given the call for methods that perform DER coordination and the modelling challenges that this bears, there is a broad range of methods in the literature that propose methods for the optimal scheduling problem of DER connected to electricity distribution networks. This section aims to provide a basic background on these studies, which can be found in detail in the next chapter of this thesis.

There are relevant studies that do not take into account parameter uncertainty ([41, 42, 43, 44, 45, 46, 47, 48, 49, 50, 51, 52, 53, 54, 55, 56]), which is important to be taken into account, in order to avoid the risk of renewable DER being curtailed

and the violation of technical constraints. There are also publications that take into account parameter uncertainty ([8, 57, 31, 58, 59, 60, 61, 62, 63, 26, 64, 65, 66, 67, 68, 27, 35, 69, 29, 30, 70, 71, 72, 28, 73, 74, 75, 76]), but either use stochastic methods to handle uncertainty (which needs the knowledge of probability distributions that requires well-known historical data, and can have limited application in large problems [77]), or IGDT (which is a conservative method to handle uncertainty [78]), and/or in terms of the power flow model: 1) do not take into account power flow equations (which creates the risk of overloading network lines, i.e. violating voltage or line current limits), 2) take into account an approximate power flow model, 3) incorporate a nonconvex power flow model (which means that only a local optimal solution can be guaranteed). Finally, there are studies that account for uncertainty using robust optimisation and a second-order cone accurate power flow model, that either propose multi-stage problems (which require a decomposition method in order to be solved, such as the column-and-constraint generation method [79], and therefore have an additional computational load) ([80, 81, 82, 83]), or propose a model that uses the probability density function of random variables: [84] (which may not always be available, as explained above for stochastic optimisation problems).

The benefits for DER coordination using methods that accurately account for technical constraints, that handle uncertainty deterministically (compared to methods that require the knowledge of probability density functions of uncertain data), and that can be solved using commercial optimisation solvers, have motivated the proposal of the model presented in this thesis. The next sections present the aim & objectives, and the main contributions of this thesis.

1.4. Aim and objectives

1.4.1. Aim

The aim of this work is to propose a model for the optimal day-ahead scheduling problem of distributed energy resources connected to radial electricity distribution networks.

1.4.2. Research objectives

This PhD research has the following two research objectives.

Objective 1

To use a convex and accurate AC power flow model, and study the impact of this AC power flow model on the optimal decisions made by the R-MISOCP model.

Objective 2

To use a method to tackle uncertainty, and study the impact of this method on the optimal decisions made by the R-MISOCP model.

1.5. Main contributions

The contributions of this work are summarised below.

1. This thesis presents a robust mixed-integer second-order cone programming model (R-MISOCP) for the optimal scheduling problem of DER connected to radial electricity distribution networks. This model captures the benefits of both convexity and robustness and can be solved using commercial optimisation solvers. Convexity is achieved using the second-order cone power flow model (SOC-PF) model proposed in [85]. This formulation is an exact approximation of the branch flow model for radial networks, given that demand is formulated as a variable which does not have an upper limit [85, 86]. Robustness is achieved using the robust approach of [87] to tackle uncertainty, where uncertain data are assumed to lie within a deterministic interval. Data uncertainty is considered in market price, demand, renewable generation (PV generation), and islanding duration. This robust approach allows the DSO and/or MG operator to control the trade-off between tolerance of uncertainty and operational performance, using a parameter Γ called the budget of uncertainty.

2. The performance of the R-MISOCP model has been evaluated through computational experiments in a number of case studies informed by real-world

data and operational scenarios. To evaluate the impact of the employed power flow model, a detailed comparison is provided between the R-MISOCP and a model that uses a piecewise linear power flow model (PWL-PF) which has been used in relevant studies. To evaluate the impact of the employed robust approach, a comparative study is provided between the proposed R-MISOCP model and a fully robust (conservative) model, where operational performance is assessed based on the cost of operation and load shedding.

In terms of the impact of the employed power flow model, computational experiments show that an AC power flow model that fails to accurately account for power flow equations, can result in a significant underestimation of both, the operational costs and the curtailed demand, and violation of technical constraints. Furthermore, the results of this research suggest that an accurate power flow formulation needs to be taken into account within the decision-making process (rather than retrospectively), as there does not seem to exist a “corrective action” that can be applied to the model that doesn’t use an accurate power flow model, in order to extract the optimal DER schedules of the R-MISOCP model (which uses an accurate power flow model). This is found to hold even if the operational costs calculated by the R-MISOCP and COMP model are very close, and for case studies with a low and a high PV penetration. In terms of the impact of the employed robust approach, computational experiments show that, for the modified IEEE-33 bus network used in research, the DSO and/or MG operator can adjust the budgets of uncertainty and achieve a sizable reduction in the day-ahead operational costs, compared to a fully robust (conservative) approach, while having a 0% probability of shedding additional load than expected.

The model proposed in this thesis has been published as follows:

[1] **N. -M. Zografou-Barredo**, C. Patsios, I. Sarantakos, P. Davison, S. L. Walker and P. C. Taylor, "MicroGrid Resilience-Oriented Scheduling: A Robust MISOCP Model," in IEEE Transactions on Smart Grid, vol. 12, no. 3, pp. 1867-1879, May 2021, doi: 10.1109/TSG.2020.3039713.

1.6. Thesis Structure

In a nutshell, chapters 1-3 present the background and methodology for the proposed R-MISOCP model, chapter 4 presents the proposed R-MISOCP model, and the remaining chapters 5-7, present the computational experiments and conclusions of this research. The content of the thesis chapters are described below and shown in figure 1.1.

- **Chapter 1 -** ***Introduction***.
  This chapter introduces this thesis and presents the aim and objectives of this PhD research.

- **Chapter 2 -** ***Literature review***.
  This chapter presents relevant studies to this research.

- **Chapter 3 -** ***Methodology***.
  This chapter presents the two main blocks that compose the proposed R-MISOCP model: the power flow mathematical formulation and the method used to deal with uncertainty.

- **Chapter 4 -** ***The R-MISOCP model***.
  Given that chapter 3 presented the main blocks of the R-MISOCP model, this chapter aims to present the mathematical formulation of the proposed R-MISOCP model.

- **Chapter 5 -** ***The impact of the accuracy of the power flow model***.
  This chapter aims to study the impact of an accurate power flow model on the scheduling decisions made by the proposed R-MISOCP model, through comparative studies with a model that does not use an accurate power flow model.

- **Chapter 6 -** ***The impact of uncertainty***.
  This chapter aims to study the impact of the employed method to deal with uncertainty on the scheduling decisions made by the proposed R-MISOCP model, through comparative studies with a fully robust (conservative) model.

Chapter	Content
Chapters 1 & 2	• Background & research motivation. • Relevant studies.
Chapters 3 & 4	• Methods used for the power flow model and the method to deal with uncertainty in the R-MISOCP model (**chapter 3**). • Mathematical formulation of the R-MISOCP model (**chapter 4**).
Chapters 5 & 6	• Computational experiments to study the impact of the employed power flow model (**chapter 5**). • Computational experiments to study the impact of the employed method to deal with uncertainty (**chapter 6**).
Chapter 7	• Main conclusions. • Proposal of future work.
Appendices	• Appendix A. Data used. • Appendix B. Power flow equations of COMP model. • Appendix C. Numerical results: Relaxation gap.

Figure 1.1: Thesis structure.

□ **Chapter 7 -** ***Conclusions & Future work***.

This chapter aims to present the main conclusions made during this PhD research, and to propose directions for future work.

□ **Appendix A -** ***Data for the modified IEEE-33 bus network***.

This Appendix presents tables which contain data used for the electricity distribution network and the distributed energy resources used in the computational experiments of chapters 5 and 6.

□ **Appendix B -** ***The Power flow formulation used in the COMP model***.

Chapter 5 presents a comparative study between the R-MISOCP model and another model, which is referred to as the *COMP* model. This Appendix presents the power flow model used for the COMP model.

□ **Appendix C -** ***Numerical results: Relaxation gap***.

This Appendix presents the relaxation gaps for constraint (4.14h) of the proposed R-MISOCP model for the computational experiments of section 5.3, chapter 5. This constraint forms part of the power flow equations, which have been used according to the study in [85].

Chapter 2. Literature review

Contents

2.1. Chapter Summary

This chapter aims to present some of the studies that are relevant with the work proposed in this thesis, and is structured as follows.

- **Section 2.2** presents relevant work to the work developed in this thesis.
- **Section 2.3** presents the main conclusions of this chapter.

2.2. Relevant work

Due to the economic and environmental benefits of DER, there is a broad range of research related to the coordination of DER connected to electricity distribution networks [88, 89, 90]. Relevant studies to this thesis are presented below, starting with a set of studies that does not incorporate a method to tackle uncertainty, and then moving on to studies that take into account uncertainty.

Furthermore, a table in figure 2.1 is shown below, in order to summarise the relevant papers of this chapter. The papers are classified according to the power flow model formulation that they use and the method used to tackle uncertainty.

Ref.	Power Flow model			Uncertainty method				
					Robust optimisation			
						Single-stage problem		
	Not used	Second-order cone PF	Other[1]	Not used	Multi-stage problem/ Problem with recourse	Using PDF[5]	PDF[5] not required	Other[2]
[35]	✓						✓	
[41]	✓			✓				
[27, 29, 30]	✓				✓			
[63, 73]	✓							✓
[42 - 45]			✓	✓				
[8, 26, 31, 57, 60-62, 72, 75]			✓					✓
[69, 70]			✓				✓	
[28, 74]			✓		✓			
[58, 59][3]		✓	✓					✓
[71][3]		✓	✓		✓			
[46-56]		✓		✓				
[64 - 67, 76]		✓						✓
[68, 80, 81, 82, 83]		✓			✓			
[84]		✓				✓		
This work (published in [1])		✓					✓	
[94][4]		✓						✓
[95][4]		✓				✓	✓	
[96][4]		✓			✓			

Notes:
1. Other power flow approaches include for example linear, non-convex PF, three-phase PF equations.
2. Other uncertainty approaches include stochastic optimisation, stochastic-robust optimisation, chance-constrained optimisation and others.
3. Papers [58, 59, 71] use a linearised second-order cone PF model.
4. The studies [94-96] propose MISOCP models, but solve real-time control and planning/investment problems, which is out of the scope of this thesis.
5. PDF: Probability density function.

Figure 2.1: Classification of relevant studies according to their power flow model formulation and method to tackle uncertainty.

Some studies that are relevant to the research of this thesis, are listed below, starting with a set of papers which do not incorporate a method to tackle uncertainty.

- The study in [41] models the day-ahead operation of a residential microgrid with a vehicle-to-grid system, and does not take into account a method to tackle uncertainty. As this work focuses on residential-level, it does not account for power flow equations, compared to the R-MISOCP model proposed in this thesis which is intended for network-level studies.

- The study in [42], proposes an optimal energy management problem of active elements of a smart distribution grid where network reconfiguration is taken into account. The proposed model is mathematically formulated as a mixed-integer nonlinear programming problem, and is solved using a genetic algorithm. Furthermore, it does not take into account a method to handle uncertainty; it rather uses reserve resources to compensate for load and renewable generation uncertainty.

- The study in [43] proposes a model for the optimal day-ahead scheduling problem of active distribution networks. A three-phase unbalanced power flow model is used. The resulting model is nonlinear nonconvex, and is solved using a novel Kriging model assisted modified fuzzy adaptive particle swarm optimization algorithm (KMA-MFAPSO) combined with constraints handling technique. Therefore, the model proposed in this work is not convex, and a method to incorporate uncertainty is not used.

- In the study of [44] a model for the optimal day-ahead scheduling problem is proposed. This study takes into account a whole energy systems approach. Three types of energy vectors are considered; electricity, gas and heat, where the interconnection between energy vectors is incorporated using the energy hub modelling method ([91]). Power flow equations are incorporated using three-phase electric network constraints, which resulted in a nonlinear model which is solved based on genetic algorithm and a nonlinear interior point method. This work does not take into account uncertainty in the proposed model.

- The study in [45], proposes a non-linear model for the optimal energy

management problem of unbalanced three-phase microgrids. This work does not take into account a method to tackle uncertainty.

- In [46], a mixed-integer second-order cone programming model for the optimal scheduling of microgrids is proposed. This study does not take into account data uncertainty.
- In [47], a framework to evaluate power system resilience is proposed. This is formulated as a mixed-integer second-order cone programming problem, but a method to consider uncertain data is not taken into account within the proposed model.
- The study in [48], proposes a service restoration method of distribution networks with an increasing PV penetration. This is mathematically formulated as a mixed-integer second-order cone programming problem. Uncertainty is not taken into account in this study.
- The study in [49] also proposes a multi-objective optimisation model for the service restoration problem of distribution networks. This problem is formulated using mixed-integer second-order cone programming. Uncertain data are not considered in this model.
- In [50], a model for the online reconfiguration of active distribution networks is proposed in order to minimise DER curtailment while respecting the technical characteristics of the network. A range of scenarios are examined in order to account for uncertainty in the load and renewable generation (namely in solar and wind generation), however, a method to tackle uncertainty is not taken into account within the proposed model.
- In [51], proposes a load restoration model in order to improve the resilience of the electricity distribution network in the face of extreme events, taking into account the formation of microgrids and network reconfiguration. This is formulated using mixed-integer second-order cone programming. Uncertainty is not taken into account in this study.
- The work in [52] proposes a mixed-integer second-order programming problem to minimise network losses and eliminate voltage violations using reactive power

optimisation and network reconfiguration. To model power flow equations, this study expands the work of [85] (which is also used in this thesis) to also model transformers. This work does not take into account uncertainty.

- The work in [53], proposes a MISOCP model for the optimal dispatch problem of active distribution networks and incorporates dynamic thermal ratings of transformers, which is out of the scope of this thesis. Uncertainty is not taken into account in this study.

- In [54], a multi-objective mixed-integer second-order cone programming problem is proposed for the energy management problem at electricity distribution networks, where the cost of energy not supplied and energy procurement cost are considered the competitive objectives. Uncertainty is not taken into account in this study.

- In [55], a method for the optimal operation scheduling problem of reconfigurable networked MGs is presented, taking into account the conflicting objectives between the distribution system operator and the microgrid operator. This is formulated as a bi-level optimisation problem which is re-formulated into a MISOCP model. Uncertainty is not taken into account in this study.

- The work in [56], proposes a model for the decentralised economic dispatch problem of an active distribution network with multiple microgrids. This is mathematically formulated using mixed-integer second-order cone programming. Data uncertainty is not taken into account in the proposed MISOCP method.

The papers presented above did not consider a method to tackle uncertainty. However, the optimal DER scheduling problem has some data that are inherently uncertain as their real-time values may differ from their forecasted values, such as the demand and the renewable generation. There is a range of methods to handle uncertainty in decision-making problems, including stochastic optimisation, robust optimisation, and others. These methods are inherently different in nature and therefore may serve different applications and problems [78].

The list below, presents a set of papers that incorporate a method to account for uncertain data.

- The study in [8], proposed a two-stage stochastic linear optimization model. In this model, unintentional islanding, load, pool price, and EV schedule were considered as random variables. Although power flow equations were included in the model, the formulation used did not have an accurate representation of network losses, which can result in a more optimistic outcome regarding the cost of operation. Additionally, the knowledge of the probability distributions of random variables is required in stochastic optimization. The latter can be a great advantage for a problem with well-known historical data. However, this is a limitation for modelling islanding uncertainty due to an interruption of power supply from the main grid, as this belongs to high-impact/low-probability events (HILP) for which historical data is rare [92, 28].

- In [57], a model for the optimal operation of photovoltaics connected to a three-phase active distribution network is proposed. The model is mathematically formulated as a multi-objective stochastic optimization problem. The two objectives of the problem are to minimize active power losses and minimize the network maximum voltage unbalance. This is developed for three-phase active and reactive power balance equations.

- The study in [31], presented a model to enhance resilience using islanded operation of MGs focusing on the event of inadequate on-site generation to feed all MG loads. The model was mathematically formulated as a nonlinear programming problem. The proposed model was not formulated as a convex model, which meant that only a local optimal solution was guaranteed. Uncertainty in renewable generation and load forecasts are take into account using their probability distribution.

- The papers in [58, 59] propose mixed-integer linear programming models for the operation of active distribution networks, and use a linearised formulation of the second-order cone power flow equations. The method proposed in [58] uses a stochastic method to tackle uncertainty related to wind speed, solar irradiance and load demand, which requires their probability density function, and the study in [59] also uses stochastic optimisation to tackle uncertainty.

- The studies in [60, 61] also propose a model for optimal operation of active

distribution networks, where stochastic optimisation is used to tackle uncertainty.

- The study in [62] presents a model for the scheduling problem of distribution networks within smart grids, which includes dynamic network reconfiguration. This is modelled using multi-objective optimisation, and the probability of a range of scenarios is used to model uncertain data.

- The study in [63] presents a methodology for the optimal day-ahead and real-time scheduling problem of multi-energy microgrids. This work considers combined cooling, heating and power (CCHP) units and ice-storage air-conditioners, PVs, wind turbines and energy storage systems. Uncertainty in wind and PV is taken into account using the methods of Latin hypercube sampling (LHS) and scenario reduction. A set of equations for the power flow model is not taken into account.

- The study in [26] proposes an optimisation method for active distribution networks, for the provision of ancillary services. The proposed model is formulated as a multi-period chance-constrained optimal power flow problem, therefore requiring probabilistic information to form the chance constraints.

- In [64], a MISOCP model is proposed which uses chance-constrained optimisation to deal with uncertainty, which proposes a direct and fast scenario generation method and uses a seven-step probability distribution to model the outputs of the renewable energy resources.

- The study of [65] presents a method for the optimal day-ahead scheduling problem of future smart distribution networks. The proposed model is mathematically formulated as a mixed-integer second-order cone programming problem. Uncertainty in wind generation and demand is modelled using a two-stage stochastic-robust optimisation approach. Power flow equations are modelled using a relaxed branch flow model. This approach uses a combination of stochastic and robust optimisation to model uncertainty, in order to avoid the conservatism of robust optimisation.

- In [66], a model for the scheduling of an AC/DC hybrid distribution system is proposed, and uses fuzzy chance-constrained programming to account for uncertainty. The problem is formulated as a mixed-integer second-order cone

programming model. This work requires information around the probability distributions of the uncertain data to be formulated.

- The study of [67], proposed a stochastic MISOCP model for the security-constrained energy management system (EMS) of microgrids. Demand and renewable generation uncertainty are taken into account. This work uses stochastic optimisation to handle uncertainty.

- In [68], a model for the both long-term planning and short-term operation of DER in active distribution network is presented. This is mathematically formulated using mixed-integer second-order cone programming, and uncertainty is modelled using data-driven distributionally robust optimisation. This method needs the knowledge of probability distribution of the given uncertain scenarios.

- The study in [27] proposed an operational framework for a MG which operated in islanded mode for an extended period of time due to interruption of supply from the main grid, and was introduced as the *resiliency-oriented MicroGrid optimal scheduling*. The proposed operational framework was mathematically formulated as a robust optimization problem. Power flow equations were not included in the model, and robustness was treated in a conservative fashion; assuming maximum expected demand and minimum expected renewable generation at all times.

- In [35], a model for the day-ahead participation of smart-home aggregators is proposed. This model uses a robust approach to handle uncertainty which uses budgets of uncertainty to control the conservatism of the solution. Since this study proposes a home energy management system, power flow equations are not taken into account.

- The study in [69] presents a method for the optimal energy management problem of microgrids under net-zero emissions, using robust optimisation to tackle uncertainty and budgets of uncertainty to control the degree of conservatism of the solution. The proposed model is nonconvex.

- The studies in [29, 30], presented resilient operation strategies for an AC/DC MG and a multi-energy MG respectively. The proposed models were mathematically

formulated as two-stage robust optimization problems. In these studies, power flow equations were not considered at all in the network model, which creates the risk of overloading network lines, i.e. violating voltage or line current limits.

- In [70], a method for planning of future microgrids in order to mitigate the severe consequences of extreme events is proposed. Robust optimisation is used to tackle uncertainty, and power flow equations were formulated using a linear approximation.
- The paper in [71] proposes a mixed-integer linear programming model for the operation of active distribution networks, and uses a linearised formulation of the second-order cone power flow equations. A two-stage robust approach with uncertainty budgets is used to tackle uncertainty. This method uses the Pearson autocorrelation and cross-correlation to account for the temporal and spatial correlation which requires the knowledge of historical data.
- The study in [72], proposes a mixed-integer linear programming model to enhance the resilience of active distribution networks. The IGDT method is used to handle uncertainty, and a linear DistFlow model is used in order to account for power flow equations.
- The study in [28], presented a two-stage robust optimization model. Load, market price, and the scheduled time of the MG islanding event were considered as uncertain parameters in this model. Power flow equations were approximated.
- In [73], an optimal economic schedule for microgrids is presented using model predictive control. Power flow equations are not considered in this work.
- The study in [74], proposes a method for island partitioning at distribution networks in the face of extreme events. This is mathematically formulated as a mixed-integer second-order cone programming model, where uncertainty is modelled using two-stage robust optimisation model. Power flow equations are formulated using a linearised DistFlow model, and uncertainty is modelled using an ellipsoidal uncertainty set.
- The study in [75], proposes a risk-averse energy management strategy in a network with DER, taking into account network reconfiguration. The information

gap decision theory (IGDT) method is used to tackle uncertainty in renewable generation, which is a non-probabilistic and non-fuzzy uncertainty method [93]. The proposed model is mathematically formulated as a mixed-integer nonlinear programming problem which is nonconvex.

- The work in [76] proposes a methodology for the operation of active distribution networks for the optimal use of the reactive power of DER, which are able to provide spinning reserve to the transmission network. Power flow equations are modelled using the second-order cone power flow model of [85]. IGDT is used to take into account spinning reserve uncertainty. However uncertainty in other data is not studied.

- In [80], a model for the day-ahead scheduling problem of microgrids is proposed. This model is mathematically formulated as a tri-level optimisation, uses robust optimisation to tackle uncertainty in renewable generation (namely wind and solar), demand, and grid electricity price and an accurate second order cone power flow model. The resulting tri-level problem, which cannot be directly solved by commercial solvers, is solved using a solution approach which includes benders decomposition.

- The publication [81] proposes a two-stage robust optimisation problem for reactive power optimisation in active distribution networks, where the wind power uncertainty is taken into account. The column and constraint generation method is used to solve this problem. This work compares the optimal decisions and computational performance between the proposed two-stage model with a deterministic approach.

- The study of [82] proposes a two-stage robust MISOCP model, and focuses on a comparison of the results of the proposed model with its deterministic approach. The robust approach of [82] does not include parameters that can control the trade-offs between tolerance of uncertainty and operational performance. The column and constraint generation method is used to solve this problem.

- The study in [83], proposes a data-driven robust multi-period distribution power flow model for the power management problem in active distribution systems with

a high PV penetration. The proposed model is formulated using mixed-integer second-order cone programming, and two-stage robust optimisation is used in order to tackle uncertainty, and is solved using the column and constraint generation algorithm.

- The study of [84] proposes a convex MISOCP model for the energy management problem of microgrids and uses a robust optimisation approach to tackle uncertainty. The robust approach of [84] assigns and uses the probability density functions of the random variables, and takes into account uncertainty in renewable generation (namely solar PV and wind turbines) and demand.
- The work in [94], proposes a multi-timescale scheduling method for active distribution networks, where the proposed method is decomposed into the day-ahead and real-time stage. Power flow equations are formulated using the second-order cone programming model of [85], making the final problem a mixed-integer second-order cone programming model. The real-time stage is the model-predictive control method which is introduced to reduce the impact of renewable generation forecasting errors, however, real-time control is not within the scope of this thesis.
- The paper [95], proposes a model for the microgrid planning problem, which is formulated using robust second-order cone programming and takes into account load uncertainty. The paper [96], presents a bi-level robust planning method for active distribution networks, taking into account uncertainty in the generation and the loads. The investment and operation levels are formulated using mixed-integer second-order cone programming. However, planning and investment decision-making is not within the scope of this thesis.

2.3. Conclusions

To conclude the above: there are relevant studies that do not take into account parameter uncertainty ([41, 42, 43, 44, 45, 46, 47, 48, 49, 50, 51, 52, 53, 54, 55, 56]), which is important to be taken into account, in order to avoid the risk of renewable DER being curtailed and the violation of technical constraints. There are also publications

that take into account parameter uncertainty ([8, 57, 31, 58, 59, 60, 61, 62, 63, 26, 64, 65, 66, 67, 68, 27, 35, 69, 29, 30, 70, 71, 72, 28, 73, 74, 75, 76]), but either use stochastic methods to handle uncertainty (which needs the knowledge of probability distributions that requires well-known historical data, and can have limited application in large problems [77]), or IGDT (which is a conservative method to handle uncertainty [78]), and/or in terms of the power flow model: 1) do not take into account power flow equations (which creates the risk of overloading network lines, i.e. violating voltage or line current limits), 2) take into account an approximate power flow model, 3) incorporate a nonconvex power flow model (which means that only a local optimal solution can be guaranteed). Furthermore, there are relevant studies that account for uncertainty using robust optimisation and a second-order cone accurate power flow model, that either propose multi-stage problems (which require a decomposition method in order to be solved, such as the column-and-constraint generation method [79], and therefore have an additional computational load) ([80, 81, 82, 83]), or propose a model that uses the probability distribution function of random variables: [84] (which may not always be available, as explained above for stochastic optimisation problems). Finally, there are studies that use mixed-integer second-order cone programming, but either focus on real-time control (e.g. [94]), or planning and investment decisions (e.g. [95, 96]).

The next chapter presents the two methods used in this thesis in order to formulate power flow equations and to handle uncertainty.

Chapter 3. Methodology

Contents

3.1. Chapter Summary

This chapter aims to introduce the two building blocks of the proposed R-MISOCP model: the power flow equations and the method to model uncertainty, and is structured as follows.

- **Section 3.2** presents the first building block of the R-MISOCP model of this thesis, which is the convex power flow model of [85, 86].
- **Section 3.3** presents the second building block of the proposed model, which is the robust optimisation approach of [87].
- **Section 3.4** concludes this chapter.

3.2. The power flow model

3.2.1. Mathematical formulation

The Optimal Power Flow problem is essential for a range of power systems applications such as, economic dispatch, unit commitment, scheduling, demand response, control, state estimation, and market clearing [97, 98]. Power flow equations capture the physical characteristics and constraints of the network under study, which include the voltage limits, the branch current limits, the network topology, and the resistance/reactance of the network lines. The first research towards the formulation of the optimal power flow problem was made in 1962 by J. Carpentier in [99], inspiring a wide range of research around the optimal power flow problem [98]. Since then, there has been a wide range of research on the optimal power flow problem at both electricity distribution and transmission level [99, 100, 101, 98, 102, 103].

Power flow equations can be categorized into two main formulations; the bus injection model and the branch flow model [98]. The bus injection model is the more widely used for power systems analysis, and focuses on variables related to system nodes, such as voltage, and power injections [98, 85]. The branch flow model, which is mainly used for radial distribution networks, focuses on the values of the branch currents and branch powers [98, 85]. An analysis on the equivalence of the bus injection and branch flow model is presented in [104]. In the R-MISOCP model

presented in this thesis, which aims to provide an optimal schedule for DER connected to electricity distribution networks, power flow equations have been modelled according to the convex optimal power flow formulation proposed in [85, 86], which is based on the branch flow model.

In [85], the nonconvex optimal power flow problem is approximated using two relaxation steps; the first is related to the angles of the voltage and the current, and the second is related to the fact that the resulting problem is formulated as a conic (and therefore convex) optimisation problem. In [85], it is shown that both relaxations are exact under two conditions. First, if the network is radial. Second, if over-satisfaction of the real/reactive demand is allowed. This means, that the optimisation problem is formulated in a way so that the demand is a decision variable (not a fixed number) which has a lower limit. Therefore, the following constraint (3.1) must hold:

$$D_{it}^{P/Q} \geq \underline{D_{it}^{P/Q}} \tag{3.1}$$

where, $D_{it}^{P/Q}$ is the real/reactive demand of the optimisation problem for bus i at time t, and $\underline{D_{it}^{P/Q}}$ its minimum limit.

The mathematical formulation of the power flow model used in this work is presented in equations (3.2a) - (3.2d) below as in [85], and is a second-order cone power flow model.

$$PF_{ijt}^{P} = \sum_{k:(j,k)\in E} PF_{jkt}^{P} + r_{ij}\, I_{ijt}^{sq} + D_{jt}^{P} - G_{jt}^{P}, \quad \forall (i,j) \in E, \forall t \in \Omega_T \tag{3.2a}$$

$$PF_{ijt}^{Q} = \sum_{k:(j,k)\in E} PF_{jkt}^{Q} + x_{ij}\, I_{ijt}^{sq} + D_{jt}^{Q} - G_{jt}^{Q}, \quad \forall (i,j) \in E, \forall t \in \Omega_T \tag{3.2b}$$

$$V_{jt}^{sq} = V_{it}^{sq} - 2\,(r_{ij}\, PF_{ijt}^{P} + x_{ij}\, PF_{ijt}^{Q}) + \left((r_{ij})^2 + (x_{ij})^2\right) I_{ijt}^{sq}, \quad \forall (i,j) \in E, \forall t \in \Omega_T \tag{3.2c}$$

$$\left.\begin{aligned} & I_{ijt}^{sq} + V_{it}^{sq} \geq \left\| \begin{bmatrix} 2\,PF_{ijt}^{P} & 2\,PF_{ijt}^{Q} & (I_{ijt}^{sq} - V_{it}^{sq}) \end{bmatrix}^{T} \right\|_2 \\ & \text{or} \\ & I_{ijt}^{sq} + V_{it}^{sq} \geq \left\| \begin{matrix} 2\,PF_{ijt}^{P} \\ 2\,PF_{ijt}^{Q} \\ (I_{ijt}^{sq} - V_{it}^{sq}) \end{matrix} \right\|_2 \end{aligned}\right\} \quad \forall (i,j) \in E,\ \forall t \in \Omega_T \tag{3.2d}$$

In equations (3.2a)-(3.2d) above [85]: equation (3.2a) represents the real power flow from bus i to bus j (sending-end), equation (3.2b) represents the reactive power flow from bus i to bus j (sending-end), equation (3.2c) represents the squared voltage on bus i, (3.2d) is the second-order cone equation which represents the squared current from bus i to bus j, and therefore makes this power flow model a second-order cone power flow formulation. The description of these symbols and equations (3.2a)-(3.2d) is based on table I-NOTATIONS of [85].

3.2.2. Exactness of conic relaxation

According to [85], for the optimal power flow (OPF) problem which uses equations (3.2a)-(3.2d), both relaxation steps mentioned above are exact, given that the network is radial and that over-satisfaction of loads is allowed (i.e. as shown in equation (3.1)). This means, that in equation (3.2d) the equality holds when the optimal solution is found. An extended analysis on the conditions of exactness for these PF equations is shown in [85].

This set of power flow equations has been used in this work where, apart from the power flow equations, there is an additional set of constraints which models the technical characteristics of distributed energy resources. The theoretical property regarding the exactness of the conic constraints (3.2d), numbered as constraint (4.14h) in the proposed R-MISOCP model, has been confirmed in this work for the computational experiments of section 5.3, chapter 5, by calculating the relaxation gaps of constraint (4.14h). The relaxation gaps for constraint (4.14h) of the proposed R-MISOCP model are shown in Appendix C of this thesis.

3.3. Modelling under uncertainty

3.3.1. Robust approach: Mathematical formulation

Robust optimisation (RO) is an approach to optimisation under uncertainty, where the solution is immunized against any realization of the uncertain data which belong to a deterministic interval [105, 36, 106]. This means, that the solution of the problem will be feasible for any value of the uncertain data within this interval. The motivation and goals

of RO are twofold [105]. First, in RO, data uncertainty is not stochastic. For example, the probability distribution function for the demand is not necessary to formulate a robust optimisation problem, as it is in the case of stochastic optimisation. Second, the RO formulation of an important class of optimisation problems (such as linear and second-order cone programming problems [105, 107, 108]) is computationally tractable. This second benefit, is a result of the technological advances and in the advances in the algorithms that solve convex optimisation problems (such as fast interior point methods) [105, 109].

In the optimal day-ahead scheduling problem, being fully robust, i.e. considering the *worst* possible case of uncertainty, may be too conservative, in the sense that too much of the operational performance may be sacrificed in order to tolerate any possible perturbation of the uncertain data, such as a very high cost of operation. Therefore, the robust approach of [87] is used for the R-MISOCP model proposed in this thesis. Using the robust approach of [87], the trade-off between tolerance of uncertainty and model performance can be controlled with a parameter, which is called the *budget of uncertainty* [87]. This parameter allows the DSO and/or MG operator to control the operational performance, while being robust against possible data perturbations with a very high probability. The Greek letter Γ will be used as a symbol for the budget of uncertainty throughout this thesis according to [87]. In this work, operational performance is evaluated according to the value of the operational cost and the load shedding levels (if load shedding takes place). Performance criteria are explained in more detailed in the next subsection (3.3.2).

The underlying deterministic model of the R-MISOCP model of chapter 4 is formulated as an MISOCP problem. The robust approach of [87] is employed to the deterministic problem (3.3a)-(3.3e), where data uncertainty only exists in the linear constraints (3.3b). Assume that the deterministic model is the following MISOCP problem.

$$\min \quad c^T \mathbf{x} + d^T \varphi + e^T \omega \tag{3.3a}$$

subject to

$$\sum_j \lambda_{ij} x_j + \sum_j \beta_{ij} \varphi_j + \sum_j \delta_{ij} \omega_j \leq \eta_i \quad \forall i \tag{3.3b}$$

$$\varkappa^T \varphi \geq \left\| \vartheta \varphi \right\|_2 \tag{3.3c}$$

$$\underline{\mathbf{x}} \leq \mathbf{x} \leq \overline{\mathbf{x}}, \quad \underline{\varphi} \leq \varphi \leq \overline{\varphi} \tag{3.3d}$$

$$\mathbf{x}, \varphi \quad \text{continuous}, \quad \omega \quad \text{binary} \tag{3.3e}$$

Assume that the coefficients λ_{ij} are uncertain, and each entry is a bounded and symmetric random variable λ_{ij} that takes values in $[\lambda_{ij} - \hat{\lambda}_{ij}, \lambda_{ij} + \hat{\lambda}_{ij}]$ [87]. Employing the robust approach of [87], the robust counterpart of problem (3.3a)-(3.3e) becomes as follows.

$$\min \quad c^T \mathbf{x} + d^T \varphi + e^T \omega \tag{3.4a}$$

subject to (3.3c)-(3.3d), and

$$\left[\sum_j \lambda_{ij} x_j + \max_{\{S_i \cup \{t_i\} | S_i \subseteq J_i, |S_i| = \lfloor \Gamma_i \rfloor, t_i \in J_i \setminus S_i\}} \left\{ \sum_{j \in S_i} \hat{\lambda}_{ij} y_j + (\Gamma_i - \lfloor \Gamma_i \rfloor) \hat{\lambda}_{it_i} y_t \right\} \right] + \sum_j \beta_{ij} \varphi_j + \sum_j \delta_{ij} \omega_j \leq \eta_i \ \forall i \tag{3.4b}$$

$$\mathbf{x}, \varphi, \mathbf{z}, \mathbf{p}, \mathbf{y} \quad \text{continuous}, \quad \omega \quad \text{binary} \tag{3.4c}$$

Following [87], the robust MISOCP becomes as follows.

$$\min \quad c^T \mathbf{x} + d^T \varphi + e^T \omega \tag{3.5a}$$

subject to (3.3c)-(3.3d), and

$$\left[\sum_j \lambda_{ij} x_j + z_i \Gamma_i + \sum_j p_{ij} \right] + \sum_j \beta_{ij} \varphi_j + \sum_j \delta_{ij} \omega_j \leq \eta_i \quad \forall i \tag{3.5b}$$

$$z_i + p_{ij} \geq \hat{\lambda}_{ij} y_j, \quad -y_j \leq x_j \leq y_j \tag{3.5c}$$

$$\mathbf{z} \geq 0, \ \mathbf{p} \geq 0, \ \mathbf{y} \geq 0 \tag{3.5d}$$

$$\mathbf{x}, \varphi, \mathbf{z}, \mathbf{p}, \mathbf{y} \quad \text{continuous}, \quad \omega \quad \text{binary} \tag{3.5e}$$

where $j \in J_i$, $\Gamma_i \in [0, |J_i|]$, and z_i, p_{ij}, y_j decision variables that result from the robust formulation of [87].

The following section presents the algorithm used in this research in order to choose the value of the budgets of uncertainty for the R-MISOCP model which is presented in chapter 4.

3.3.2. The Budget of Uncertainty (BoU) algorithm

In this thesis, the budgets of uncertainty are calculated using an algorithm which is based on the thesis [110] and the publication [87]. It will be referred to as the *budget of uncertainty algorithm*, or for simply *BoU algorithm*. The BoU algorithm is applicable for problems that solve the optimal day-ahead scheduling problem for DER connected to electricity distribution networks, and is not a generic algorithm to find the budgets of uncertainty such as the methods presented in section 4 of the article [87].

The BoU algorithm calculates probabilistic information in order to evaluate the suitability of the budgets of uncertainty for the DSO and/or MG operator according to operational performance criteria. Two performance criteria are considered in this work: the probability of underestimating the operational cost (PoU) and the probability of load shedding (PLS). These two criteria are defined as follows. PoU is the probability that the actual cost of operation, when considering data perturbations within the full range of uncertainty, will exceed the day-ahead operational cost calculated by the robust model. Respectively, PLS is the probability that the actual load shedding will exceed the load shedding calculated by the robust model, again when considering data perturbations in the full range of uncertainty. In these definitions, the *actual cost of operation* refers to the cost of operation in real-time, and the *robust model* refers to the proposed R-MISOCP model which is presented in chapter 4. The BoU algorithm is explained with a numerical example below for more clarity. During the explanation below there will be reference to figure 3.1 which shows the BoU algorithm in the form of a flow chart.

Assume that the optimal scheduling problem for DER connected to electricity distribution networks is formulated as in (3.5a)-(3.5e), and that the budget of uncertainty Γ corresponds to the uncertain parameter λ, such that $\lambda \in [\lambda_{ij} - \hat{\lambda}_{ij}, \lambda_{ij} + \hat{\lambda}_{ij}]$ and $\Gamma \in [0, 1]$. This means that the BoU Γ can take any value within the range [0,1],

such as Γ = 0.004, Γ = 1/3, Γ = 0.78. In a nutshell, the BoU algorithm calculates the PoU and PLS that correspond to each one of the different values of this BoU Γ. This is implemented using Monte Carlo simulations as follows.

First, a finite number of values for the BoU Γ are chosen within the interval [0,1]. For example, the five following values can be chosen Γ_1 = 0, Γ_2 = 0.25, Γ_3 = 0.5, Γ_4 = 0.75, Γ_5 = 1 (shown in Step no. 1 of figure 3.1). The R-MISOCP optimal DER schedules are considered as fixed numbers in the power flow model. Therefore, the R-MISOCP optimal DER schedules are imported in the beginning of the BoU algorithm. The R-MISOCP operational cost and load shedding are also imported at this point for the calculation of the PoU and PLS (shown in Step no. 2 of figure 3.1). Then, a set of Monte Carlo simulations of N=10 000 loops is run for each one of these different BoUs to calculate: 1) the number of times that the operational cost exceeds the day-ahead cost of operation, and 2) the number of times that the actual load shedding exceeds the day-ahead load shedding (shown in Steps no. 3 - 6 of figure 3.1). The Monte Carlo simulations basically represent the range of possible values that the uncertain data can take during the actual (real-time) operation. Therefore, in each one of the 10 000 Monte Carlo simulations, the value of the uncertain parameter λ takes a random value within the full range of uncertainty $\lambda \in [\lambda_{ij} - \hat{\lambda}_{ij}, \lambda_{ij} + \hat{\lambda}_{ij}]$. In this thesis, the random values of λ are calculated using the function *unifrnd* of MATLAB (shown in Step no. 4 of figure 3.1). Within the Monte Carlo simulations, the actual operation (i.e. the real-time operation) is simulated by running a power flow problem. In this thesis, the power flow problem is implemented using the *runpf()* function by the package MATPOWER [9] (shown in Step no. 5 of figure 3.1). When the N loops are completed, the DSO and/or MG operator is presented with the calculated probabilistic metrics (PoU, PLS) in order to choose the most suitable value for the budget of uncertainty (shown in Step no. 7 of figure 3.1).

The next section provides a discussion regarding the two building blocks of the R-MISOCP model of this thesis and concludes this chapter.

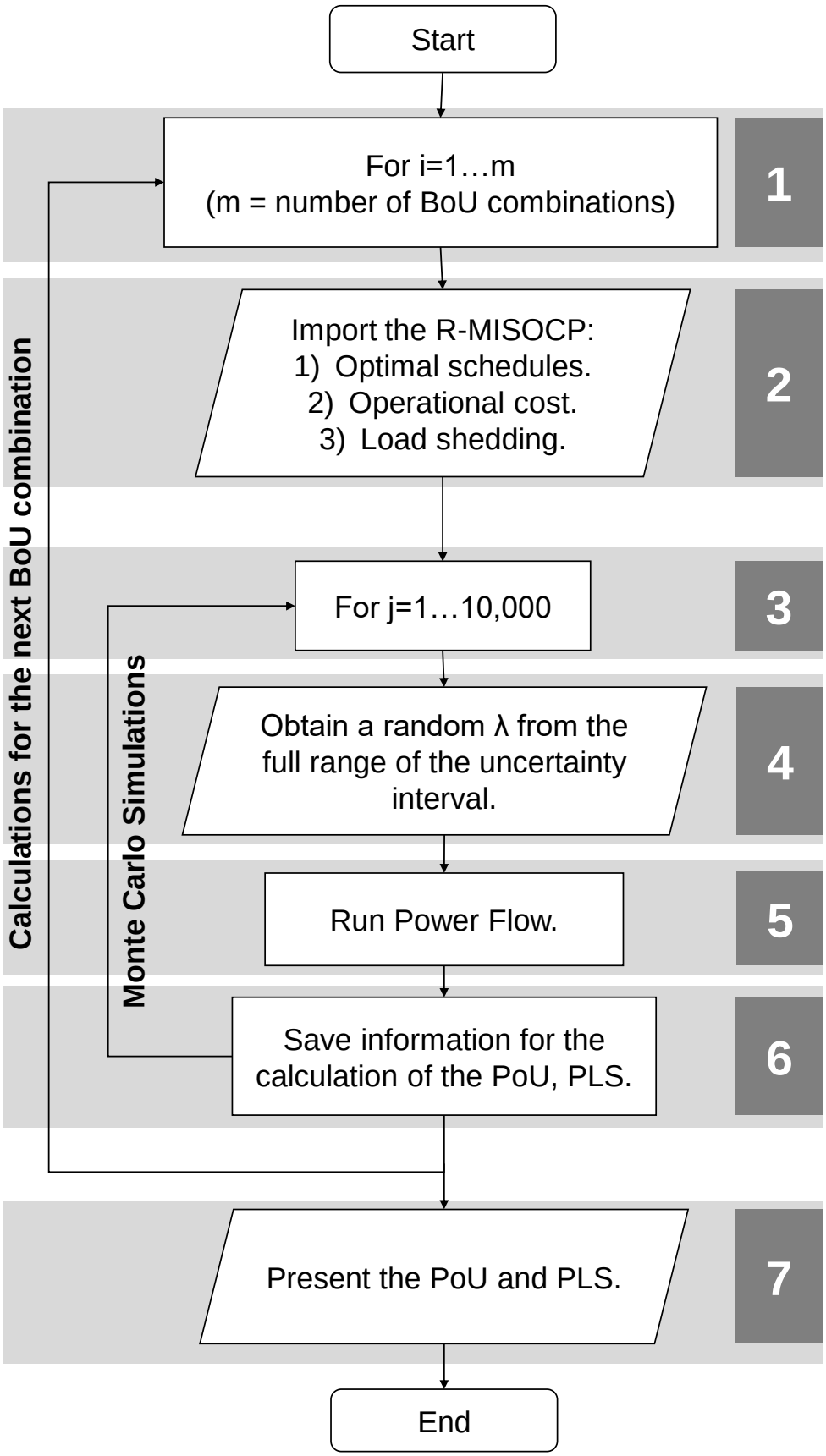

Figure 3.1: Flow chart for the Budget of uncertainty algorithm.

3.4. Conclusions and discussion

This chapter presented the methods used for the two building blocks of the R-MISOCP model proposed in this thesis. These are the power flow model of [85] and the method to model uncertainty of [87]. Some points to discuss follow below.

The R-MISOCP model of this thesis uses AC power flow equations which are mathematically formulated using second-order cone power flow model. The second-order cone power flow model used in this work (3.2a)-(3.2d), is exact an approximation of the nonconvex branch flow model under two conditions: 1) if the network is radial, and 2) if over-satisfaction of the real/reactive demand is allowed [85, 86]. The latter means that the optimisation problem is formulated in a way so that the demand is a decision variable (not a fixed number) which does not have an upper limit. As there will be no reference to *DC* power flow formulations in this research, the terms *AC power flow* and *power flow* are used interchangeably throughout this thesis. Furthermore, this power flow formulation takes into account network losses which are represented in equation (3.2a) by the term $[r_{ij}\, I^{sq}_{ijt}]$. In the computational experiments of chapter 5, it is shown through a detailed comparative study between the R-MISOCP model and a model that uses a piecewise linear power flow formulation that does not account for network losses, that losses significantly affect the calculation of the operational cost and optimal DER schedules.

In order to account for uncertainty in the market price, the demand and the renewable generation, the robust approach of [87] is used in the R-MISOCP which is presented in section 3.3 above. In this robust approach, the trade-off between tolerance of uncertainty and model performance can be controlled with a parameter, which is called the *budget of uncertainty* [87]. This parameter allows the DSO and/or MG operator to control the operational performance, while being robust against possible data perturbations with a very high probability. This probability is calculated using the BoU algorithm presented in section 3.3.2 which is based on the thesis [110] and the publication [87]. The BoU algorithm can be used for problems with one or more budgets of uncertainty. In this thesis, the BoU algorithm is used in a case where there are four BoUs (shown in the computational experiments of chapter 6). Furthermore, the research hereby has used the PoU and PLS metrics as performance criteria. Depending on the application and case study, this algorithm can easily be

adjusted to evaluate the budgets of uncertainty against other criteria as well. For example, calculate which is the probability that a network line will be overloaded. The studies [87, 110] used the following metrics: probability of underperforming (PoU) in [87], probability of success (PoS) in [110], and probability of constraint violation (PoCV) [87, 110]. The next chapter presents the R-MISOCP model proposed in this thesis which uses the two methods presented hereby.

Chapter 4. The R-MISOCP model

Contents

4.1. Chapter Summary

This chapter presents the R-MISOCP model developed in this work and is structured as follows.

- **Section 4.2** presents the mathematical formulation for the underlying deterministic problem of the proposed R-MISOCP model, and the mathematical formulation for the R-MISOCP model.
- **Section 4.3** provides a discussion and concludes the chapter.

4.2. Mathematical formulation

The following subsections present the mathematical formulation of the underlying deterministic model, and the proposed robust model, respectively. In these models, it is assumed that the distribution network has the following assets: energy storage systems, dispatchable generators, an electric vehicle parking lot and renewable generation.

4.2.1. The underlying deterministic model

The underlying deterministic model of the R-MISOCP model is presented in the model (4.1)-(4.8) below. A description of these constraints is provided below.

• **Objective function:**

Constraint (4.1) is the objective function of the MISOCP deterministic optimization problem. The objective function aims to minimize the operational cost. The cost of operation includes: the DG generation cost (using DG cost functions), the start-up/shut-down costs, the cost to buy power from the main grid, and the cost for load shedding when there is insufficient generation to feed the demand.

$$\min \sum_{i\in\Omega_G}\sum_{t\in\Omega_T}\left(b_i\,P_{it}^{DG} + a_i\,u_{it} + c_{SU_i}\,SU_{it} + c_{SD_i}\,SD_{it}\right) + \sum_{i\in\Omega_{Slack}}\sum_{t\in\Omega_T} m_{it}\,P_{it}^{Grid} + \sum_{i\in\Omega_N}\sum_{t\in\Omega_T} c^{Shed}\,D_{it}^{P^{Shed}} \tag{4.1}$$

where P_{it}^{DG}, u_{it}, SU_{it}, SD_{it}, P_{it}^{Grid}, D_{it}^{PShed} are decision variables, and b_i, a_i, c_{SU_i}, c_{SD_i}, m_{it}, c^{Shed} are parameters.

• **Unit commitment constraints:**

The set of constraints (4.2) represents unit commitment decisions.

$$u_{it} - u_{i(t-1)} \leq SU_{it}, \quad t > 1, \quad \forall i \in \Omega_G \tag{4.2a}$$

$$u_{i(t-1)} - u_{it} \leq SD_{it}, t > 1, \quad \forall i \in \Omega_G \tag{4.2b}$$

$$u_{it} \leq SU_{it}, \quad t = 1, \quad \forall i \in \Omega_G \tag{4.2c}$$

$$-u_{it} \leq SD_{it}, t = 1, \quad \forall i \in \Omega_G \tag{4.2d}$$

$$u_{it} \in \{0, 1\}, \quad \forall t \in \Omega_T, \quad \forall i \in \Omega_G \tag{4.2e}$$

$$SU_{it} \in \{0, 1\}, \quad \forall t \in \Omega_T, \quad \forall i \in \Omega_G \tag{4.2f}$$

$$SD_{it} \in \{0, 1\}, \quad \forall t \in \Omega_T, \quad \forall i \in \Omega_G \tag{4.2g}$$

where u_{it}, SU_{it}, SD_{it} are decision variables.

• **Ramp up/down limits:**

The set of constraints (4.3) represents ramp-up/down limits for the dispatchable generators.

$$P_{it}^{DG} - P_{i(t-1)}^{DG} \leq RU_i, \quad t > 1, \quad \forall i \in \Omega_G \tag{4.3a}$$

$$P_{i(t-1)}^{DG} - P_{it}^{DG} \leq RD_i, \quad t > 1, \quad \forall i \in \Omega_G \tag{4.3b}$$

$$P_{it}^{DG} \leq RU_i, \quad t = 1, \quad \forall i \in \Omega_G \tag{4.3c}$$

where P_{it}^{DG} are decision variables, and RU_i, RD_i are parameters.

• **DG limits:**

Constraints (4.4) represent the upper and lower limits of the DG.

$$u_{it}\,\underline{P_{it}^{DG}} \leq P_{it}^{DG} \leq u_{it}\,\overline{P_{it}^{DG}}, \quad \forall t \in \Omega_T, \quad \forall i \in \Omega_G \tag{4.4a}$$

$$u_{it}\,\underline{Q_{it}^{DG}} \leq Q_{it}^{DG} \leq u_{it}\,\overline{Q_{it}^{DG}}, \quad \forall t \in \Omega_T, \quad \forall i \in \Omega_G \tag{4.4b}$$

where u_{it}, P_{it}^{DG}, Q_{it}^{DG} are decision variables, and $\underline{P_{it}^{DG}}$, $\overline{P_{it}^{DG}}$, $\underline{Q_{it}^{DG}}$, $\overline{Q_{it}^{DG}}$ are parameters.

• **Power flow equations [85]:**

Constraints (4.5) represent the second-order cone power flow model along with the upper and/or lower limits of the demand, load shedding, renewable generation and voltage.

$$PF_{ijt}^{P} = \sum_{k:(j,k)\in E} PF_{jkt}^{P} + r_{ij}\, l_{ijt}^{sq} + D_{jt}^{P} - G_{jt}^{P}, \quad \forall t \in \Omega_T, \quad \forall (i,j) \in E \tag{4.5a}$$

$$PF_{ijt}^{Q} = \sum_{k:(j,k)\in E} PF_{jkt}^{Q} + x_{ij}\, l_{ijt}^{sq} + D_{jt}^{Q} - G_{jt}^{Q}, \quad \forall t \in \Omega_T, \quad \forall (i,j) \in E \tag{4.5b}$$

$$v_{jt}^{sq} = v_{it}^{sq} - 2\,(r_{ij}\, PF_{ijt}^{P} + x_{ij}\, PF_{ijt}^{Q}) + (r_{ij}^2 + x_{ij}^2)\, l_{ijt}^{sq}, \quad \forall t \in \Omega_T, \quad \forall (i,j) \in E \tag{4.5c}$$

$$P_{it}^{Grid} = PF_{ijt}^{P}, \quad \forall t \in \Omega_T, \quad i = 1, \forall (i,j) \in E \tag{4.5d}$$

$$Q_{it}^{Grid} = PF_{ijt}^{Q}, \quad \forall t \in \Omega_T, \quad i = 1, \forall (i,j) \in E \tag{4.5e}$$

$$
\begin{aligned}
G_{it}^{P} = & \sum_{i \in \Omega_{EV}} \left(P_{it}^{Dch,EV} + P_{it}^{Ch,EV} \right) + \\
& \sum_{i \in \Omega_{N}} D_{it}^{P,shed} + \\
& \sum_{i \in \Omega_{G}} P_{it}^{DG} + \\
& \sum_{i \in \Omega_{ESS}} \left(P_{it}^{Dch,ESS} - P_{it}^{Ch,ESS} \right) + \\
& \sum_{i \in \Omega_{Ren}} P_{it}^{Ren} + \\
& \sum_{i \in \Omega_{Slack}} P_{it}^{Grid}, \quad \forall t \in \Omega_{T}, \quad \forall i \in \Omega_{N}
\end{aligned}
\tag{4.5f}
$$

$$
G_{it}^{Q} = \sum_{i \in \Omega_{Slack}} Q_{it}^{Grid} + \sum_{i \in \Omega_{N}} Q_{it}^{DG}, \quad \forall t \in \Omega_{T}, \quad \forall i \in \Omega_{N} \tag{4.5g}
$$

$$
I_{ijt}^{sq} + v_{it}^{sq} \geq \left\| \begin{bmatrix} 2\,PF_{ijt}^{P} & 2\,PF_{ijt}^{Q} & (I_{ijt}^{sq} - v_{it}^{sq}) \end{bmatrix}^{T} \right\|_{2}, \quad \forall t \in \Omega_{T}, \quad \forall (i,j) \in E \tag{4.5h}
$$

$$
P_{it}^{Ren} \leq \overline{P_{it}^{Ren}}, \quad \forall t \in \Omega_{T}, \quad \forall i \in \Omega_{Ren} \tag{4.5i}
$$

$$
D_{it}^{P} \geq \underline{D_{it}^{P}}, \quad \forall t \in \Omega_{T}, \quad \forall i \in \Omega_{N} \tag{4.5j}
$$

$$
0 \leq D_{it}^{P,shed} \leq \underline{D_{it}^{P}}, \quad \forall t \in \Omega_{T}, \quad \forall i \in \Omega_{N} \tag{4.5k}
$$

$$
D_{it}^{Q} \geq \underline{D_{it}^{Q}}, \quad \forall t \in \Omega_{T}, \quad \forall i \in \Omega_{N} \tag{4.5l}
$$

$$
0 \leq I_{ijt}^{sq} \leq \overline{I_{ijt}^{sq}}, \quad \forall t \in \Omega_{T}, \quad \forall (i,j) \in E \tag{4.5m}
$$

$$
\underline{v_{it}^{sq}} \leq v_{it}^{sq} \leq \overline{v_{it}^{sq}}, \quad \forall t \in \Omega_{T}, \quad \forall i \in \Omega_{N} \tag{4.5n}
$$

$$
v_{it}^{sq} = v_{it}^{ref}, \quad \forall i \in \Omega_{Slack}, \quad \forall t \in \Omega_{T} \tag{4.5o}
$$

where $PF_{ijt}^{\{P,Q\}}$, I_{ijt}^{sq}, $D_{it}^{\{P,Q\}}$, $G_{it}^{\{P,Q\}}$, v_{it}^{sq}, $\{P,Q\}_{it}^{Grid}$, $P_{it}^{Dch,\{EV,\ ESS\}}$, $P_{it}^{Ch,\{EV,\ ESS\}}$, $D_{it}^{P,shed}$, $\{P,\ Q\}_{it}^{DG}$, P_{it}^{Ren} are decision variables, and r_{ij}, x_{ij}, $\overline{P_{it}^{Ren}}$, $\underline{D_{it}^{\{P,Q\}}}$, $\overline{I_{ijt}^{sq}}$, $\underline{v_{it}^{sq}}$, $\overline{v_{it}^{sq}}$, v_{it}^{ref} are parameters.

- **Main grid real and reactive power limits:**

Constraints (4.6) present the main grid import limits for the real and reactive power.

$$0 \leq P_{it}^{Grid} \leq \overline{P_{it}^{Grid}}, \quad \forall i \in \Omega_{Slack}, \quad \forall t \in \Omega_T \tag{4.6a}$$

$$0 \leq Q_{it}^{Grid} \leq \overline{Q_{it}^{Grid}}, \quad \forall i \in \Omega_{Slack}, \quad \forall t \in \Omega_T \tag{4.6b}$$

where P_{it}^{Grid}, Q_{it}^{Grid} are decision variables, and $\overline{P_{it}^{Grid}}$, $\overline{Q_{it}^{Grid}}$ are parameters.

- **Energy Storage System model:**

The energy storage system model is formulated by constraints (4.7).

$$SOC_{it}^{ESS}\, C_i^{ESS,Max} = \begin{cases} SOC_{i,initial}^{ESS}\, C_i^{ESS,Max} + (\eta_i\, P_{it}^{Ch,ESS} - P_{it}^{Dch,ESS}/\eta_i)\, D\tau, \\ \quad t = 1, \quad \forall i \in \Omega_{ESS} \\ SOC_{i(t-1)}^{ESS}\, C_i^{ESS,Max} + (\eta_i\, P_{it}^{Ch,ESS} - P_{it}^{Dch,ESS}/\eta_i)\, D\tau, \\ \quad t > 1, \forall i \in \Omega_{ESS} \end{cases} \tag{4.7a}$$

$$0 \leq SOC_{it}^{ESS} \leq 1, \quad \forall i \in \Omega_{ESS}, \quad \forall t \in \Omega_T \tag{4.7b}$$

$$0 \leq P_{it}^{Dch,ESS} \leq u_{it}^{ESS}\overline{P_{it}^{Dch,ESS}}, \quad \forall i \in \Omega_{ESS}, \quad \forall t \in \Omega_T \tag{4.7c}$$

$$0 \leq P_{it}^{Ch,ESS} \leq v_{it}^{ESS}\overline{P_{it}^{Ch,ESS}}, \quad \forall i \in \Omega_{ESS}, \quad \forall t \in \Omega_T \tag{4.7d}$$

$$u_{it}^{ESS} + v_{it}^{ESS} \leq 1, \quad \forall i \in \Omega_{ESS}, \quad \forall t \in \Omega_T \tag{4.7e}$$

$$u_{it}^{ESS} \in \{0, 1\}, \quad \forall i \in \Omega_{ESS}, \quad \forall t \in \Omega_T \tag{4.7f}$$

$$v_{it}^{ESS} \in \{0, 1\}, \quad \forall i \in \Omega_{ESS}, \quad \forall t \in \Omega_T \tag{4.7g}$$

where SOC_{it}^{ESS}, $P_{it}^{\{Ch,Dch\},ESS}$, u_{it}^{ESS}, v_{it}^{ESS} are decision variables, and η_i, $D\tau$, $\overline{P_{it}^{Dch,ESS}}$, $\overline{P_{it}^{Ch,ESS}}$, $SOC_{i,initial}^{ESS}$, $C_i^{ESS,Max}$ are parameters.

• **Electric Vehicle Parking lot constraints [8, 2]:**

The EV parking lot is modelled as an aggregated EV, using the set of linear constraints (4.8) based on [8, 2], where constraints (4.8a) represent the arrival and departure state of charge. The EVs follow the CC to CV (Constant Current to Constant Voltage) charging method for Li-ion batteries, presented in the Appendix of the study in [2].

$$SOC_{it}^{EV} = \begin{cases} SOC_{arrival}^{EV}\, C_i^{EV,Max}, & t = t_{Min}^{EV}, \quad \forall i \in \Omega_{EV} \\ SOC_{departure}^{EV}\, C_i^{EV,Max}, & t = t_{Max}^{EV}, \quad \forall i \in \Omega_{EV} \end{cases} \tag{4.8a}$$

$$SOC_{it}^{EV} = SOC_{i(t-1)}^{EV} + (-\eta_i\, P_{it}^{Ch,EV} - P_{it}^{Dch,EV}/\eta_i)\, D\tau, \quad \forall i \in \Omega_{EV}, \quad \forall t \in \Omega_T \tag{4.8b}$$

$$P_{it}^{EV} = P_{it}^{Dch,EV} - P_{it}^{Ch,EV}, \quad \forall i \in \Omega_{EV}, \quad \forall t \in \Omega_T \tag{4.8c}$$

$$P_{it}^{EV} \leq \overline{P_{it}^{EV}}\, EV_{it}^{schdl}, \quad \forall i \in \Omega_{EV}, \quad \forall t \in \Omega_T \tag{4.8d}$$

$$P_{it}^{EV} \leq \overline{P_{it}^{EV}}\, EV_{it}^{schdl}\, \frac{1 - SOC_{it}^{EV}}{1 - SOC_i^{Sat,EV}}, \quad \forall i \in \Omega_{EV}, \quad \forall t \in \Omega_T \tag{4.8e}$$

$$P_{it}^{Dch,EV} \leq \overline{P_{it}^{EV}}\, u_{it}^{EV}, \quad \forall i \in \Omega_{EV}, \quad \forall t \in \Omega_T \tag{4.8f}$$

$$P_{it}^{Ch,EV} \leq \overline{P_{it}^{EV}}\, (1 - u_{it}^{EV}), \quad \forall i \in \Omega_{EV}, \quad \forall t \in \Omega_T \tag{4.8g}$$

$$SOC_{it}^{EV} \geq 0, \quad \forall i \in \Omega_{EV}, \quad \forall t \in \Omega_T \tag{4.8h}$$

$$P_{it}^{Dch,EV} \geq 0, \quad \forall i \in \Omega_{EV}, \quad \forall t \in \Omega_T \tag{4.8i}$$

$$P_{it}^{Ch,EV} \leq 0, \quad \forall i \in \Omega_{EV}, \quad \forall t \in \Omega_T \tag{4.8j}$$

$$-\overline{P_{it}^{EV}} \leq P_{it}^{EV} \leq \overline{P_{it}^{EV}}, \quad \forall i \in \Omega_{EV}, \quad \forall t \in \Omega_T \tag{4.8k}$$

$$u_{it}^{EV} \in \{0, 1\}, \quad \forall i \in \Omega_{EV}, \quad \forall t \in \Omega_T \tag{4.8l}$$

where SOC_{it}^{EV}, $P_{it}^{\{Ch,\ Dch\},EV}$, P_{it}^{EV}, u_{it}^{EV} are decision variables, and $SOC_{\{arrival,\ departure\}}^{EV}$, η_i, $D\tau$, $\overline{P_{it}^{EV}}$, EV_{it}^{schdl}, $SOC_i^{Sat,EV}$, $C_i^{EV,Max}$ are parameters.

Finally, it is noted that in the model above, the constraints that have been used along with the power flow equations of [85, 86] are linear, and the underlying deterministic MISOCP problem (4.1)-(4.8) is convex in terms of its continuous variables [111].

4.2.2. The R-MISOCP model

The robust formulation of the deterministic problem (4.1)-(4.8) above, is presented in constraints (4.9)-(4.21) below. Constraints related to the unit commitment decisions, ramp-up/down limits, the energy storage model and the electric vehicle parking lot are not altered in the R-MISOCP problem. However, these constraints are re-written below for completeness.

The objective of the R-MISOCP model is to minimize the cost of operation. The cost of operation includes: DG generation cost (using DG cost functions), start-up/shut-down costs, the cost to buy power from the main grid, and the cost for load shedding when (during the times that the network operates disconnected from the main grid) there is insufficient generation to feed the demand. Constraints represent: the SOC-PF model, branch current limits, unit commitment decisions, ramp-up/down limits, the ESS model, the EV parking lot model, and upper/lower limits of variables (namely of fixed loads, curtailable loads, bus voltage, DGs and grid power).

The R-MISOCP model has binary and continuous decision variables. Binary decision variables represent: unit commitment decisions, charging/discharging state of the energy storage system (ESS), charging/discharging state of the electric vehicle (EV) parking lot, and the state of connection between the distribution network and

the main grid (grid-connected/islanded). Continuous decision variables represent: scheduling of network assets (DGs, charged/discharged power of ESS and EV parking lot), imported power from the main grid, bus voltages, power flows, line losses, ESS state-of-charge, loads (fixed and curtailed), and auxiliary decision variables as a result of the robust formulation.

As explained in section 3.3, chapter 3, robust optimisation according to [87] is used to handle uncertainty, where uncertainty is formulated within a deterministic interval that requires the mean and range of the uncertain data, and can be calculated using historical and/or forecasted data [28, 77]. Data uncertainty is considered in the market price, the demand, the renewable generation, and time and duration of an islanding event (for example, due to an upstream maintenance or a foreseeable natural disaster such as a hurricane [1, 27, 8, 28]). A description of constraints (4.9)-(4.21) is provided below.

The objective function of the underlying deterministic problem is dropped to the constraint (4.10), in order to model market price uncertainty. The value of the R-MISOCP objective function is calculated by the right-hand side value of constraint (4.10). Constraints (4.11) model the unit commitment decisions for the dispatchable generators. Constraints (4.12) represent the dispatchable generator's ramp-up/down limits, and constraints (4.13) the upper and lower limits of DG. Constraints (4.14) model the power flow equations, and take into account renewable generation uncertainty and demand uncertainty. The energy storage system model is presented in constraints (4.15). The electric vehicle parking lot is modelled in constraints (4.16).

Constraints (4.17) represent the market price uncertainty, where the budget of uncertainty adjusts the time periods that the market price deviates from its forecasted value, and therefore takes values in the interval [0, $|\Omega_T|$]. In this thesis, $|\Omega_T|$ = 144 time periods. Constraints (4.18) represent the demand uncertainty, where the budget of uncertainty adjusts the percentage that the demand deviates from its forecasted value, and takes values in the interval [0, 1]. Constraints (4.19) represent the renewable generation uncertainty, where the budget of uncertainty adjusts the percentage that the renewable generation deviates from its forecasted value, and takes values in the interval [0, 1]. Constraints (4.20) present the constraints for the islanding event uncertainty which are based on the study [28], where the budget of uncertainty adjusts

the time periods that the network interruption deviates from its forecasted value, and takes values in the interval [0, $\overline{\gamma^{I,Left}}$ + $\overline{\gamma^{I,Right}}$]. The parameter $\overline{\gamma^{I,Left}}$, represents the maximum number of time periods that the network is predicted to operate disconnected from the main grid before the time that the scheduled interruption is expected to start. Respectively, the parameter $\overline{\gamma^{I,Right}}$, represents the maximum number of time periods that the network is predicted to operate disconnected from the main grid after the time that the scheduled interruption is expected to end. In this thesis, $\overline{\gamma^{I,Left}}$ = $\overline{\gamma^{I,Right}}$ = 3 time periods. Finally, the main grid upper and lower limits are presented in constraints (4.21), which have been modified compared to the constraints (4.6) of the deterministic problem above, in order to be in line with the decisions made by the islanding event uncertainty.

The R-MISOCP model is presented below in equations (4.9)-(4.21).

Robust Mixed Integer Second Order Cone Programming model (the R-MISOCP model):

$$\min \quad \rho \tag{4.9}$$

subject to

$$\begin{aligned}\rho \geq \sum_{i\in\Omega_G}\sum_{t\in\Omega_T}\left(b_i\,P_{it}^{DG} + a_i\,u_{it} + c_{SU_i}\,SU_{it} + c_{SD_i}\,SD_{it}\right) + \\ \sum_{i\in\Omega_{Slack}}\sum_{t\in\Omega_T} m_{it}\,P_{it}^{Grid} + z^M\,\Gamma^M + \sum_{i\in\Omega_{Slack}}\sum_{t\in\Omega_T} p_{it}^M + \\ \sum_{i\in\Omega_N}\sum_{t\in\Omega_T} c^{Shed}\,D_{it}^{Shed}\end{aligned} \tag{4.10}$$

Unit commitment constraints:

$$u_{it} - u_{i(t-1)} \leq SU_{it}, \quad t > 1, \quad \forall i \in \Omega_G \tag{4.11a}$$

$$u_{i(t-1)} - u_{it} \leq SD_{it}, \quad t > 1, \quad \forall i \in \Omega_G \tag{4.11b}$$

$$u_{it} \leq SU_{it}, \quad t = 1, \quad \forall i \in \Omega_G \tag{4.11c}$$

$$-u_{it} \leq SD_{it}, \quad t = 1, \quad \forall i \in \Omega_G \tag{4.11d}$$

$$u_{it} \in \{0, 1\}, \quad \forall t \in \Omega_T, \quad \forall i \in \Omega_G \tag{4.11e}$$

$$SU_{it} \in \{0, 1\}, \quad \forall t \in \Omega_T, \quad \forall i \in \Omega_G \tag{4.11f}$$

$$SD_{it} \in \{0, 1\}, \quad \forall t \in \Omega_T, \quad \forall i \in \Omega_G \tag{4.11g}$$

Ramp up/down limits:

$$P_{it}^{DG} - P_{i(t-1)}^{DG} \leq RU_i, \quad t > 1, \quad \forall i \in \Omega_G \tag{4.12a}$$

$$P_{i(t-1)}^{DG} - P_{it}^{DG} \leq RD_i, \quad t > 1, \quad \forall i \in \Omega_G \tag{4.12b}$$

$$P_{it}^{DG} \leq RU_i, \quad t = 1, \quad \forall i \in \Omega_G \tag{4.12c}$$

DG limits:

$$u_{it} \underline{P_{it}^{DG}} \leq P_{it}^{DG} \leq u_{it} \overline{P_{it}^{DG}}, \quad \forall t \in \Omega_T, \quad \forall i \in \Omega_G \tag{4.13a}$$

$$u_{it} \underline{Q_{it}^{DG}} \leq Q_{it}^{DG} \leq u_{it} \overline{Q_{it}^{DG}}, \quad \forall t \in \Omega_T, \quad \forall i \in \Omega_G \tag{4.13b}$$

Power flow equations [85]:

$$PF_{ijt}^{P} = \sum_{k:(j,k)\in E} PF_{jkt}^{P} + r_{ij}\, I_{ijt}^{sq} + D_{jt}^{P} + z_t^D\, \Gamma_t^D + p_{jt}^{D} - G_{jt}^{P}, \quad \forall t \in \Omega_T, \quad \forall (i,j) \in E \tag{4.14a}$$

$$PF_{ijt}^{Q} = \sum_{k:(j,k)\in E} PF_{jkt}^{Q} + x_{ij}\, I_{ijt}^{sq} + D_{jt}^{Q} - G_{jt}^{Q}, \quad \forall t \in \Omega_T, \quad \forall (i,j) \in E \tag{4.14b}$$

$$v_{jt}^{sq} = v_{it}^{sq} - 2\,(r_{ij}\, PF_{ijt}^{P} + x_{ij}\, PF_{ijt}^{Q}) + (r_{ij}^2 + x_{ij}^2)\, I_{ijt}^{sq}, \quad \forall t \in \Omega_T, \quad \forall (i,j) \in E \tag{4.14c}$$

$$P_{it}^{Grid} = PF_{ijt}^{P}, \quad \forall t \in \Omega_T, \quad i = 1, \forall (i,j) \in E \tag{4.14d}$$

$$Q_{it}^{Grid} = PF_{ijt}^{Q}, \quad \forall t \in \Omega_T, \quad i = 1, \forall (i,j) \in E \tag{4.14e}$$

$$
\begin{aligned}
G_{it}^{P} = \sum_{i\in\Omega_{EV}} \left(P_{it}^{Dch,EV} + P_{it}^{Ch,EV}\right) + \\
\sum_{i\in\Omega_{N}} D_{it}^{P,shed} + \\
\sum_{i\in\Omega_{G}} P_{it}^{DG} + \\
\sum_{i\in\Omega_{ESS}} \left(P_{it}^{Dch,ESS} - P_{it}^{Ch,ESS}\right) + \\
\sum_{i\in\Omega_{Ren}} \left(P_{it}^{Ren} - z_{t}^{Ren}\,\Gamma_{t}^{Ren} - p_{it}^{Ren}\right) + \\
\sum_{i\in\Omega_{Slack}} P_{it}^{Grid}, \quad \forall t \in \Omega_{T}, \quad \forall i \in \Omega_{N}
\end{aligned}
\tag{4.14f}
$$

$$
G_{it}^{Q} = \sum_{i\in\Omega_{Slack}} Q_{it}^{Grid} + \sum_{i\in\Omega_{N}} Q_{it}^{DG}, \quad \forall t \in \Omega_{T}, \quad \forall i \in \Omega_{N} \tag{4.14g}
$$

$$
I_{ijt}^{sq} + v_{it}^{sq} \geq \left\| \left[2\,PF_{ijt}^{P} \quad 2\,PF_{ijt}^{Q} \quad (I_{ijt}^{sq} - v_{it}^{sq}) \right]^{T} \right\|_{2}, \quad \forall t \in \Omega_{T}, \quad \forall (i,j) \in E \tag{4.14h}
$$

$$
P_{it}^{Ren} \leq \overline{P_{it}^{Ren}}, \quad \forall t \in \Omega_{T}, \quad \forall i \in \Omega_{Ren} \tag{4.14i}
$$

$$
D_{it}^{P} \geq \underline{D_{it}^{P}}, \quad \forall t \in \Omega_{T}, \quad \forall i \in \Omega_{N} \tag{4.14j}
$$

$$
0 \leq D_{it}^{P,shed} \leq \underline{D_{it}^{P}}, \quad \forall t \in \Omega_{T}, \quad \forall i \in \Omega_{N} \tag{4.14k}
$$

$$
D_{it}^{Q} \geq \underline{D_{it}^{Q}}, \quad \forall t \in \Omega_{T}, \quad \forall i \in \Omega_{N} \tag{4.14l}
$$

$$
0 \leq I_{ijt}^{sq} \leq \overline{I_{ijt}^{sq}}, \quad \forall t \in \Omega_{T}, \quad \forall (i,j) \in E \tag{4.14m}
$$

$$
\underline{v_{it}^{sq}} \leq v_{it}^{sq} \leq \overline{v_{it}^{sq}}, \quad \forall t \in \Omega_{T}, \quad \forall i \in \Omega_{N} \tag{4.14n}
$$

$$
v_{it}^{sq} = v_{it}^{ref}, \quad \forall i \in \Omega_{Slack}, \quad \forall t \in \Omega_{T} \tag{4.14o}
$$

Energy Storage System model:

$$SOC_{it}^{ESS}\, C_i^{ESS,Max} = \begin{cases} SOC_{i,initial}^{ESS}\, C_i^{ESS,Max} + (\eta_i\, P_{it}^{Ch,ESS} - P_{it}^{Dch,ESS}/\eta_i)\, D\tau, \\ \quad t = 1, \quad \forall i \in \Omega_{ESS} \\ SOC_{i(t-1)}^{ESS}\, C_i^{ESS,Max} + (\eta_i\, P_{it}^{Ch,ESS} - P_{it}^{Dch,ESS}/\eta_i)\, D\tau, \\ \quad t > 1, \quad \forall i \in \Omega_{ESS} \end{cases} \tag{4.15a}$$

$$0 \leq SOC_{it}^{ESS} \leq 1, \quad \forall i \in \Omega_{ESS}, \quad \forall t \in \Omega_T \tag{4.15b}$$

$$0 \leq P_{it}^{Dch,ESS} \leq u_{it}^{ESS} \overline{P_{it}^{Dch,ESS}}, \quad \forall i \in \Omega_{ESS}, \quad \forall t \in \Omega_T \tag{4.15c}$$

$$0 \leq P_{it}^{Ch,ESS} \leq v_{it}^{ESS} \overline{P_{it}^{Ch,ESS}}, \quad \forall i \in \Omega_{ESS}, \quad \forall t \in \Omega_T \tag{4.15d}$$

$$u_{it}^{ESS} + v_{it}^{ESS} \leq 1, \quad \forall i \in \Omega_{ESS}, \quad \forall t \in \Omega_T \tag{4.15e}$$

$$u_{it}^{ESS} \in \{0, 1\}, \quad \forall i \in \Omega_{ESS}, \quad \forall t \in \Omega_T \tag{4.15f}$$

$$v_{it}^{ESS} \in \{0, 1\}, \quad \forall i \in \Omega_{ESS}, \quad \forall t \in \Omega_T \tag{4.15g}$$

Electric Vehicle Parking lot constraints [8, 2]:

$$SOC_{it}^{EV} = \begin{cases} SOC_{arrival}^{EV}\, C_i^{EV,Max}, & t = t_{Min}^{EV}, \quad \forall i \in \Omega_{EV} \\ SOC_{departure}^{EV}\, C_i^{EV,Max}, & t = t_{Max}^{EV}, \quad \forall i \in \Omega_{EV} \end{cases} \tag{4.16a}$$

$$SOC_{it}^{EV} = SOC_{i(t-1)}^{EV} + (-\eta_i\, P_{it}^{Ch,EV} - P_{it}^{Dch,EV}/\eta_i)\, D\tau, \quad \forall i \in \Omega_{EV}, \quad \forall t \in \Omega_T \tag{4.16b}$$

$$P_{it}^{EV} = P_{it}^{Dch,EV} - P_{it}^{Ch,EV}, \quad \forall i \in \Omega_{EV}, \quad \forall t \in \Omega_T \tag{4.16c}$$

$$P_{it}^{EV} \leq \overline{P_{it}^{EV}}\, EV_{it}^{schdl}, \quad \forall i \in \Omega_{EV}, \quad \forall t \in \Omega_T \tag{4.16d}$$

$$P_{it}^{EV} \leq \overline{P_{it}^{EV}}\, EV_{it}^{schdl}\, \frac{1 - SOC_{it}^{EV}}{1 - SOC_{i}^{Sat,EV}}, \quad \forall i \in \Omega_{EV}, \quad \forall t \in \Omega_T \tag{4.16e}$$

$$P_{it}^{Dch,EV} \leq \overline{P_{it}^{EV}}\, u_{it}^{EV}, \quad \forall i \in \Omega_{EV}, \quad \forall t \in \Omega_T \tag{4.16f}$$

$$P_{it}^{Ch,EV} \leq \overline{P_{it}^{EV}}\, (1 - u_{it}^{EV}), \quad \forall i \in \Omega_{EV}, \quad \forall t \in \Omega_T \tag{4.16g}$$

$$SOC_{it}^{EV} \geq 0, \quad \forall i \in \Omega_{EV}, \quad \forall t \in \Omega_T \tag{4.16h}$$

$$P_{it}^{Dch,EV} \geq 0, \quad \forall i \in \Omega_{EV}, \quad \forall t \in \Omega_T \tag{4.16i}$$

$$P_{it}^{Ch,EV} \leq 0, \quad \forall i \in \Omega_{EV}, \quad \forall t \in \Omega_T \tag{4.16j}$$

$$-\overline{P_{it}^{EV}} \leq P_{it}^{EV} \leq \overline{P_{it}^{EV}}, \quad \forall i \in \Omega_{EV}, \quad \forall t \in \Omega_T \tag{4.16k}$$

$$u_{it}^{EV} \in \{0, 1\}, \quad \forall i \in \Omega_{EV}, \quad \forall t \in \Omega_T \tag{4.16l}$$

Market price uncertainty [87]:

$$z^M + p_{it}^M \geq \widehat{m_{it}}\, y_{it}^M, \quad \forall t \in \Omega_T, \quad i \in \Omega_{Slack} \tag{4.17a}$$

$$-y_{it}^M \leq P_t^{Grid} \leq y_{it}^M, \quad \forall t \in \Omega_T, \quad i \in \Omega_{Slack} \tag{4.17b}$$

$$z^M \geq 0 \tag{4.17c}$$

$$p_{it}^M \geq 0, \quad \forall t \in \Omega_T, \quad i \in \Omega_{Slack} \tag{4.17d}$$

$$y_{it}^M \geq 0, \quad \forall t \in \Omega_T, \quad i \in \Omega_{Slack} \tag{4.17e}$$

$$\Gamma^M \in [0, |\Omega_T|] \tag{4.17f}$$

Demand uncertainty [87]:

$$z_t^D + p_{it}^D \geq \widehat{d}\, y_{it}^D, \quad \forall i \in \Omega_N, \quad \forall t \in \Omega_T \tag{4.18a}$$

$$-y_{it}^D \leq D_{it}^P \leq y_{it}^D, \quad \forall i \in \Omega_N, \quad \forall t \in \Omega_T \tag{4.18b}$$

$$z_t^D \geq 0, \quad \forall t \in \Omega_T \tag{4.18c}$$

$$p_{it}^D \geq 0, \quad \forall i \in \Omega_N, \quad \forall t \in \Omega_T \tag{4.18d}$$

$$y_{it}^D \geq 0, \quad \forall i \in \Omega_N, \quad \forall t \in \Omega_T \tag{4.18e}$$

$$\Gamma_t^D \in [0, 1], \quad \forall t \in \Omega_T \tag{4.18f}$$

Renewable generation uncertainty [87]:

$$z_t^{Ren} + p_{it}^{Ren} \geq \widehat{p^{Ren}}\, y_{it}^{Ren}, \quad \forall i \in \Omega_{Ren}, \quad \forall t \in \Omega_T \tag{4.19a}$$

$$-y_{it}^{Ren} \leq P_{it}^{Ren} \leq y_{it}^{Ren}, \quad \forall i \in \Omega_{Ren}, \quad \forall t \in \Omega_T \tag{4.19b}$$

$$z_t^{Ren} \geq 0, \quad \forall t \in \Omega_T \tag{4.19c}$$

$$p_{it}^{Ren} \geq 0, \quad \forall i \in \Omega_{Ren}, \quad \forall t \in \Omega_T \tag{4.19d}$$

$$y_{it}^{Ren} \geq 0, \quad \forall i \in \Omega_{Ren}, \quad \forall t \in \Omega_T \tag{4.19e}$$

$$\Gamma_t^{Ren} \in [0, 1], \quad \forall t \in \Omega_T \tag{4.19f}$$

Islanding event uncertainty [28]:

$$\Gamma^I = \gamma^{I,Left} + \gamma^{I,Right} \tag{4.20a}$$

$$\gamma^{I,Left} = \sum_{t \in \Omega T} isl_t^L \tag{4.20b}$$

$$\gamma^{I,Right} = \sum_{t \in \Omega T} isl_t^R \tag{4.20c}$$

$$0 \leq \gamma^{I,Left} \leq \overline{\gamma^{I,Left}} \tag{4.20d}$$

$$0 \leq \gamma^{I,Right} \leq \overline{\gamma^{I,Right}} \tag{4.20e}$$

$$0 \leq (I_t + isl_t^L + isl_t^R) \leq 1, \quad \forall t \in \Omega_T \tag{4.20f}$$

$$\sum_{t \in \Omega(T)} (I_t + isl_t^L + isl_t^R) = \sum_{t \in \Omega_T} I_t + \Gamma^I \tag{4.20g}$$

$$isl_t^L + I_t \leq isl_{t+1}^L + I_{t+1}, \quad t \leq (t_{start}^{isl} + \overline{\gamma^{I,Left}} + 1) \tag{4.20h}$$

$$isl_t^R + I_t \geq isl_{t+1}^R + I_{t+1}, \quad t \geq (t_{end}^{isl} - \overline{\gamma^{I,Right}} - 1) \tag{4.20i}$$

$$isl_t^L = 0, \quad \forall t \in \Omega_T, \quad t \notin [t_{start}^{isl} - \overline{\gamma^{I,Left}} - 1, t_{start}^{isl} + \overline{\gamma^{I,Left}} + 1] \tag{4.20j}$$

$$isl_t^R = 0, \quad \forall t \in \Omega_T, \quad t \notin [t_{end}^{isl} - \overline{\gamma^{I,Right}} - 1, t_{end}^{isl} + \overline{\gamma^{I,Right}} + 1] \tag{4.20k}$$

$$\Gamma^I \in [0, \overline{\gamma^{I,Left}} + \overline{\gamma^{I,Right}}] \cap \mathbb{Z} \tag{4.20l}$$

$$\gamma^{I,Left} \in \mathbb{Z} \tag{4.20m}$$

$$\gamma^{I,Right} \in \mathbb{Z} \tag{4.20n}$$

$$isl_t^L \in \{0, 1\}, \quad \forall t \in \Omega_T \tag{4.20o}$$

$$isl_t^R \in \{0,1\}, \quad \forall t \in \Omega_T \tag{4.20p}$$

Main grid real and reactive power limits:

$$0 \leq P_{it}^{Grid} \leq \overline{P_{it}^{Grid}}\,[1-(I_t + isl_t^{Left} + isl_t^{Right})], \quad \forall i \in \Omega_{Slack}, \quad \forall t \in \Omega_T \tag{4.21a}$$

$$0 \leq Q_{it}^{Grid} \leq \overline{Q_{it}^{Grid}}\,[1-(I_t + isl_t^{Left} + isl_t^{Right})], \quad \forall i \in \Omega_{Slack}, \quad \forall t \in \Omega_T \tag{4.21b}$$

4.3. Discussion and conclusions

This chapter presented the mathematical formulation of the proposed R-MISOCP model for the optimal day-ahead scheduling problem of DER connected to electricity distribution networks. Some points to discuss follow below.

The inputs of the R-MISOCP model are the budgets of uncertainty (BoUs) and the data that correspond to the network under study. The BoUs can be calculated according to the BoU algorithm that is presented in Chapter 3. The outputs of the R-MISOCP model are the decision variables that correspond to the DER optimal schedules, the operational cost, and the remaining decision variables (such as line current, branch flows, etc.). To run the R-MISOCP model (4.9)-(4.21) for business-as-usual case studies (where no network interruption from the main grid is expected), the parameters I_t, t_{start}^{isl}, t_{end}^{isl} can be set equal to zero: $I_t = 0$, $\forall\, t \in \Omega_T$ and $t_{start}^{isl} = t_{end}^{isl} = 0$. Furthermore, the proposed R-MISOCP model can be reformulated to a mixed-integer linear programming problem using the ϵ-polyhedral approximation of [112] with a very high accuracy. This ability can be found very useful, particularly for studies where, mathematically, a linear model formulation is preferable.

Finally, the R-MISOCP model takes into account the following distributed energy resources: dispatchable generators, photovoltaics, energy storage system and electric vehicle parking lot based on the publication [8]. However, depending on the case study, these assets can be removed or other assets can be included in the R-MISOCP model without loss of generality. The next chapters, 5 - 6, present computational experiments that have been conducted in this PhD research using the R-MISOCP model in order to: a) demonstrate the impact that the accuracy of the power flow modelling has on

scheduling decisions, and b) study the effects of adjusting the budgets of uncertainty to achieve reductions in operational cost while minimising the probability of load shedding.

Chapter 5. The impact of the accuracy of the power flow model

Contents

5.1. Chapter Summary

Chapter 5 is structured as follows.

- **Section 5.2** presents the case study and modelling tools that have been used for the computational experiments of this Chapter.
- In **sections 5.3** and **5.4**, computational experiments are performed in order to demonstrate the impact that accuracy in power flow modelling has on the operational cost and the optimal scheduling decisions, and to demonstrate the risks of scheduling DER without the use of an accurate power flow formulation.
- **Section 5.5** discusses the scalability of mixed-integer second-order cone programming on electricity distribution problems according to the existing bibliography.
- **Section 5.6** concludes this chapter.

5.2. Case Study and Modelling Environment

The test network used in this chapter is a modified IEEE 33 bus radial distribution network. The topology of this network is according to [3]. The positioning of distributed energy resources follows the one presented in article [8]. The network under study is presented in figure 5.1. Network data is extracted from [3]. The demand has been modified according to feeder data from the Customer-Led Network Revolution project [4], and has been adjusted in the network buses according to the demand used in the publication [3]. The PV generation represents data from the solar PV of the Urban Sciences Building in Newcastle University UK [6] which has been modified for the case study of this research. The market price (which represents the cost to import power from the main grid) is extracted from Elexon [5]. This data is shown in figure 5.2. Dispatchable generators, energy storage systems, and electric vehicle parking lot data are extracted from the article [8], and the cost of the DGs is assumed to be equal to 54.66 £/MWh (which is a modification of the DG cost presented in [8]).

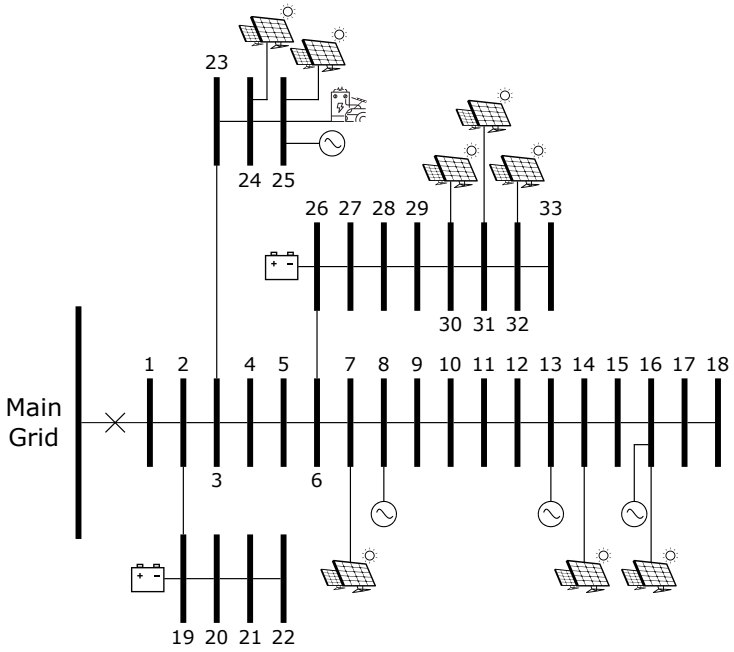

Figure 5.1: Test Network [1].

The current limits of all lines is assumed to be 400A (which has been set according to the upper limits of the first 9 lines of the IEEE-33 network of the publication [113]). DER and network data used in this research can also be found in tables C.1-A.3 of Appendix A of this thesis. Data granularity is 10-minute time intervals over a 24-hour scheduling horizon; i.e. $6\times24 = 144$ periods. The 24-hour demand is 206 MWh. Some computational experiments are performed for a network that is connected to the main grid (grid-connected operation) and some are performed for a network that is not (islanded operation), which operates in isolation from the rest of the grid between 17:00 and 20:00. The lower plot in figure 5.2 shows the duration that the network will be disconnected from the main grid using a transparent gray curtain.

Computational experiments are run using the GAMS IDE environment. Optimisation problems are solved using the CPLEX and the MOSEK solver [114]. Figures and secondary codes are produced in MATLAB (MATLAB versions used are R2017a, R2018a, and R2020b). Numerical experiments of the R-MISOCP need less than 30 seconds to run, using a desktop with an Intel Core i5-6600 CPU at 3.30 GHz and 32 GB of RAM. In the computational experiments of section 5.4, optimisation models (namely the R-MISOCP, COMP and HYBR models) are solved using the MOSEK solver and are run using a laptop with an Intel Core i7-7500 CPU at 2.70 GHz and 16 GB of RAM. Finally, to provide an estimation of the problem size, according to

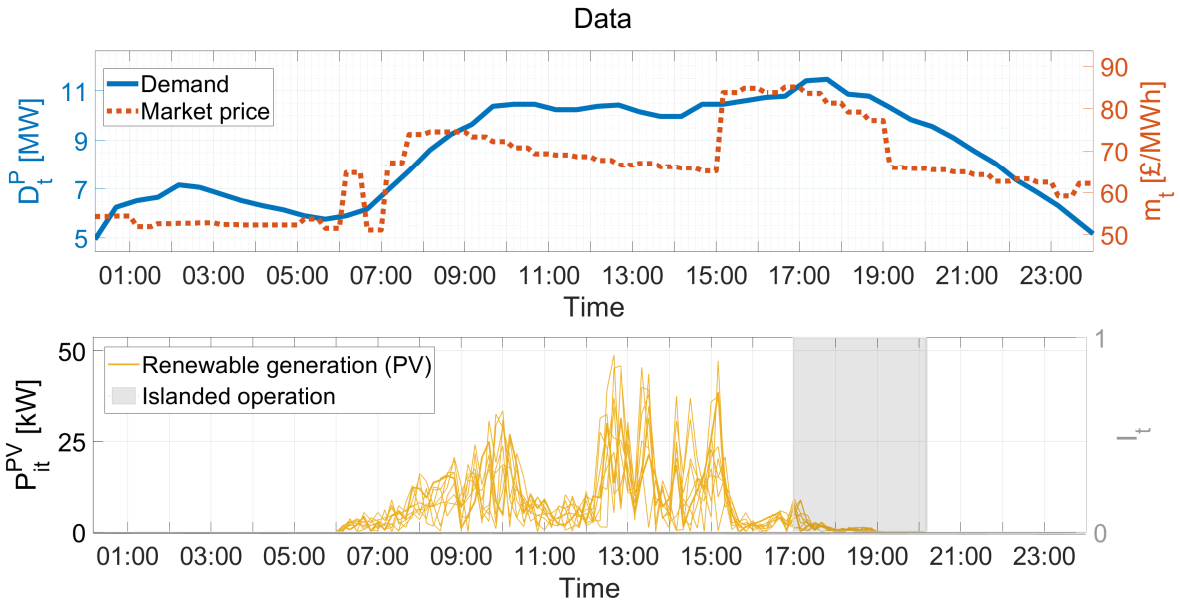

Figure 5.2: **Upper plots:** Demand (left y-axis) [3, 4]. Market price (right y-axis) [5]. **Lower plot:** PV (renewable) generation (left y-axis) [6]. Duration of islanding event (right y-axis). [1].

the statistics of the GAMS IDE environment, the R-MISOCP model of section 5.3, has 70 170 equations and 77 466 variables, out of which 2 162 are discrete variables.

5.3. A comparative study: Results and discussion

5.3.1. Introduction: The COMP model

The proposed R-MISOCP model uses the second order cone power flow formulation of [85]. In section 5.3, the R-MISOCP model is compared with an optimal scheduling model that uses a piecewise linear power flow formulation. The latter will be referred to as the COMP model (as it is the model used in this COMParative study).

As this section focuses on the power flow model formulation, the COMP model is compared to the R-MISOCP model results for all Γ equal to zero. This means that the expected values of the uncertain parameters are considered in this subsection (uncertainty is not studied in this chapter, as it is the subject of chapter 6). The COMP model is described by the same constraints to model DER as the R-MISOCP model, but differs in the power flow formulation; i.e. the COMP model does not include equations (4.14a)-(4.14h).

To preserve the comparison within day-ahead scheduling for DER connected to electricity distribution networks, the power flow model formulation of [8] is chosen for the COMP model. The power flow model of [8] is mathematically formulated as a piecewise linear model according to [115], and the linearization follows the algorithm proposed in [7]. The power flow equations for the COMP model are formulated following these studies (i.e. [8, 115, 7]). The assumption of [8], that the voltage angles between adjacent buses ($\theta_i - \theta_j$) range within $\pm 10^\circ$, is preserved. The power flow formulation used for the COMP model is presented in Appendix B of this thesis, in equations (B.2a)-(B.2g).

In the remainder of section 5.3, subsections 5.3.2 - 5.3.4, discuss the impact that the power flow formulation has on the schedules and the operational costs produced by the R-MISOCP and the COMP model. Subsection 5.3.5, also presents a discussion regarding the schedules and the operational costs produced by the R-MISOCP and the COMP model, but for a higher PV penetration compared to the one used in subsections 5.3.2 - 5.3.4.

5.3.2. Part I: Operational costs and network losses

Simulation results show that the COMP model underestimates the value of network losses, compared to the R-MISOCP model (table 5.1). In particular, for a demand of 206 MWh, the R-MISOCP model calculates that the network losses are equal to 8.1 MWh, and the COMP model calculates that the network losses are equal to 0.0046$\approx$0 MWh (table 5.1). Therefore, the R-MISOCP produces a generation mix that is 8.1 MWh higher than the COMP model (or 3.9% of the total demand). The different calculation in network losses has also resulted in the two models calculating different schedules for the generation units and therefore different operational costs. More specifically, the R-MISOCP operational cost is £12 925, whereas the COMP operational cost is £11 443; which means, that the R-MISOCP is 11.47% more expensive than the COMP model, for the network under study (table 5.1). This is elaborated below.

Network losses constitute practically an additional demand. This additional demand causes: 1) extra generation and 2) extra load shedding during the islanding event. Therefore, the network losses (which are incorporated in the R-MISOCP), manifest themselves as: 1) extra generation cost, and 2) extra load shedding cost. These

	R-MISOCP	COMP
Operational Cost	£12 925	£11 443
Cost Difference (%)	$\frac{(12\ 925 - 11\ 443)}{12\ 925}\ 100\% = 11.47\%$	
Losses	8.05 MWh	0 MWh
Load shedding	1.89 MWh	0.2 MWh

Table 5.1: RESULTS: R-MISOCP AND COMP MODEL

two costs, account for a 11.47%≈12% cost difference between the R-MISOCP and COMP model. Load shedding cost accounts for an ≈8% of this 12%. The generation cost (composed of the main grid and dispatchable generation), accounts for the remaining almost 4% difference between the two models. This is expected, since the load shedding cost is 600 [£/MWh], and the market price (used for the main grid power) varies between 51.5 - 85.1 [£/MWh] and the DG cost is 54.66 [£/MWh]. A detailed comparison between the two models in terms of their schedules and individual operational costs for the main grid, the dispatchable generators and the load shedding follows below.

5.3.3. Part II: Optimal schedules

In figure 5.3, the main grid schedules for the R-MISOCP and COMP models are shown. During times 00:00am-06:00am, when market price is low, both models draw high levels of power from the main grid. However, a visible difference is observed between the two models (particularly during 00:00am-06:00am), as the R-MISOCP schedules a lower amount of power to be drawn from the main grid than the COMP model. During the same period, the R-MISOCP model also prioritizes dispatching of the DGs as, although they are more expensive, they are electrically closer to the load at the given time window (figure 5.4). This is a result of the R-MISOCP model having a more accurate calculation of network losses.

Amongst all DGs, the schedule for DG at bus 8 differs significantly between the two models in the period 00:00am - 06:00am. This is attributed to the fact that bus 8 has a high demand, and it is located *before* the DGs at buses 13 and 16 (see figure 5.1).

In particular, the demand during 00:00am-06:00am, at buses 8, 13, 16 and 25 is: 8.40 MWh 2.52 MWh, 2.52 MWh, and 17.63 MWh respectively. During the rest of the day (i.e. from 06:00am onwards), the DG optimal schedules remain relatively similar between the two models, due to three reasons. The DG cost is lower or very close to the market price cost, the DGs have reached their upper limits (figure 5.4, and table A.1), and the demand is at its highest levels (figure 5.2).

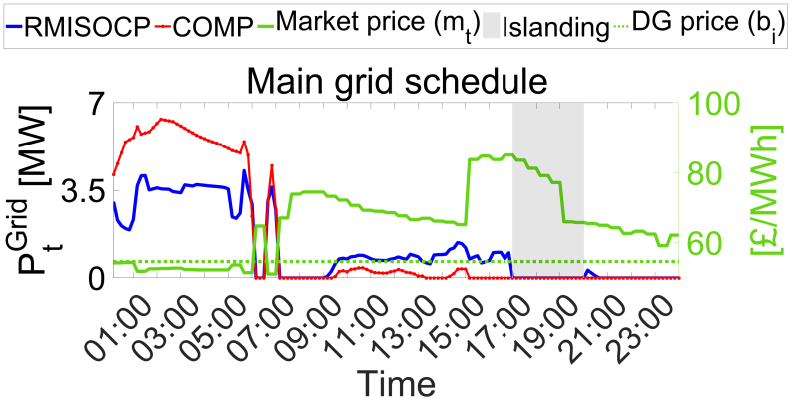

Figure 5.3: **Left y-axis:** Main grid power schedule: by the R-MISOCP model and the COMP model. **Right y-axis (green colour):** The market price and the cost of the dispatchable generators. The islanding event takes place between 17:00 and 20:00 (shown in transparent gray colour) [1].

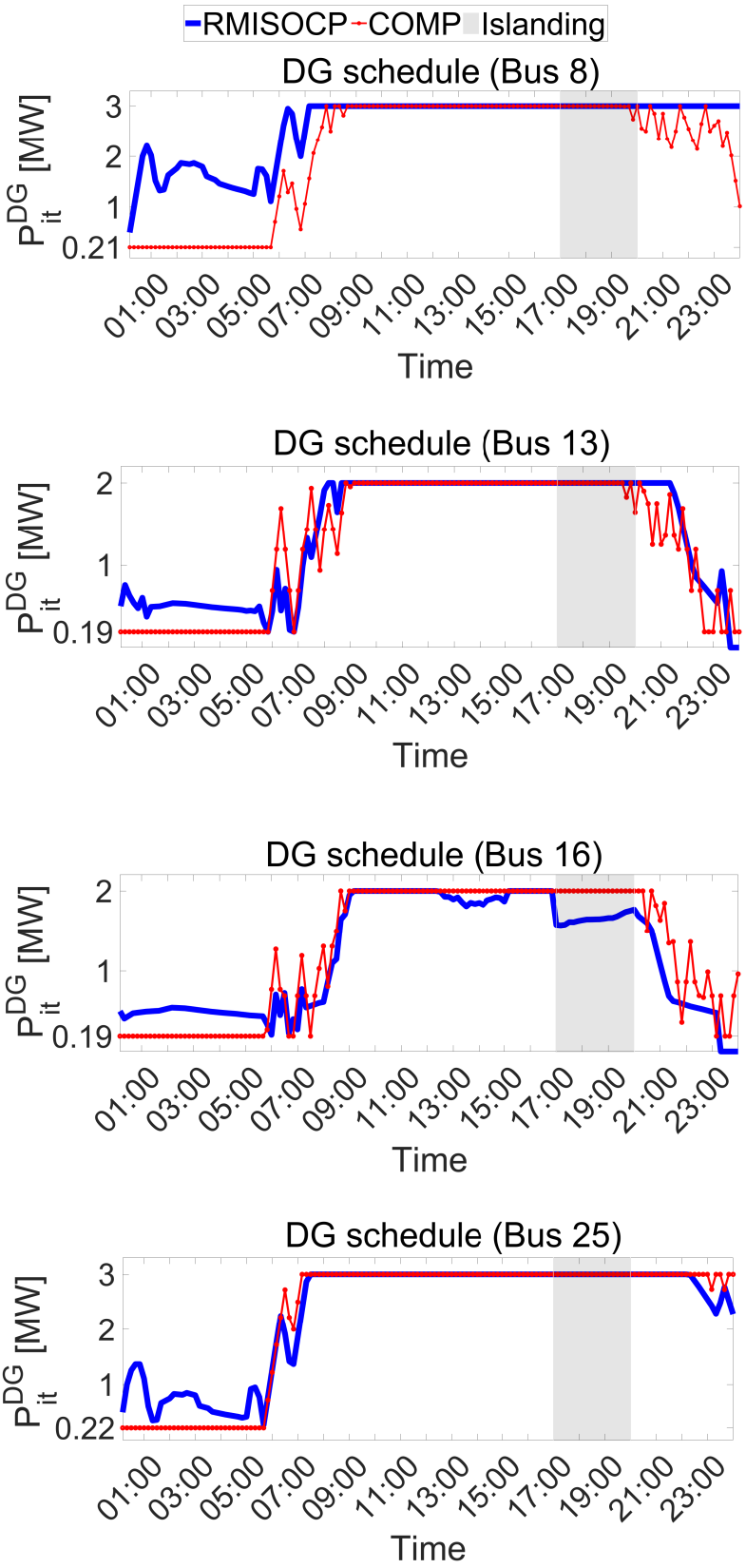

Figure 5.4: Dispatchable generation schedules by the R-MISOCP model (blue colour) and the COMP model (red colour). The islanding event takes place between 17:00 and 20:00 (shown in transparent gray colour) [1].

Figure 5.5 presents the ESS schedules for the R-MISOCP and COMP model. The ESSs are at buses 19 and 26. Bus 19 and bus 26, are both located close to the main grid bus (figure 5.1); no other generator is located between the ESSs and the main grid. ESS schedules also vary between the R-MISOCP and the COMP model, due to the calculated losses especially when discharging. In the COMP model, the dominant factor for dispatching the ESSs is market price. However, in the R-MISOCP model, the ESS schedules are affected by the occurrence of the islanding event as well (especially when discharging). This difference is noticeable between $\approx$15:00 and 20:00 (i.e. before and during the islanding event).

Figure 5.5 also presents the EV parking lot schedule for the R-MISOCP and the COMP model. The EV parking lot is located at bus 25, and EVs arrive at 8:30am and depart at 17:30, assuming that this parking lot is used within office working hours. This is shown with two thick vertical lines at figure 5.5. Simulation results show that both models schedule the EVs according to the market price. More specifically, both models discharge the EVs when the market price is high: which is shown after 15:00 until 17:30. The R-MISOCP model mainly charges the EVs when the market price is low (shown from around 12:00 midday until 15:00 with a blue line in the negative values of figure 5.5). However, the COMP model does not schedule EV charging between 8:30am and 17:30.

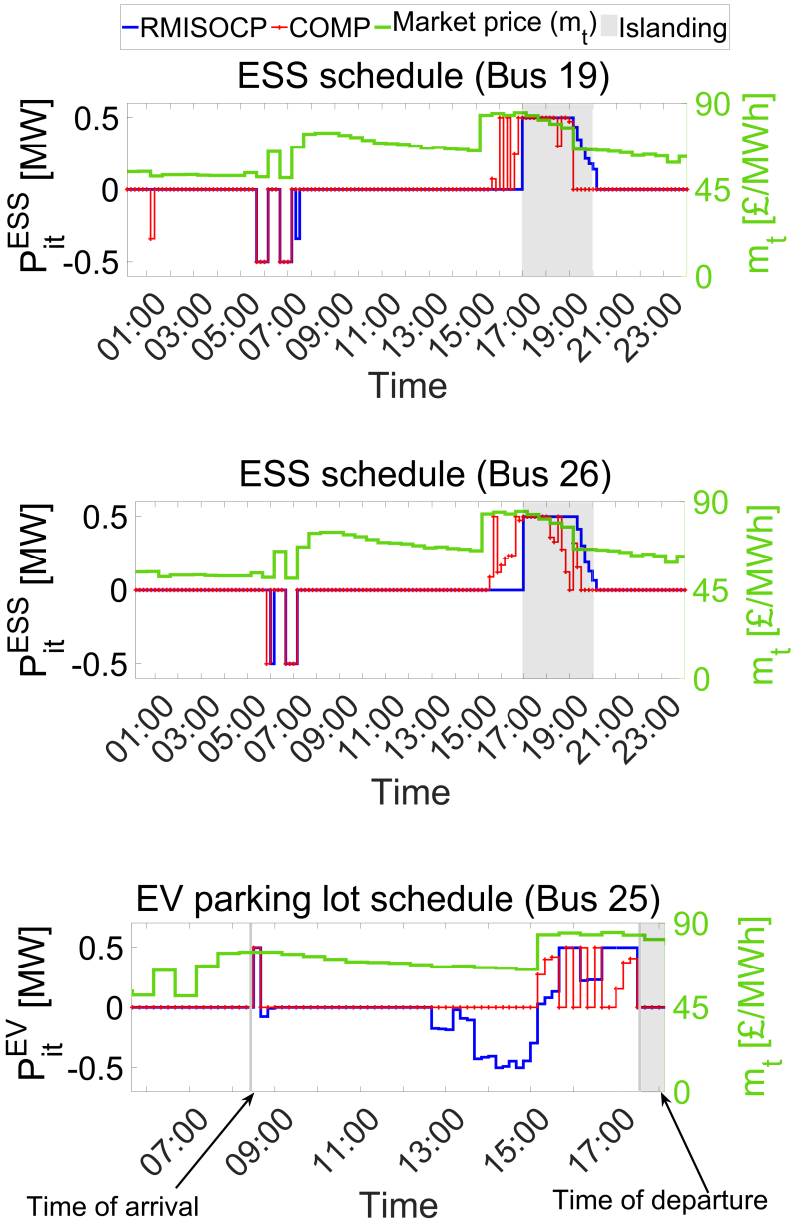

Figure 5.5: **Left y-axis:** ESS and EV parking lot schedules by the R-MISOCP (blue colour) and the COMP model (red colour). **Right y-axis (green colour):** The market price. The islanding event takes place between 17:00 and 20:00 (shown in transparent gray colour). **Positive values:** Discharge state. **Negative values:** Charge state. [1]

5.3.4. Part III: Comparing the main grid, the dispatchable generator and the load shedding costs

The operational cost (for both models) is the summation of: the main grid cost, the dispachable generators' cost, the load shedding cost, and the unit commitment cost. This means that the operational cost is affected, and also affects the schedules

produced by the generation units. These costs are shown in figure 5.6 for both the R-MISOCP and the COMP model. In these figures, the left axis (blue colour) presents the cumulative costs, and the right axis (red colour) presents the costs per time-step.

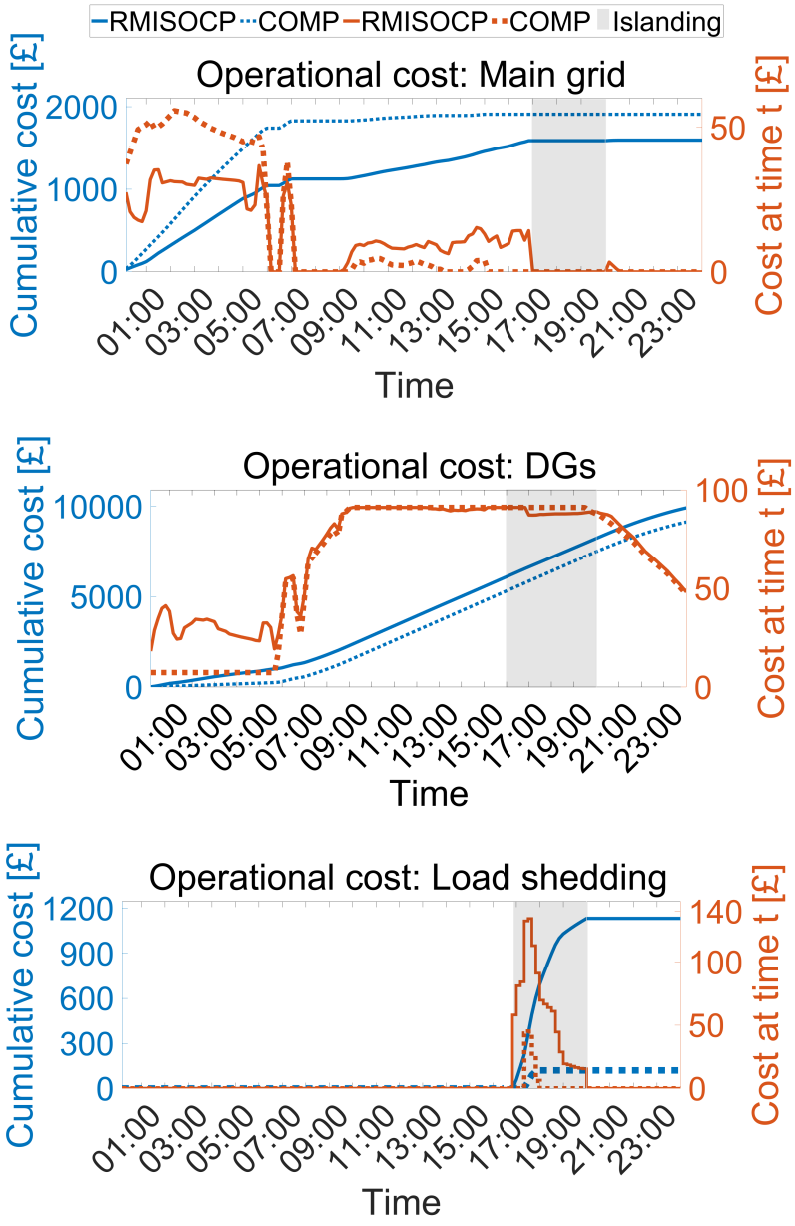

Figure 5.6: Results for both the R-MISOCP model and the COMP model. **Left y-axis** Cumulative costs. **Right y-axis:** Costs per timestep. The islanding event takes place between 17:00 and 20:00 (shown in transparent gray colour). [1]

More specifically, the fact that the COMP model schedules more power from the main grid (figure 5.3) is reflected on the cumulative main grid cost, shown in the first plot of figure 5.6. Furthermore, the R-MISOCP model uses the dispatchable generators more than the COMP model, especially during 00:00am-06:00am (figure 5.4), which is also shown in the cumulative cost of DGs in the second plot of figure 5.6.

The difference in the calculation of network losses also resulted in a lower level of load shedding by the COMP model, compared to the R-MISOCP model (third plot of figure 5.6). In particular, for a demand of 33.89 MWh during the time of the islanding (17:00 - 20:00), the R-MISOCP sheds 1.89 MWh and the COMP model sheds 0.2 MWh. As explained earlier, the network losses constitute practically an additional demand. This additional demand results in the need of a higher generation. Therefore, the R-MISOCP model needs to schedule DER to cover both the demand and network losses to supply this demand. However, as the on-site generation does not suffice in order to cover the demand plus the network losses, the R-MISOCP sheds more loads than the COMP model during the islanding event.

For a load shedding cost of $c_{i,t}^{Shed}$=£600/MWh, the cumulative cost due to load shedding, for both models, is shown in the third plot of figure 5.6. Finally, the total unit commitment cost throughout the 24-hour scheduling horizon is the same for both models, and equal to £280.1. This is expected as, for both cases, DGs start-up at 00:00am and operate continuously throughout the day (figure 5.4).

It is noted that the load shedding cost varies remarkably in the literature (for example, from 475.18 [£/MWh] in [116], to 16 940 [£/MWh] in [117]). The value for this research was chosen according to computational experimentation, in order for loads not to be shed unless the generation cannot meet the demand, which is the cost for load shedding also used in the thesis [118], i.e. 600 £/MWh [1].

[1] This can be found for the residential load presented in table 4.1 of page 61 in [118] which is 0.846 [$/kWh]. For a conversion of 1 GBP = 1.41 USD, this is 0.846 [$/kWh] = 846 [$/MWh] = $\frac{846[\$/MWh]}{1.41\$/£}$ = 600 [£/MWh].

5.3.5. A case study with a higher PV penetration

Finally, inspired by the upcoming changes in future electricity distribution networks, one more set of results is presented hereby in order to test the impact of an accurate power flow model. In this experiment, the network is connected to the main grid at all times, and the PV generation is 20 times higher than the one used in the set of experiments above. This level of PV generation is chosen based on the 2050 Distribution Future Energy Scenario (DFES) for the city of Newcastle upon Tyne (UK) by Northern Powergrid [2], and has been adjusted for the case study of this section.

For this set of experiments, figures 5.7 and 5.8 present the optimal schedules for both models. The main difference between the two models can be seen in the schedules of the DG at bus 8 and the main grid (shown in the first plots of figures 5.7 and 5.8), which is due to the fact that the R-MISOCP model takes into account network losses, whereas the COMP model not (as explained in the discussion above for the DG at bus 8 and the main grid). The ESS and the EV parking lot optimal schedules (shown in figure 5.8), have similar discharging patterns in both models. Discharging of the ESSs and the EV parking lot takes place during the times that the market price is high, and the charging when the market price is low. However, the two models do not have similar charging schedules, which is particularly shown around 5:30am-7:00am in the ESS charging schedules by the R-MISOCP model (blue line, in the negative values of the ESS schedules of figure 5.8), and around 8:30am-10:30am in the EV charging schedule of the R-MISOCP model (blue line, in the negative values of the ESS schedules of figure 5.8).

[2]This DFES can be found in the website `https://odileeds.github.io/northern-powergrid/2020-DFES/`, which was accessed on 25th June 2021.

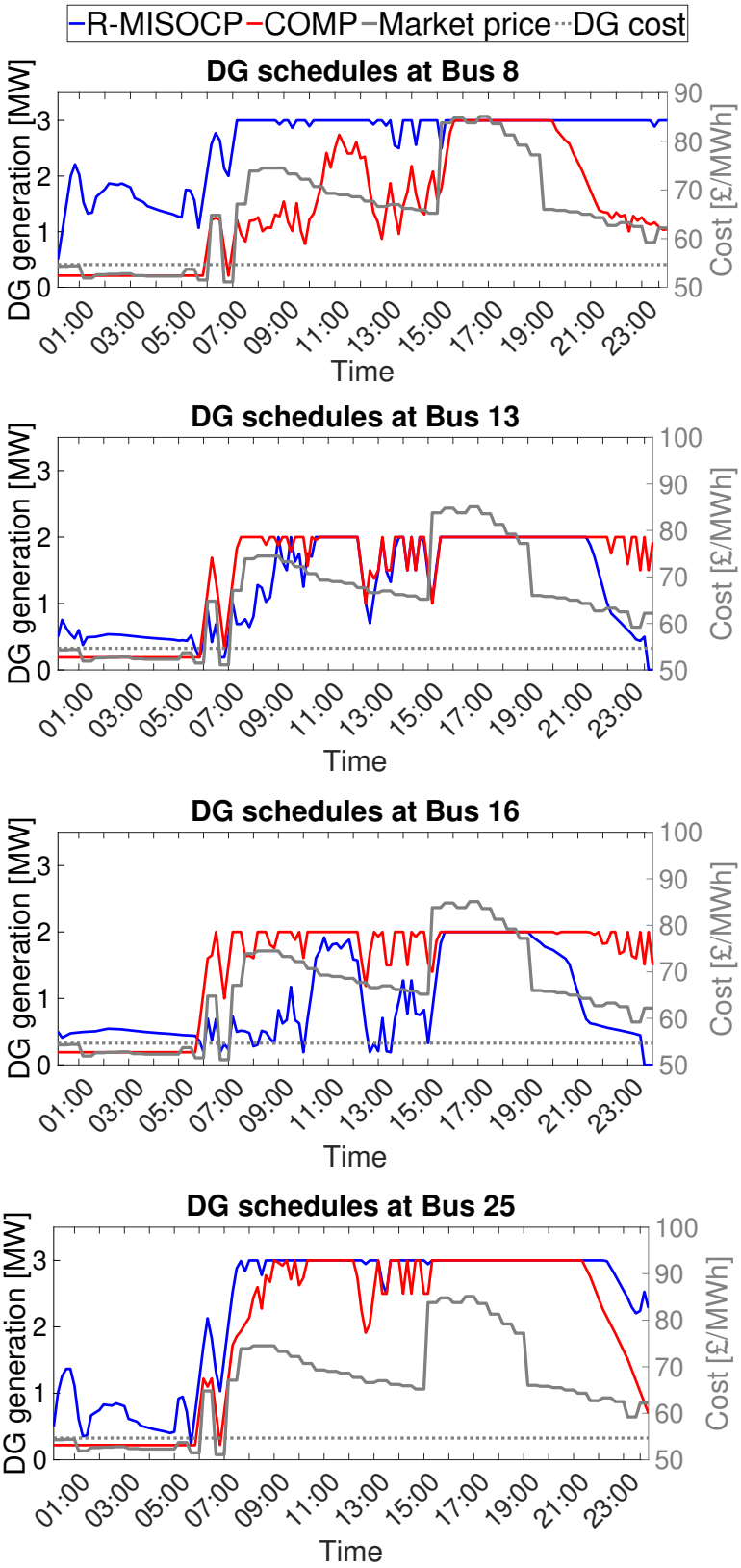

Figure 5.7: **Left y-axis:** Optimal schedules for the main grid and the dispatchable generators by the R-MISOCP and COMP model. **Right y-axis (gray colour):** Market price and the cost of the dispatchable generators. Islanding event (17:00-20:00): shown in transparent gray colour.

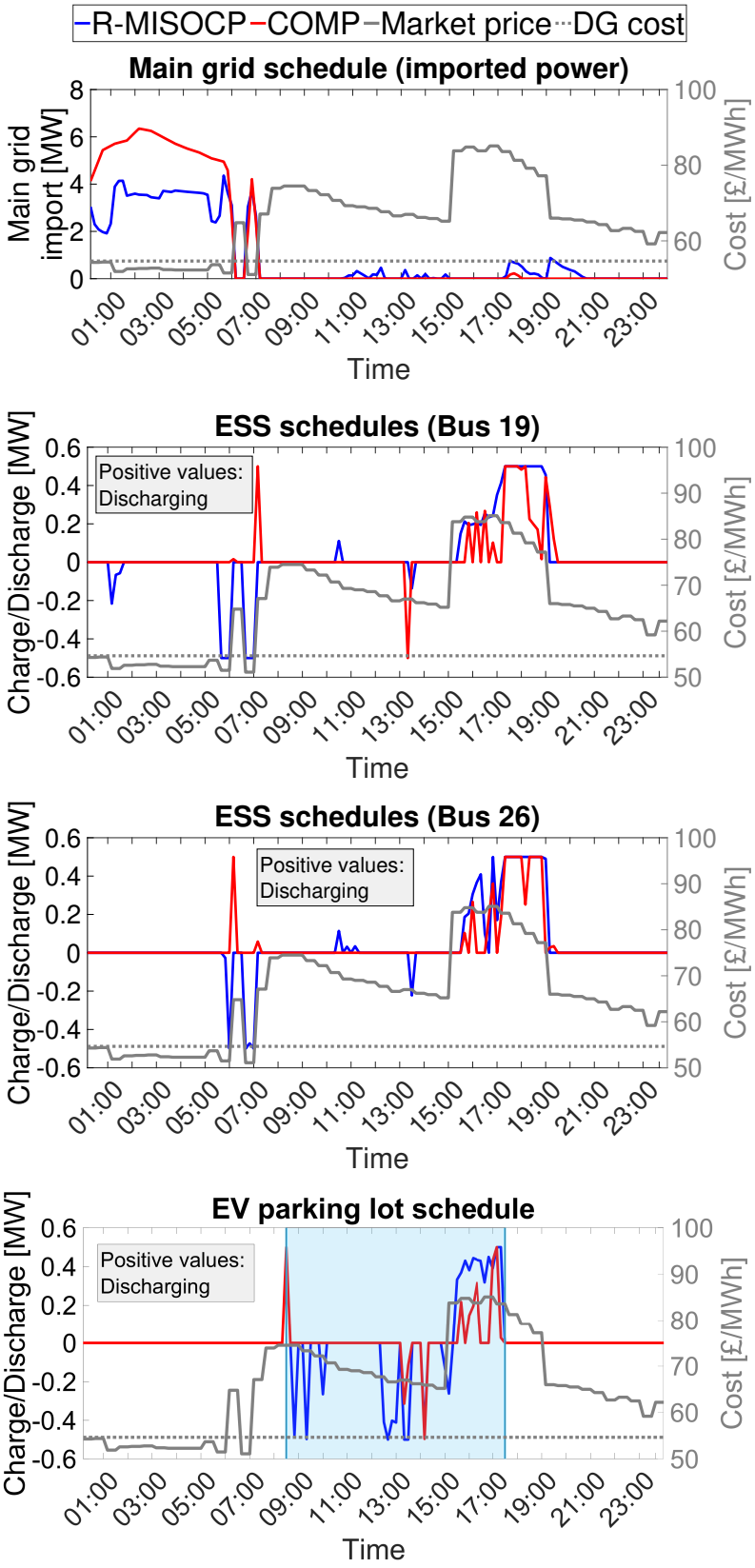

Figure 5.8: **Left y-axes:** ESS and EV parking lot optimal schedules by the R-MISOCP (blue colour) and COMP (red colour) model. **Last plot:** EVs operate from 8:30-17:30 (shown with a light blue curtain). **Right y-axes (gray colour):** Market price and DG cost.

In terms of costs, the R-MISOCP model calculates that the operational cost is £10 884 and the COMP model £10 423. These operational costs are closer compared to the costs of the previous comparative study, as in this case study the R-MISOCP model is 4.23% more expensive than the COMP model (compared to the 12% difference that the two models had in the previous case study). A reduction in the operational cost in this case study in both models (compared to the previous experiments) is expected, since the penetration of PV generation is higher in than the previous case study and has no cost. The smaller difference between the two models is attributed to the fact that in this grid-connected case study no load shedding took place. However, the COMP model does not account for network losses, and the R-MISOCP calculates that the network losses are almost 7 MWh in this study where PV penetration is high. This means that in the actual operation, where network losses actually occur, the operational cost of the COMP model would be expected to be higher than the current cost of £10 423, since network losses manifest themselves as extra generation (this is also discussed in the next section).

In terms of the optimal DER schedules, this last set of computational experiments shows that, there is not a direct connection between the optimal DER schedules calculated by the R-MISOCP model (which accounts for network losses) and the COMP model (which does not account for network losses), regardless of the proximity of their operational costs. This shows that there does not seem to exist a "corrective action" that can be performed on the optimal DER schedules calculated by the COMP model in order to extract the R-MISOCP model results, and that an accurate power flow model needs to be taken into account *within* the decision-making process of the optimal DER scheduling problem, rather than retrospectively.

To conclude, the computational experiments of this section show that the incorporation of network losses in the power flow model can impact both the operational cost and calculation of generation schedules. For the network under study in particular, this has resulted in the following main differences between the two models. First, in terms of the operational costs, the R-MISOCP is 12% more expensive than the COMP model, since accounting for network losses in the R-MISOCP results in increased generation and increased load shedding. Second, in terms of the day-ahead schedules, the COMP model schedules, are mainly driven by the cost

of generation, whereas the R-MISOCP schedule calculations, apart from the cost of generation, are also sensitive to the electrical location of the generation units. Furthermore, the simulations of this section show that there does not seem to exist a specific pattern between the optimal schedules calculated by a model that accounts for network losses and one that doesn't, regardless of their operational costs. Therefore, these experiments indicate that an accurate power flow model needs to be taken into account within the optimal DER scheduling problem, and not retrospectively using a type of "corrective action" to the optimal schedules which did not account for network losses.

5.4. The risk of constraint violations

The previous section presented a comparative study between two models, namely the R-MISOCP and the COMP model, which are using different formulations to represent the power flow equations. The R-MISOCP model takes into account network losses to calculate the optimal DER schedules, whereas the COMP model not. In the previous section, the comparative study focused on the operational costs, the optimal DER schedules, and the network losses calculated by these two models. This section aims to extend these computational experiments and study: *How would the network operation be affected if the optimal DER schedules of the COMP model were implemented in conditions where network losses are taken into account?*

In order to test this, the optimal schedules calculated by the COMP model (which does not account for network losses) are inserted as fixed parameters in the R-MISOCP model (which accounts for network losses). Using the first case study of section 5.3 (i.e. the case study of subsections 5.3.1-5.3.4), these are the optimal schedules of the energy storage system (for both charging and discharging), the electric vehicle parking lot optimal schedules (for both charging and discharging), and the dispatchable generators. The R-MISOCP model that uses the COMP model optimal schedules will be referred to as *HYBR* model, as it is a hybrid model which has the mathematical formulation of the R-MISOCP model, and uses the COMP model optimal DER schedules. Two sets of computational experiments are run for the HYBR model. Scenario 1, runs a business-as-usual case study, i.e. where there is only

grid-connected operational mode. Scenario 2, runs the first case study of the previous section, i.e. where the network is expected to be islanded from 17:00 to 20:00.

Overall, in the computational experiments below it is shown that the R-MISOCP model results in a technically better performing network compared to the COMP model. In particular, it is shown that implementing the optimal DER schedules calculated by the COMP model in conditions where network losses are taken into account, resulted in violations of technical constraints and load shedding.

Scenario 1

Table 5.2 presents the operational cost, the network losses, and the load shedding calculated by the COMP, the R-MISOCP model, and the HYBR model. It is shown, that there is a significant increase in the HYBR operational cost of 17.52% compared to the R-MISOCP model, as the R-MISOCP model calculates a cost of £11 908, and the HYBR model calculates cost of £14 437 (whereas the COMP model calculated that the operational cost is £11 338). This is attributed to the fact that the HYBR model accounts for network losses, whereas the COMP model doesn't, and therefore needs to produce a higher generation. Also, even though in this scenario the network operates only in the grid-connected mode, the HYBR model calculates load shedding which is equal to 4.58 MWh. This happened in order to avoid a violation of the line current constraints in lines 1-2 and 2-3 of the network (the network topology is shown in figure 5.1), as it is explained below.

The computational experiments show that the HYBR model reaches the upper limits of the line current in line 1-2 from ≈00:00 to ≈06:00, which is shown in figure 5.9. The upper plot of figure 5.9 presents the line currents calculated by the initial R-MISOCP model, and it is shown that they are not equal or close to reaching their upper limits

	COMP	R-MISOCP	HYBR
Operational Cost	£11 338	£11 908	£14 437
Losses	0 MWh	8.084 MWh	8.58 MWh
Load shedding	0 MWh	0 MWh	4.58 MWh

Table 5.2: SCENARIO 1: GRID-CONNECTED MODE

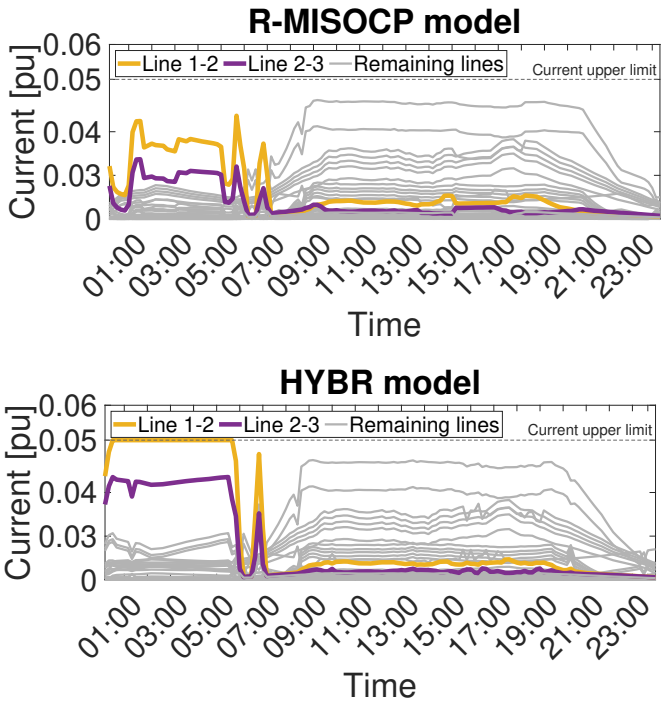

Figure 5.9: **Scenario 1 - Grid-connected mode.** General Description: Line current for all lines of the network in figure 5.1. Lines 1-2 and 2-3 are shown with two thicker lines for clarity. **Upper Plot:** R-MISOCP model results. **Lower Plot:** HYBR model results.

in any of the network lines. However, the HYBR model, in the lower plot of figure 5.9, reaches the upper limits of the line current in line 1-2 between ≈00:00 until ≈06:00. Line 2-3, is also significantly increased but does not reach its upper current limits (lines 1-2 and 2-3 are plotted with a thicker line compared to the other line currents). As the COMP model results did not account for network losses, the optimal schedules for the three sets of assets used in the HYBR model were calculated in order to satisfy only the network loads. Therefore, the network losses would be supplied by the power which is imported from the main grid. However, the upper limits of the line current for line 1-2 do not allow all the required power from the main grid to be imported, and this results in some loads being shed, which are equal to 4.58 MWh.

Scenario 2

In scenario 2, the network is islanded from 17:00 to 20:00. The COMP, the R-MISOCP, and the HYBR model results for the operational cost, the network losses and the load shedding are presented in table 5.3. It is shown that, in this scenario as well, there

is a significant increase in the operational cost of the HYBR model, compared to the R-MISOCP model. In particular, the R-MISOCP model has an operational cost of £12 925 and the HYBR model an operational cost of £15 877 (whereas the COMP model calculated that the operational cost is £11 443). This is equal to an increase of 18.59%. As in scenario 1 above, this is also attributed to the fact that the HYBR model accounts for network losses, whereas the COMP model, whose DER optimal schedules are used to run the HYBR model, doesn't account for network losses.

There is also a significant increase in the load shedding, from 0.2 MWh in the COMP model, to 7.21 MWh in the HYBR model. The R-MISOCP model has a higher amount of load shedding compared to the COMP model, which occurs only during the period that the network is islanded, and is equal to 1.89 MWh (but is still significantly less than 7.21 MWh). The additional load shedding in scenario 2, also occurs in order to avoid violation of the line current limits in line 1-2 (figure 5.10). In the upper plot of figure 5.10, it shown that the line currents calculated by the R-MISOCP model are not equal or close to reaching their upper limits in any of the network lines. However, in the lower plot of figure 5.10, which shows the line current calculated by the HYBR model, the line current limits are very high and equal to their upper limits between ≈00:00-06:00.

To conclude, this section presents a comparative study in order to study the effect of the optimal schedules that are calculated without taking into account network losses in the operation of the network. In this comparative study, the R-MISOCP model results are compared with the COMP model results, and with the HYBR model. The *HYBR* model, is a hybrid model which has the mathematical formulation of the R-MISOCP model but uses the COMP model optimal DER schedules. Two scenarios were tested: one where the network is operating connected to the main grid, and one where the network is operating is isolation from the main grid from 17:00-20:00. It is found that, in both scenarios, the HYBR model not only had a higher operational cost compared to the R-MISOCP model, but it also shed loads in order to avoid a violation of the constraints set for the line currents. Also, the HYBR model has a significantly higher cost of operation compared to the R-MISOCP model, which in these computational experiments was 17.52% higher when operating in grid-connected mode (scenario 1) and 18.59% higher when the network was islanded between 17:00 and 20:00 (scenario 2).

	COMP	R-MISOCP	HYBR
Operational Cost	£11 443	£12 925	£15 877
Losses	0 MWh	8.05 MWh	8.85 MWh
Load shedding	0.2 MWh	1.89 MWh	7.21 MWh

Table 5.3: SCENARIO 2: ISLANDED MODE FROM 17:00 TO 20:00

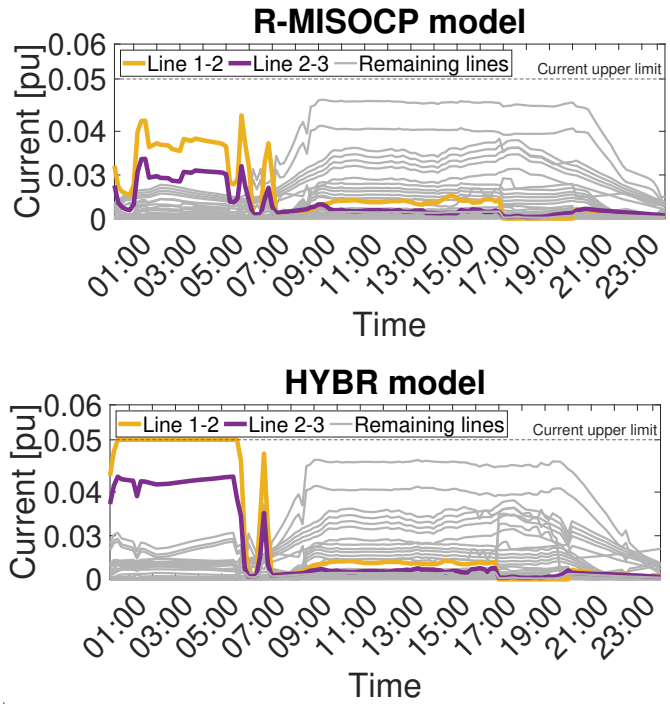

Figure 5.10: **Scenario 2 - Islanded mode 17:00-20:00.** General Description: Line current for all lines of the network in figure 5.1. Lines 1-2 and 2-3 are shown with two thicker lines for clarity. **Upper Plot:** R-MISOCP model results. **Lower Plot:** HYBR model results.

5.5. Model scalability

The simulations in this work are performed on the IEEE 33-bus electricity distribution network which is a test network that has been widely used in relevant studies, such as in [8, 28, 42, 50, 52]. However, models that are mathematically formulated using mixed-integer second-order cone programming (MISOCP) can also be used in

larger electricity distribution networks which would result in larger power distribution problems. This has been shown by relevant studies in the literature that propose models using MISOCP and have implemented their computational experiments on cases ranging from 69- to 1300-bus distribution networks.

In particular, the study in [49] proposes an MISOCP model which is tested, apart from the IEEE 33-bus network, on the IEEE 69-bus network. The study in [52] proposes an MISOCP model and uses the IEEE 33-bus and the IEEE 123-bus network for its computational experiments. The study in [48] proposes an MISOCP model and uses a 135-bus network and a 540-bus distribution network. Finally, the study in [55] proposes an MISOCP model, using the 84-bus 11.4 kV Taiwan Power Company (TPC) distribution system, and the IEEE 119-bus and IEEE 1300-bus systems.

5.6. Conclusions

This chapter presents computational experiments for the Robust Mixed-Integer Second Order Cone Programming model of this work for the optimal day-ahead scheduling problem. The main focus of the computational experiments is to demonstrate the impact of an accurate power flow model on the operational cost and scheduling decisions.

In terms of the operational costs, for the network under study, comparing the proposed model with a model that uses a piecewise linear power flow formulation that does not take into account network losses, this underestimation is found to be 11.47%. In terms of the optimal DER schedules, it is shown that when network losses are not taken into account, the scheduling decisions are mainly driven by the cost of generation units, whereas, when accounting for network losses, the scheduling decisions are sensitive to both the cost of on-site generators and their electrical location within the network. Also, the computational experiments hereby suggest that there does not seem to exist a “corrective action” that can be applied on the optimal DER results which are calculated without considering network losses, in order to extract the R-MISOCP model results, regardless of the proximity of the operational costs between the COMP and the R-MISOCP model. This means, that the accurate power flow model needs to be taken into account within the decision-making process

of the optimal DER scheduling, rather than retrospectively. Finally, it was shown that taking into account an accurate power flow model which accounts for network losses in the optimal DER scheduling problem, is important in order to avoid constraint violations, as network losses basically constitute an additional demand that could lead to load shedding in order to respect the technical constraints of the network.

Chapter 6. The impact of uncertainty

Contents

6.1. Chapter Summary

Chapter 6 is structured as follows.

- **Section 6.2** presents the case study and modelling tools that have been used for the computational experiments of this Chapter.
- **Section 6.3** presents numerical simulations which test the benefits of the uncertainty modelling approach used in the R-MISOCP model for the optimal day-ahead scheduling problem. In particular, it aims to present the impact of the uncertain parameters on the operational cost and load shedding, by showing results for a range of combinations for the budgets of uncertainty, and to present a case study which shows how to choose the budgets of uncertainty.
- **Section 6.4** discusses the scalability of robust mixed-integer second-order cone programming on electricity distribution problems according to the existing bibliography.
- **Section 6.5** concludes this chapter.

6.2. Case Study and Modelling Environment

The test network used is the modified IEEE 33 bus radial distribution network following DER positioning of [8], presented in Fig. 5.1 of the previous chapter. Network data is extracted from [119]. DGs, ESSs, EV parking lot data are extracted from [8]. The cost of DGs is set to 54.66 [£/MWh] (which is a modification of the DG cost presented in [8]). This data is given in detail in Appendix A of this thesis. Data granularity is 10-minute time intervals over a 24-hour scheduling horizon; i.e. $6 \times 24 = 144$ periods. The nominal values of the uncertain parameters are presented in Fig. 5.2; namely market price, renewable generation, demand, and islanding event. Total 24-hour demand is 206 MWh. Market price, renewable generation (PV), and demand uncertainty are set to $\pm 10\%$ [27]. The islanding event takes place at 5pm-8pm with an hour window of uncertainty, i.e. (5pm$\pm$30 minutes)-(8pm$\pm$30 minutes). GAMS IDE environment and the MOSEK solver are used for optimization problems [114]. Figures and secondary codes are produced in MATLAB R2017a, R2018a and R2020b.

In the following section, computational experiments are performed in order to study the effects of adjusting the budgets of uncertainty to achieve reductions in operational cost while minimizing the probability of load shedding.

6.3. Choosing the budgets of uncertainty

This subsection aims to show how the DSO and/or MG operator can choose the budgets of uncertainty according to performance criteria. The aim of the R-MISOCP model is to minimize operational costs. Operational costs include DG generation cost, unit commitment costs, main grid import costs, and the cost for load shedding.

Load shedding takes place during the islanded operation if there is insufficient on-site generation to supply the demand. The four sets of uncertain data with their respective budgets of uncertainty are the following: market price with $\Gamma^{M} \in [0, 144]$, demand with $\Gamma_{t}^{D} \in [0, 1]$, renewable generation (PV) with $\Gamma_{t}^{RG} \in [0, 1]$, and islanding duration with $\Gamma^{I} \in \{0, 6\}$. The upper limit of the auxiliary budgets of uncertainty used in the islanding event uncertainty are set to $\overline{\gamma^{I,Left}} = 3$ and $\overline{\gamma^{I,Right}} = 3$.

For any value of the uncertain parameters within the boundaries defined by these budgets of uncertainty, the DSO and/or MG operator is guaranteed that the actual operational costs and load shedding will not exceed the predicted values calculated by the R-MISOCP model. For example, if $\Gamma_{t}^{D} = 1$, then it is guaranteed that for any value of the demand between D_{it}^{P} and $D_{it}^{P} + 10\% D_{it}^{P}$ $\forall i \in \Omega_{B}, t \in \Omega_{T}$, the actual operational costs and load shedding will not exceed the predicted values calculated by the R-MISOCP model. Otherwise, if $\Gamma_{t}^{D} = 0$, then no uncertainty in the values of the demand is considered, and there is no guarantee that the actual operational costs and load shedding will not exceed the predicted values calculated by the R-MISOCP model.

The ranges of the budgets of uncertainty for market price, demand, and renewable generation, depend on the number of uncertain parameters per constraint, as shown in [87] or Chapter 3 of this thesis. For example, the budget of uncertainty for market price takes values in $\Gamma_{t}^{D} \in [0, 144]$, since there are up to 144 uncertain parameters of the market price in each constraint (4.10) (as this study uses 10-minute data, that result in 144 time steps). The range of the budget of uncertainty for the islanding event

depends on the uncertainty in the duration of the islanding event, and represents the number of uncertain time periods. For example, if Γ^{I} = 6, the islanding event duration is increased by six 10-minute time periods, i.e. the islanding event occurs between 16:30 and 20:30, instead of 17:00-20:00.

However, considering the upper limits of the budgets of uncertainty can lead to conservative solutions. Therefore, the simulations below focus on how to adjust the budgets of uncertainty in order to reach a desirable trade-off between: the level of uncertainty considered, and the day-ahead operational cost and load shedding levels.

In this subsection, the appropriate levels of the parameters Γ are evaluated according to the probability of underestimating operational cost (PoU) and the probability of load shedding (PLS):

- PoU is the probability that the actual cost of operation, when considering data perturbations within the full range of uncertainty, will exceed the day-ahead operational cost calculated by the R-MISOCP model.

- Respectively, PLS is the probability that the actual load shedding will exceed the load shedding calculated by the R-MISOCP model, again when considering data perturbations in the full range of uncertainty.

In this work, loads are shed at a cost during the islanding period. However, the DSO and/or MG operator can choose the budgets of uncertainty appropriately in order to ensure that this will be limited while preserving an overall low operational cost. First, the sensitivity of the optimal day-ahead operational cost and load shedding against the four uncertain sets of data are tested. Optimal day-ahead operational cost and load shedding range from: £12 925 with 1.89 MWh, which represents <1% of total 24-hour demand, when accounting for no uncertainties (all Γ =0); up to £16 551 with 5.89 MWh, which represents <3% of total 24-hour demand, when accounting for the full range of uncertainty (fully robust case). Therefore, the DSO and/or MG operator is presented with a significant range of options regarding trade-offs between the tolerance of uncertainty, and the day-ahead operational cost and load shedding levels.

According to table 6.1, two of the parameters that profoundly impact the day-ahead cost of operation and the load shedding are: the Γ_{t}^{D} for demand uncertainty, and Γ^{I} for islanding duration uncertainty. As Γ^{M} and Γ_{t}^{RG} do not largely affect the performance for

Γ_t^D	Γ^I	Γ^M	Γ_t^{RG}	**Day-ahead operational cost**	**Load shedding [MWh]**
0	0	0	0	**£12 925**	**1.89**
1	0	0	0	£15 670	4.53
0	6	0	0	£13 239	2.49
0	0	144	0	£13 024	1.89
0	0	0	1	£12 931	1.89

Table 6.1: MODEL SENSITIVITY TO BUDGETS OF UNCERTAINTY

this case, it is chosen to tolerate for these the maximum uncertainty, i.e. the maximum budgets of uncertainty are assigned for these parameters.

The levels of PoU and PLS are calculated for 21 combinations of $\Gamma_t^D - \Gamma^I$ using the BoU algorithm presented in section 3.3.2, chapter 3 (tables 6.2-6.3). The PoU and PLS are calculated by running 10 000 Monte Carlo simulations for each combination. Each iteration of the Monte Carlo simulations runs a power flow model where the inputs are: the R-MISOCP schedules (for the DGs, ESSs, and EV parking lot), and the random yields of demand spanning within its minimum and maximum limits (i.e. $D_{it}^P \pm 10\% D_{it}^P \ \forall i \in \Omega_B, t \in \Omega_T$), for Γ^I={0, 3 or 6}. PoU is calculated as the fraction of the number of times that the actual operational cost (produced by the Monte Carlo iterations) exceeds the R-MISOCP day-ahead operational cost, over the total number of iterations. Similarly, PLS is calculated as the fraction of the number of times that the load shedding (produced by the Monte Carlo iterations) exceeds the R-MISOCP load shedding, over the total number of iterations. Power flow simulations are run using the software package of MATPOWER [9]. For the 21 combinations of $\Gamma_t^D - \Gamma^I$, the R-MISOCP day-ahead operational cost and load shedding values are presented in tables 6.4 and 6.5 respectively, and the PoU and PLS results in tables 6.2 and 6.3 respectively.

Γ_t^D	$\Gamma^I = 0$	$\Gamma^I = 3$	$\Gamma^I = 6$ (max)
0	49.71%	49.59%	50.97%
0.001	43.46%	42.29%	42.57%
0.005	16.94%	16.51%	16.43%
0.01	3.32%	2.75%	2.62%
0.02	0.01%	0.02%	0.01%
0.03	**0%**	0%	0%
1 (max)	0%	0%	**0%**

Table 6.2: POU ($\Gamma^M = 144$, $\Gamma_t^{RG} = 1$) [1]

Γ_t^D	$\Gamma^I = 0$	$\Gamma^I = 3$	$\Gamma^I = 6$ (max)
0	49.51%	49.71%	50.61%
0.001	45.82%	44.46%	44.30%
0.005	27.52%	25.77%	24.41%
0.01	11.55%	9.77%	8.62%
0.02	0.81%	0.49%	0.27%
0.03	**0%**	0%	0%
1 (max)	0%	0%	**0%**

Table 6.3: PLS ($\Gamma^M = 144$, $\Gamma_t^{RG} = 1$) [1]

Γ_t^D	$\Gamma^I = 0$	$\Gamma^I = 3$	$\Gamma^I = 6$ (max)
0	£13 031	£13 169	£13 342
0.001	£13 039	£13 182	£13 351
0.005	£13 077	£13 222	£13 393
0.01	£13 123	£13 272	£13 445
0.02	£13 217	£13 371	£13 550
0.03	**£13 310**	£13 471	£13 657
1 (max)	£15 849	£16 183	**£16 551**

Table 6.4: DAY-AHEAD OPERATIONAL COST ($\Gamma^M = 144$, $\Gamma_t^{RG} = 1$) [1]

Γ_t^D	$\Gamma^I = 0$	$\Gamma^I = 3$	$\Gamma^I = 6$ (max)
0	1.88 MWh	2.15 MWh	2.49 MWh
0.001	1.89 MWh	2.17 MWh	2.50 MWh
0.005	1.93 MWh	2.20 MWh	2.54 MWh
0.01	1.97 MWh	2.25 MWh	2.59 MWh
0.02	2.05 MWh	2.34 MWh	2.69 MWh
0.03	**2.13 MWh**	2.44 MWh	2.80 MWh
1 (max)	4.52 MWh	5.17 MWh	**5.89 MWh**

Table 6.5: LOAD SHEDDING ($\Gamma^M = 144$, $\Gamma_t^{RG} = 1$) [1]

In order to account for data perturbations in all the range of uncertainty, the DSO and/or MG operator would operate the network in a fully robust case for a cost of £16 551 (table 6.4), with a PoU=0% probability of exceeding this cost during the actual operation (table 6.2), and a PLS=0% probability of shedding more loads than 5.89 MWh (tables 6.3 and 6.5 respectively). However, by selecting Γ_t^D =0.03, Γ^I =0, Γ^M =144 and Γ_t^{RG} =1 for the R-MISOCP model, it can be guaranteed that the load shedding will not exceed 2.13 MWh (table 6.5) with a probability which is also 0% (table 6.3), for a significantly lower operational cost of £13 310, with an also 0% probability of exceeding this cost during the actual operation (table 6.2).

These computational experiments result in the following two conclusions.

1. By adjusting the budgets of uncertainty, the DSO and/or MG operator can achieve a $\frac{\text{£16 551–£13 310}}{\text{£16 551}}$ = 19.58% reduction in the day-ahead operational cost, compared to a fully robust schedule. The data for this calculation has been extracted from the values that have been highlighted in gray colour in table 6.4.

2. Moreover, the R-MISOCP model can guarantee $\frac{\text{5.89MWh–2.13MWh}}{\text{5.89MWh}}$ = 63.83% lower load shedding compared to a fully robust schedule, while preserving a 0% probability of additional load shedding during the actual operation. The data for this calculation has been extracted from the values that have been highlighted in gray colour in table 6.5.

Finally, the results of the Monte Carlo simulations are also visually presented in figures 6.1-6.4 below for four representative levels of the PoU: 49.71%, 16.51%, 2.62%, and 0% (shown in tables 6.2 and 6.4). In particular, figure 6.1, presents the results for the budgets of uncertainty Γ_t^D =0, Γ^I =0, Γ^M =144 and Γ_t^{RG} =1. For these values, the blue dots show the 10 000 different values that represent the actual operational costs found by the Monte Carlo simulations. The day-ahead cost calculated by the R-MISOCP model is shown with a red line, in the centre of the plot. This means that around half of the actual (real-time) costs are above the operational cost which is calculated by the R-MISOCP model (which is £13 031), and around half of these actual (real-time) costs are below the operational cost which is calculated by the R-MISOCP model (which is £13 031), which corresponds to the value of the PoU being: PoU = 49.71%.

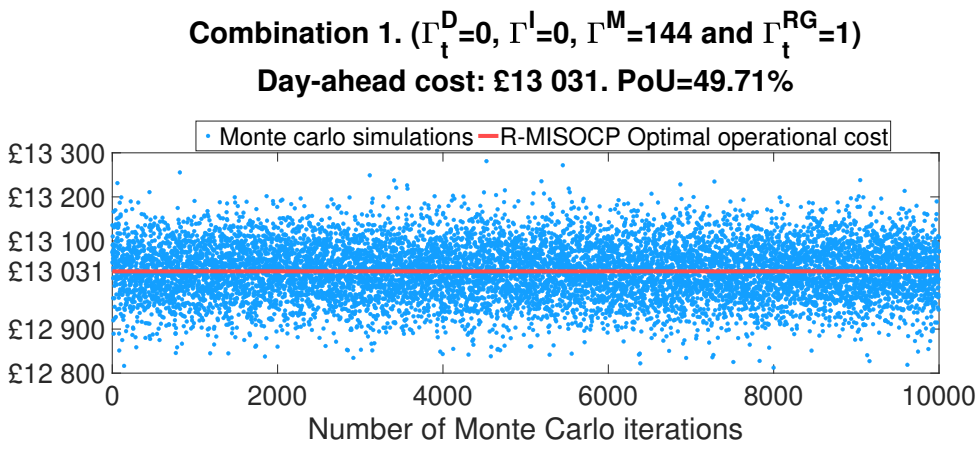

Figure 6.1: Visual representation of the results for combinations of the budgets of uncertainty used in this chapter. **X-axis:** Number of Monte Carlo simulations. **Y-axis:** Operational cost for each of these combinations using the optimal DER schedules calculated by the R-MISOCP model.

Γ_t^D	Γ^I = 0	Γ^I = 3	Γ^I = 6 (max)
0	**49.71%**	49.59%	50.97%
0.001	43.46%	42.29%	42.57%
0.005	16.94%	16.51%	16.43%
0.01	3.32%	2.75%	2.62%
0.02	0.01%	0.02%	0.01%
0.03	0%	0%	0%
1 (max)	0%	0%	0%

Table 6.6: PoU

Γ^I = 0	Γ^I = 3	Γ^I = 6 (max)
£13 031	£13 169	£13 342
£13 039	£13 182	£13 351
£13 077	£13 222	£13 393
£13 123	£13 272	£13 445
£13 217	£13 371	£13 550
£13 310	£13 471	£13 657
£15 849	£16 183	£16 551

Table 6.7: Day-Ahead Cost

In the BoU combinations of figures 6.2, 6.3 it is shown that the majority of the values calculated within the Monte Carlo simulations are below the red line, which represents the operational cost calculated by the R-MISOCP model. Therefore, figures 6.2 and 6.3 present a PoU equal to 16.51% and 2.62% respectively.

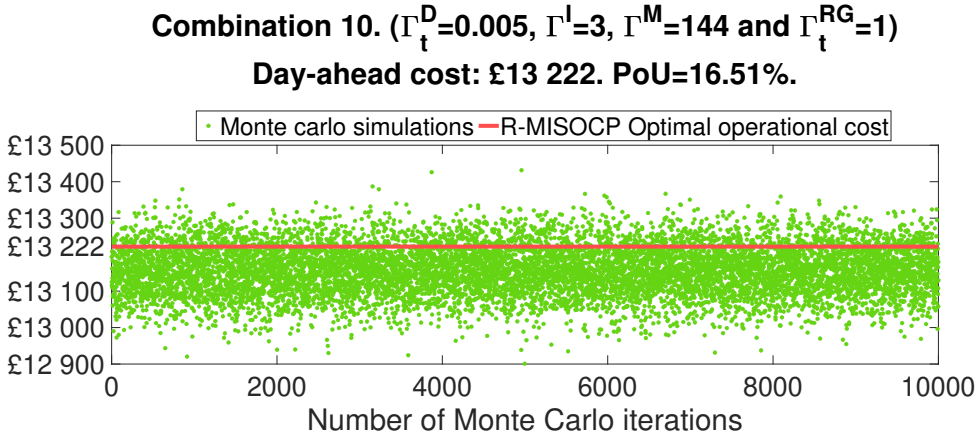

Figure 6.2: Visual representation of the results for combinations of the budgets of uncertainty used in this chapter. **X-axis:** Number of Monte Carlo simulations. **Y-axis:** Operational cost for each of these combinations using the optimal DER schedules calculated by the R-MISOCP model.

Γ_t^D	Γ^I = 0	Γ^I = 3	Γ^I = 6 (max)
0	49.71%	49.59%	50.97%
0.001	43.46%	42.29%	42.57%
0.005	16.94%	**16.51%**	16.43%
0.01	3.32%	2.75%	2.62%
0.02	0.01%	0.02%	0.01%
0.03	**0%**	0%	0%
1 (max)	0%	0%	0%

Table 6.8: PoU

Γ^I = 0	Γ^I = 3	Γ^I = 6 (max)
£13 031	£13 169	£13 342
£13 039	£13 182	£13 351
£13 077	**£13 222**	£13 393
£13 123	£13 272	£13 445
£13 217	£13 371	£13 550
£13 310	£13 471	£13 657
£15 849	£16 183	£16 551

Table 6.9: Day-Ahead Cost

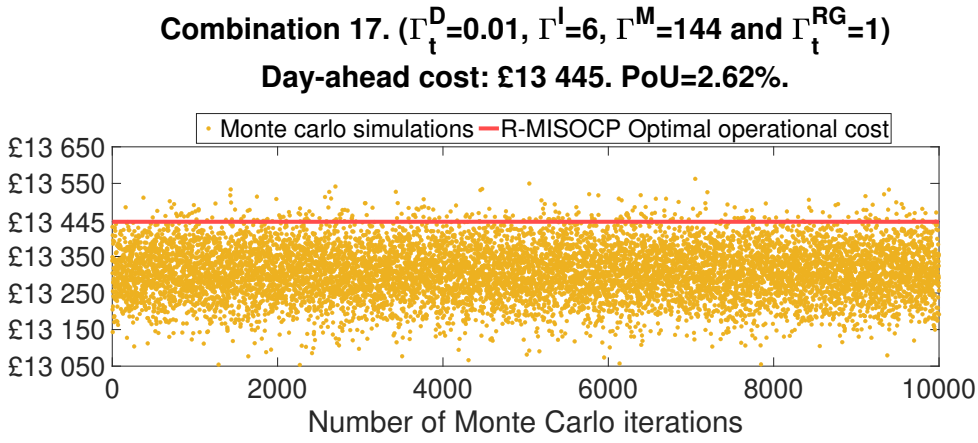

Figure 6.3: Visual representation of the results for combinations of the budgets of uncertainty used in this chapter. **X-axis:** Number of Monte Carlo simulations. **Y-axis:** Operational cost for each of these combinations using the optimal DER schedules calculated by the R-MISOCP model.

Γ_t^D	Γ^I = 0	Γ^I = 3	Γ^I = 6 (max)
0	49.71%	49.59%	50.97%
0.001	43.46%	42.29%	42.57%
0.005	16.94%	16.51%	16.43%
0.01	3.32%	2.75%	**2.62%**
0.02	0.01%	0.02%	0.01%
0.03	0%	0%	0%
1 (max)	0%	0%	0%

Table 6.10: PoU

Γ^I = 0	Γ^I = 3	Γ^I = 6 (max)
£13 031	£13 169	£13 342
£13 039	£13 182	£13 351
£13 077	£13 222	£13 393
£13 123	£13 272	£13 445
£13 217	£13 371	£13 550
£13 310	£13 471	£13 657
£15 849	£16 183	£16 551

Table 6.11: Day-Ahead Cost

Finally, figure 6.4 corresponds to a PoU = 0%, as all costs calculated within the Monte Carlo simulations are below the red line, which represents the operational cost calculated by the R-MISOCP model, which outperforms the fully robust (conservative) case as discussed earlier.

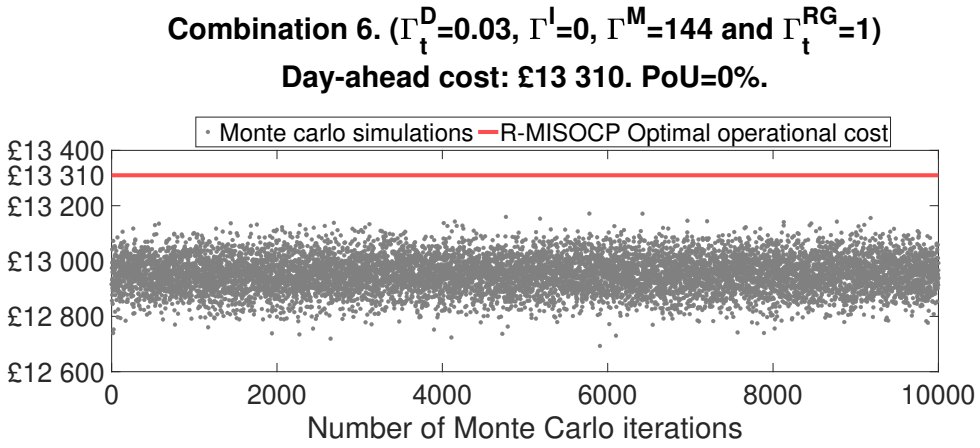

Figure 6.4: Visual representation of the results for combinations of the budgets of uncertainty used in this chapter. **X-axis:** Number of Monte Carlo simulations. **Y-axis:** Operational cost for each of these combinations using the optimal DER schedules calculated by the R-MISOCP model.

Γ_t^D	Γ^I = 0	Γ^I = 3	Γ^I = 6 (max)
0	49.71%	49.59%	50.97%
0.001	43.46%	42.29%	42.57%
0.005	16.94%	16.51%	16.43%
0.01	3.32%	2.75%	2.62%
0.02	0.01%	0.02%	0.01%
0.03	**0%**	0%	0%
1 (max)	0%	0%	0%

Table 6.12: PoU

Γ^I = 0	Γ^I = 3	Γ^I = 6 (max)
£13 031	£13 169	£13 342
£13 039	£13 182	£13 351
£13 077	£13 222	£13 393
£13 123	£13 272	£13 445
£13 217	£13 371	£13 550
£13 310	£13 471	£13 657
£15 849	£16 183	£16 551

Table 6.13: Day-Ahead Cost

6.4. Model scalability

This section uses the IEEE 33-bus distribution network of [3] to perform simulations on the proposed R-MISOCP model. However, models that are mathematically formulated using robust mixed-integer second-order cone programming can also be used in larger electricity distribution networks which would result in larger power distribution problems. These studies use a range of robust approaches to model uncertainty (a classification of these methods can be found in chapter 2, which presents the literature review of this thesis) and have implemented their computational experiments using 69-, 123- and 136-bus distribution networks.

In particular, the studies in [80, 82, 120] propose robust mixed-integer second-order cone programming models which are tested using a 69-bus network. The study in [120] proposes a robust mixed-integer second-order cone programming model and implements computational experiments using a 33-, a 69- and a 123-bus network. The study in [84] proposes a robust mixed-integer second-order cone programming model which is tested using a 136-node network.

6.5. Conclusions

To conclude, this chapter aims to show the benefits and applicability of the uncertainty method used in the proposed R-MISOCP model. A case study with DER connected to a radial electricity distribution network is presented using the IEEE-33 modified network, assuming that the network will undergo a scheduled interruption. Four sources of uncertainty are taken into account for the computational experiments: market price, demand, solar PV generation and the uncertainty in the time and duration of the interruption from the main grid, and therefore four BoU are used.

The BoU algorithm is used in order to calculate probabilistic metrics which allow the DSO and/or MG operator to control the trade-off between operational performance and robustness. Operational performance is evaluated using the probability of underperforming (PoU) and the probability of load shedding (PLS). Computational experiments perform a comparative study between the proposed R-MISOCP model, and a fully robust (conservative) model.

It is shown, that with the R-MISOCP model the DSO and/or MG operator can achieve a significant trade-off between tolerance of data perturbations of the uncertain data, and operational performance. In particular, computational experiments show that by adjusting the budgets of uncertainty, the DSO and/or MG operator can achieve a 19.58% reduction in the day-ahead operational cost, compared to a fully robust schedule. Moreover, the R-MISOCP model can guarantee 63.83% lower load shedding compared to a fully robust schedule, while preserving a 0% probability of additional load shedding during the actual operation. In general, the computational experiments show that the employed robust approach to deal with uncertainty presents a range of economic options to the DSO and/or MG operator, and allows them to control the risks they are willing to take depending on their preferences and priorities.

Chapter 7. Conclusions & Future work

Contents

7.1. Chapter Summary

This chapter is structured as follows.

- **Section 7.2** discusses the main conclusions of this PhD.
- **Section 7.3** proposes future research directions.

7.2. Discussion and conclusions

This PhD proposes a model to optimally schedule DER connected to radial distribution networks, aiming at delivering improvements in operational cost, security of supply and environmental sustainability. This model is mathematically formulated using robust mixed-integer second-order cone programming, and takes into account an accurate power flow model for radial networks, and a robust approach to deal with uncertainty in the market price, demand, renewable generation and time and duration of a scheduled interruption from the main grid. Computational experiments demonstrated the suitability of the proposed model in a number of case studies informed by real-world data and operational scenarios, with a particular focus on the impact of the employed power flow model and uncertainty method, on the operational cost and the optimal DER schedules.

To study the impact of the employed accurate power flow model (which was proposed in [85]) for radial networks on the optimal DER scheduling problem, two sets of comparative studies are performed. First, a comparative study is performed (section 5.3, chapter 5), between the proposed R-MISOCP model (which uses a second-order cone power flow model that accounts for network losses), and a model that is named *COMP* model (which uses a piecewise linear power flow model that does not account for network losses). This comparative study showed that the incorporation of network losses can impact both the operational cost and the optimal DER schedules. In terms of the operational costs, for the first case study of section 5.3, it was shown that the R-MISOCP model is almost 12% more expensive than the COMP model. This difference is attributed to the fact that accounting for network losses the R-MISOCP model calculates a higher generation (to cover both the demand and the losses) and a higher amount of load shedding which occurs while the network is not connected

to the main grid (as in this case study a scheduled interruption is assumed to take place). Subsequently, a second case study is also performed, for a network that is operating continuously connected to the main grid which has a high PV penetration. In this case, the R-MISOCP model is found to have an operational cost that is very close to the operational cost calculated by the COMP model, and that it is around 4% more expensive than the COMP model.

However, this proximity was not reflected on the optimal DER decisions calculated by the R-MISOCP and the COMP models. In particular, in section 5.3, the computational experiments for the optimal DER schedules show that the decisions made by the COMP model are mainly driven by the cost of generation, whereas the optimal DER schedules calculated by the R-MISOCP model, apart from the cost of operation, are also sensitive to the electrical location of the distributed energy resources. This was shown to hold for both a low and a high penetration of solar PV generation (which is the source of renewable generation in the network under study).

These computational experiments also demonstrated that there is not a relation or pattern between the optimal DER schedules calculated by the R-MISOCP model and the optimal DER schedules calculated by the COMP model, suggesting that there does not seem to exist some kind of “corrective action” that can be applied on the optimal DER schedules calculated by the COMP model retrospectively (which does not account for network losses), in order to extract the optimal DER schedules calculated by the proposed R-MISOCP model (which takes into account network losses). In fact, in the case where there is a high PV penetration the difference in the optimal DER schedules between the R-MISOCP and the COMP model is even more evident, as increasing the PV generation allowed more “room” for the two models to calculate how to dispatch the rest of the DER in order to supply the demand. Furthermore, these simulations provide an indication that the proximity or not of the operational cost between the R-MISOCP and the COMP model does not form a metric of evaluating the performance of the COMP model, as in these computational experiments, the results with the closer operational costs between the two models also were the ones with the larger difference between their optimal DER schedules.

Further to these conclusions, a second comparative study is performed in section 5.4, chapter 5, in order to study the effect of the optimal DER schedules calculated

by the COMP model (which does not account for network losses) on the operational decisions. In order to implement this, this section compares the results produced by the R-MISOCP model, and a model that is named *HYBR* model, as it is a hybrid model which has the R-MISOCP mathematical formulation but uses the optimal DER schedules calculated by the COMP model. The HYBR model aims to indicate which would be the actual operational cost using the optimal DER schedules calculated by the COMP model, as it takes into account network losses.

Two scenarios are compared in this set of computational experiments: one where the network under study is continuously connected to the main grid, and one where the network under study is assumed to operate in isolation from the main grid during a period of the day. In both scenarios, the HYBR model resulted in a higher operational cost compared to the R-MISOCP model, which is found to be 17.52% higher in the first scenario, and 18.59% higher in the second scenario. Furthermore, it is found that the HYBR model has high load shedding levels in both scenarios (either with or without a scheduled interruption occurring), which also explains its high operational cost. It is found that load shedding occurred in both scenarios of this case study, in order to not exceed the line current limits in the first two lines of the network when importing power from the main grid. These experiments demonstrated that apart from the underestimation of the operational cost, the COMP model due to the fact that it doesn't account for network losses, can also provide optimal DER schedules that result in violation of network operating constraints, and can result in an expensive operation and/or customers experiencing power cuts.

To study the impact of the employed robust approach for optimal DER scheduling in electricity distribution networks, the operational performance of the R-MISOCP model is compared against a fully robust (conservative) model. Uncertainty is taken into account in the market price, demand, renewable generation (which is the solar PV generation in this case study). The time and duration of a scheduled network interruption from the main grid is also considered uncertain, which is applicable for cases where the network represents a microgrid (MG). This uncertainty can be used when the main grid is not available, either due to a scheduled interruption, e.g. an upstream maintenance, or a foreseeable natural disaster such as a hurricane [27, 8, 28].

The R-MISOCP model uses the robust approach proposed in [87], which allows the DSO and/or MG operator to control the trade-off between the operational performance and the tolerance of uncertainty using a parameter called the *budget of uncertainty*, whereas the fully robust model assumes that the uncertain parameters take their *worst* values, making the problem highly conservative (and therefore expensive). The operational performance is evaluated using two metrics: the probability of underperforming (PoU), and the probability of load shedding (PLS). The PoU measures the probability that the actual cost of operation will exceed the day-ahead operational cost calculated by the R-MISOCP model. The PLS measures the probability that the actual load shedding will exceed the load shedding calculated by the R-MISOCP model. These two operational performance criteria are evaluated through Monte Carlo simulations.

Computational experiments are performed in order to assess the impact of the robust approach on the optimal DER scheduling problem. The results showed that, for the network under study, depending on the value of the budgets of uncertainty, the DSO and/or MG operator is presented with a broad range of operational costs from £13 031 to £16 551, and a broad range of load shedding levels from 1.88 MWh to 5.89 MWh, for a demand of 206 MWh.

For the network under study, the fully robust model is found to have a 0% probability of underperforming as well as a 0% probability of load shedding. However, the computational results showed that by using the proposed R-MISOCP model, the DSO and/or MG operator can also be guaranteed a 0% probability of underperforming and a 0% probability of load shedding, while having a 19.58% lower operational cost and a 63.83% lower load shedding compared to the fully robust model. The PoU and PLS values are shown for 21 different combinations of the budgets of uncertainty.

The PoU and PLS values ranged from 0% to 50%, with the values that were very close to 50% belonging to the deterministic case study (where no uncertainty is taken into account). This method to deal with uncertainty can also be extended for other operational performance criteria, such as the probability of optimisation constraint violations (see the analysis for linear and discrete optimisation problems in [87]). In general, the computational experiments show that the employed robust approach to deal with uncertainty presents a range of economic options to the DSO and/or MG

operator, and allows them to control the risks they are willing to take depending on their preferences and priorities.

Overall, the computational experiments performed in this thesis, demonstrated the suitability of the proposed R-MISOCP model in a number of case studies informed by real-world data and operational scenarios. It is shown that an accurate power flow model and an uncertainty approach that accounts for data that belong to a deterministic interval, both hold an important role in the optimal scheduling of DER connected to electricity distribution networks. The proposed model can be used by a range of stakeholders including, microgrid operators, distribution system operators, and DER owners, and can be implemented under the framework of active network management and for the operation of microgrids. The whole system benefits that DER provide, including in the global battle against climate change, and the developments in modelling power flow equations and in the methods to handle uncertainty, have pushed the scientific limits in the field of DER operation. Research on fast and efficient methods for DER coordination, including robust mixed-integer second-order cone programming methods, will continue to flourish over the next years, heading towards the provision of methods that are both interesting scientifically, but also attractive for industry and system operators.

7.3. Future research directions

This work can be extended towards different directions, some of which are presented below.

This research can be extended for cases where the electricity distribution network is mesh, which would require a separate analysis to study the accuracy of the power flow model and set of case studies. There is a range of methodologies to formulate power flow equations for mesh networks, including the work proposed in the publications [85, 121], where the paper [121] forms the second part of the study which proposed the power flow model used in this thesis.

The concepts of whole energy systems modelling and multi-energy systems due to their economic and environmental benefits, are a hot topic in power systems research. Another possible future research direction is towards using a range of energy vectors apart from electricity (e.g. heat and transport), as this work can be extended for cases where DER is coordinated using the concepts of multi-energy microgrids [122, 123] or the energy hub concept [91, 124].

In this context, apart from the DER used in work, a different DER portfolio can also be investigated (such as heat pumps, wind turbines and combined heat and power plants). This can also include the interactions of the on-site generation with flexibility methods [125] (such as flexible loads/demand response).

Finally, coordinating DER in a range of different market frameworks including peer-to-peer trading [126], energy communities and networked microgrids (or multi-microgrids) can also form subject of future work. Further to this, the economic and operational impacts of a range of stakeholders which coexist in power systems at distribution level (such as aggregators, distribution network/system operators, DER owners) with potentially conflicting objectives, can also be a subject of future work.

Appendix A. Data for the modified IEEE-33 bus network

This appendix presents the data introduced in chapter 5. The DG, ESS and EV parking lot technical constraints are shown in tables C.1, A.2, A.4 respectively. Branch data are shown in table A.3.

Bus	$\underline{P_{it}^{DG}}$ [MW]	$\overline{P_{it}^{DG}}$ [MW]	$\underline{Q_{it}^{DG}}$ [MVar]	$\overline{Q_{it}^{DG}}$ [MVar]	b_i [£/MWh]	a_i [£]
8	0.21	3	-2.1	2.1	54.66	0
13	0.19	2	-1.9	1.9	54.66	0
16	0.19	2	-1.9	1.9	54.66	0
25	0.22	3	-2.2	2.2	54.66	0

Table A.1: DG TECHNICAL CONSTRAINTS [8]

Bus	$C_i^{ESS,Max}$ [MWh]	$SOC_{i,initial}$ [%]	$\overline{P_{it}^{Ch,ESS}}$ [MW]	$\overline{P_{it}^{Dch,ESS}}$ [MW]	η_i [%]
19	1.5	66.6	0.5	0.5	90
26	1.5	80	0.5	0.5	90

Table A.2: ESS TECHNICAL CONSTRAINTS [8]

Branch	r_{ij} [Ω]	x_{ij} [Ω]	Branch	r_{ij} [Ω]	x_{ij} [Ω]
1 - 2	0.0922	0.0470	17 - 18	0.7320	0.5740
2 - 3	0.4930	0.2511	2 - 19	0.1640	0.1565
3 - 4	0.3660	0.1864	19 - 20	1.5042	1.3554
4 - 5	0.3811	0.1941	20 - 21	0.4095	0.4784
5 - 6	0.8190	0.7070	21 - 22	0.7089	0.9373
6 - 7	0.1872	0.6188	3 - 23	0.4512	0.3083
7 - 8	0.7114	0.2351	23 - 24	0.8980	0.7091
8 - 9	1.0300	0.7400	24 - 25	0.8960	0.7011
9 - 10	1.0440	0.7400	6 - 26	0.2030	0.1034
10 - 11	0.1966	0.0650	26 - 27	0.2842	0.1447
11 - 12	0.3744	0.1238	27 - 28	1.0590	0.9337
12 - 13	1.4680	1.1550	28 - 29	0.8042	0.7006
13 - 14	0.5416	0.7129	29 - 30	0.5075	0.2585
14 - 15	0.5910	0.5260	30 - 31	0.9744	0.9630
15 - 16	0.7463	0.5450	31 - 32	0.3105	0.3619
16 - 17	1.2890	1.7210	32 - 33	0.3410	0.5302

Table A.3: NETWORK DATA [3, 9]

Bus	$\overline{C_i^{EV,Max}}$	$\overline{P_{it}^{EV}}$	$SOC_{arrival}^{EV}$	$SOC_{departure}^{EV}$	$SOC_i^{Sat,EV}$	$t_{Min}^{EV} - t_{Max}^{EV}$
	[MW]	[MWh]	[%]	[%]	[%]	[period]
25	2	0.5	10	50	85	51 - 105 (8:30am - 5:30pm)

Table A.4: EV PARKING LOT TECHNICAL CONSTRAINTS [8]

Appendix B. The Power flow formulation used in the COMP Model

This section presents the Piecewise Linear Power Flow formulation (PWL-PF) of the COMP model used in this thesis, as presented in the article [1]. For completeness, the non-convex formulation of the piecewise linear power flow model is first presented, and subsequently the piecewise linear formulation (PWL-PF).

The non-convex formulation of the power flow model formulation used in [8] is shown in equations (B.1a)-(B.1b) below.

$$PF^{P}_{ij,t} = g_{ij}\,(V^{2}_{it} - V_{it}\,V_{jt}\,\cos(\theta_{it} - \theta_{jt})) - b_{ij}\,(V_{it}\,V_{jt}\,\sin(\theta_{it} - \theta_{jt})), \quad \forall (i,j) \in E, \forall t \in \Omega_T \tag{B.1a}$$

$$PF^{Q}_{ij,t} = -b_{ij}\,(V^{2}_{it} - V_{it}\,V_{jt}\,\cos(\theta_{it} - \theta_{jt})) - g_{ij}\,(V_{it}\,V_{jt}\,\sin(\theta_{it} - \theta_{jt})), \quad \forall (i,j) \in E, \forall t \in \Omega_T \tag{B.1b}$$

According to [8, 7, 115], equation (B.1a) is linearized to (B.2a), and equation (B.1b) is linearized to (B.2b), as shown below.

$$PF^{P}_{ij,t} = g_{ij}\,(V_{it} - V_{jt} - \omega^{PWL}_{ij,t} + 1) - b_{ij}\,(\theta_{it} - \theta_{jt}), \quad \forall (i,j) \in E, \forall t \in \Omega_T \tag{B.2a}$$

$$PF^{Q}_{ij,t} = -b_{ij}\,(V_{it} - V_{jt} - \omega^{PWL}_{ij,t} + 1) - g_{ij}\,(\theta_{it} - \theta_{jt}), \quad \forall (i,j) \in E, \forall t \in \Omega_T \tag{B.2b}$$

The term $\cos(\theta_{it} - \theta_{jt})$ of equations (B.1a)-(B.1b) is approximated by the linear segments shown in (B.2c), using the algorithm proposed in [7] for the calculation of the terms h_n and d_n.

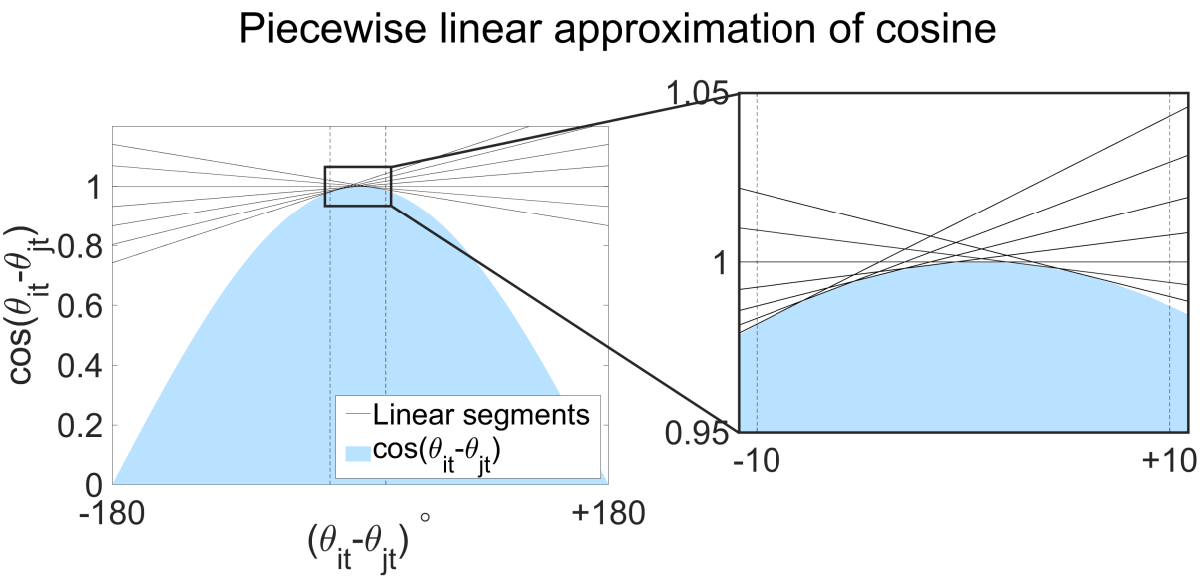

Figure B.1: Piecewise linearization of $\cos(\theta_{it} - \theta_{jt})$ for $|\theta_{it} - \theta_{jt}| \leq 10^{\circ}$ using seven linear segments according to [7].

$$\omega_{ij,t}^{PWL} \leq h_n(\theta_{it} - \theta_{jt}) + d_n, \quad \forall (i,j) \in E, \forall t \in \Omega_T, \forall n \tag{B.2c}$$

where n is the number of linear inequalities used to approximate the $\cos(\theta_{it} - \theta_{jt})$. The piecewise linearization of $\cos(\theta_{it} - \theta_{jt})$ for $|\theta_{it} - \theta_{jt}| \leq 10^{\circ}$ (following the study in [8]), is shown in figure B.1 for seven linear segments.

Along with equations (B.2a)-(B.2c), the COMP model power flow formulation is also comprised of the following equations:

$$\sum_{j:(i,j)\in E} PF_{ij,t}^{P} = G_{it}^{P} - D_{it}^{P} \tag{B.2d}$$

$$\sum_{j:(i,j)\in E} PF_{ij,t}^{Q} = G_{it}^{Q} - D_{it}^{Q} \tag{B.2e}$$

$$PF_{ij,t}^{P} + PF_{ji,t}^{P} \leq PF_{ij}^{loss} \tag{B.2f}$$

$$PF_{ij}^{loss} = \frac{g_{ij}}{g_{ij}^2 + b_{ij}^2} \overline{I_{ij}} \tag{B.2g}$$

where, (B.2d) and (B.2e) are the real and reactive power flow balance respectively, and (B.2f)-(B.2g) represent the feeder loss, which is comprised of the summation of the active power injections [8].

Appendix C. Numerical results: Relaxation gap

C.1. Mathematical formulation

This appendix presents the relaxation gaps for constraint (4.14h) of the proposed R-MISOCP model. The relaxation gaps are shown for the case study of section 5.3, chapter 5, for the following three scenarios. Scenario A, where the network is disconnected from the main grid from 17:00 to 20:00 (which is the case study of sections 5.3.2 - 5.3.4). Scenario B, where the network is continuously connected to the main grid (which is the case study of sections 5.3.2 - 5.3.4, but without a disconnection from the main grid). Scenario C, where the network is continuously connected to the main grid but there is a 20-times higher PV penetration than the one used in scenarios A and B (which is the case study of section 5.3.5).

Figures C.1, C.2, and C.3 present the relaxation gaps of constraint (4.14h) for each scenario, which has been calculated as shown in equation (C.1) below. The relaxation gap for this set of power flow equations has also been verified in a similar way in section 5 of the relevant study in [55].

$$\text{Relaxation Gap} = \left| \frac{(I_{ijt}^{sq} + v_{it}^{sq})^2 - (2\,PF_{ijt}^{P})^2 - (2\,PF_{ijt}^{Q})^2 - (I_{ijt}^{sq} - v_{it}^{sq})^2}{(2\,PF_{ijt}^{P})^2 + (2\,PF_{ijt}^{Q})^2 + (I_{ijt}^{sq} - v_{it}^{sq})^2} \right| \times 100\ \%, \qquad \forall t \in \Omega_T, \quad \forall (i,j) \in E \tag{C.1}$$

Finally, it is noted that this calculation is based on the fact that constraint (4.14h) has the following equivalent formulation, which is shown in equation (C.2) below.

$$\text{Constraint (4.14h):}\ \ I_{ijt}^{sq} + v_{it}^{sq} \geq \left\| \begin{bmatrix} 2\,PF_{ijt}^{P} & 2\,PF_{ijt}^{Q} & (I_{ijt}^{sq} - v_{it}^{sq}) \end{bmatrix}^T \right\|_2 \implies$$

$$(I_{ijt}^{sq} + v_{it}^{sq})^2 \geq (2\,PF_{ijt}^{P})^2 + (2\,PF_{ijt}^{Q})^2 + (I_{ijt}^{sq} - v_{it}^{sq})^2, \quad \forall t \in \Omega_T, \quad \forall (i,j) \in E \tag{C.2}$$

C.2. Numerical results

Overall, the relaxation gaps in the three scenarios below span from 5.11 $\times 10^{-11}$ [%] to 4.64 $\times 10^{-6}$ [%]. For each scenario in particular this is shown in table C.1 below.

SCENARIO	Min Relaxation gap [%]	Max Relaxation gap [%]
A	5.11 $\times 10^{-11}$	3.49 $\times 10^{-6}$
B	4.65 $\times 10^{-8}$	4.64 $\times 10^{-6}$
C	4.66 $\times 10^{-8}$	2.61 $\times 10^{-6}$

Table C.1: MIN AND MAX RELAXATION GAPS [%] FOR THE THREE SCENARIOS

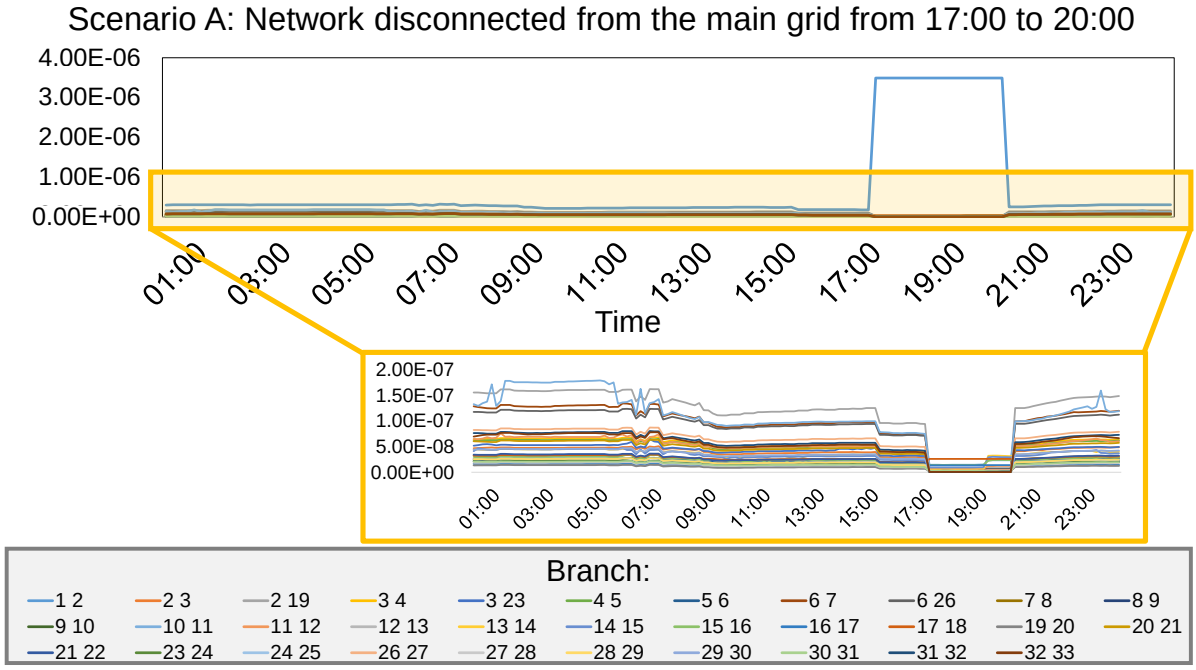

Figure C.1: Relaxation gap [%] for Scenario A: Network disconnected from the main grid between 17:00 and 20:00 during the 24-hour scheduling horizon.

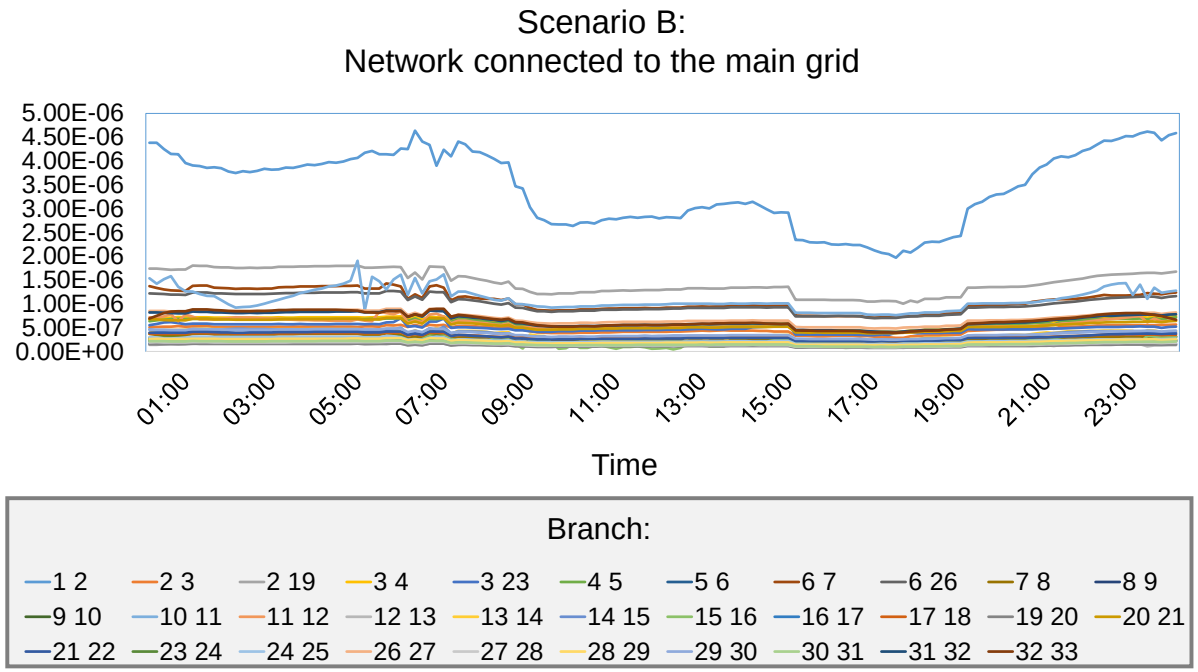

Figure C.2: Relaxation gap [%] for Scenario B: Network continuously connected to the main grid during the 24-hour scheduling horizon.

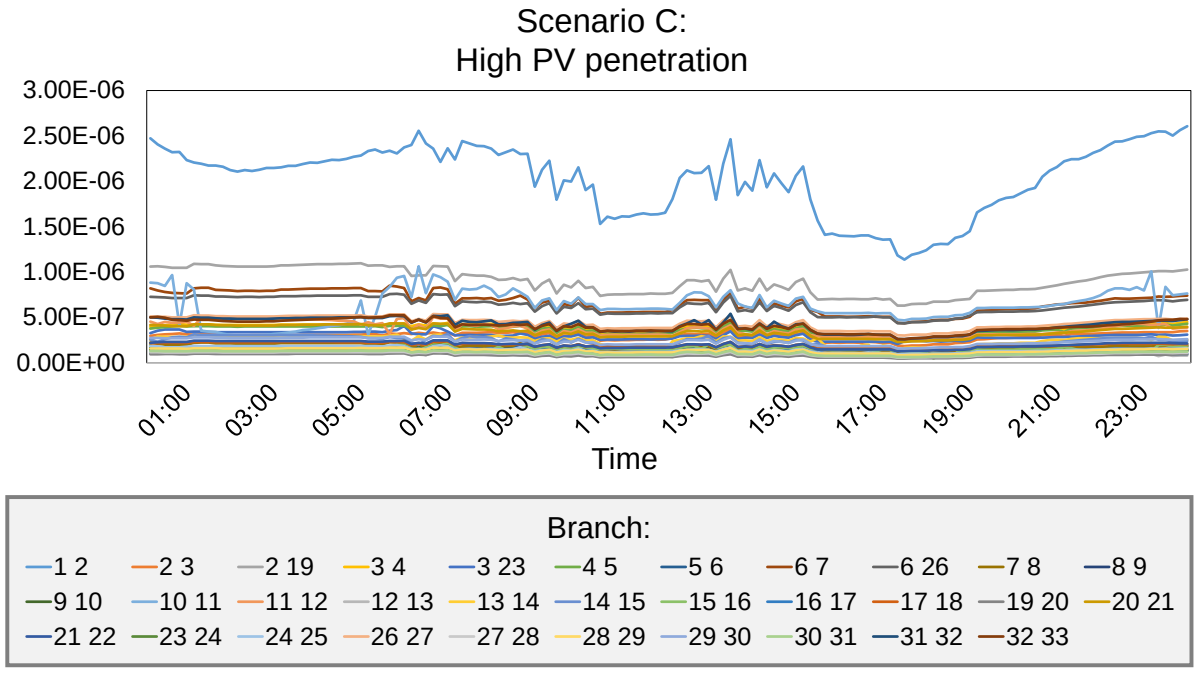

Figure C.3: Relaxation gap [%] for Scenario C: Network continuously connected to the main grid during the 24-hour scheduling horizon with a 20-times higher PV penetration than scenarios A and B.

Bibliography

[1] Natalia-Maria Zografou-Barredo, Charalampos Patsios, Ilias Sarantakos, Peter Davison, Sara Louise Walker, and Philip C. Taylor. MicroGrid Resilience-Oriented Scheduling: A Robust MISOCP Model. *IEEE Transactions on Smart Grid*, 12(3):1867–1879, May 2021.

[2] S. I. Vagropoulos and A. G. Bakirtzis. Optimal Bidding Strategy for Electric Vehicle Aggregators in Electricity Markets. *IEEE Transactions on Power Systems*, 28(4):4031–4041, Nov. 2013.

[3] M. E. Baran and F. F. Wu. Network reconfiguration in distribution systems for loss reduction and load balancing. *IEEE Transactions on Power Delivery*, 4(2):1401–1407, April 1989.

[4] Northern Powergrid (Northeast) plc. Customer-Led Network Revolution. `http://www.networkrevolution.co.uk/`. (Accessed: 08.07.2021).

[5] ELEXON. System Sell & System Buy Prices. (https://www.elexon.co.uk/), London, U.K., 2019.

[6] Newcastle University. Urban Sciences Building. `https://www.ncl.ac.uk/cesi/research/demo/usb/`. (Accessed: 08.07.2021).

[7] Carleton Coffrin and Pascal Van Hentenryck. A Linear-Programming Approximation of AC Power Flows. *INFORMS Journal on Computing*, 26, June 2012.

[8] A. Gholami, T. Shekari, F. Aminifar, and M. Shahidehpour. Microgrid Scheduling With Uncertainty: The Quest for Resilience. *IEEE Transactions on Smart Grid*, 7(6):2849–2858, Nov. 2016.

[9] R. D. Zimmerman, C. E. Murillo-Sanchez, and R. J. Thomas. MATPOWER: Steady-State Operations, Planning, and Analysis Tools for Power Systems Research and Education. *IEEE Transactions on Power Systems*, 26(1):12–19, Feb. 2011.

[10] Department for Business, Energy & Industrial Strategy, U.K. UK sets ambitious new climate target ahead of UN Summit. `https://www.gov.uk/government/news/uk-sets-ambitious-new-climate-target-ahead-of-un-summit`, December 2020. (Accessed: 23.06.2021).

[11] J. A. P. Lopes, C. L. Moreira, and A. G. Madureira. Defining control strategies for MicroGrids islanded operation. *IEEE Transactions on Power Systems*, 21(2):916–924, May 2006.

[12] F. Katiraei and M. R. Iravani. Power Management Strategies for a Microgrid With Multiple Distributed Generation Units. *IEEE Transactions on Power Systems*, 21(4):1821–1831, Nov. 2006.

[13] Office of Gas and U.K. Electricity Markets (Ofgem). Review of GB energy system operation. *(Report)*, 2021.

[14] Robert H. Lasseter, Abbas A. Akhil, Chris Marnay, John Stephens, Jeffery E. Dagle, Ross T. Guttromson, A. Sakis Meliopoulous, Robert J Yinger, and Joseph H Eto. Integration of Distributed Energy Resources: The CERTS MicroGrid Concept. Technical report, CERTS, 10/2003 2003.

[15] UK Power Networks. Distributed Energy Resources. `https://www.ukpowernetworks.co.uk/electricity/distribution-energy-resources`. (Accessed: June 2021).

[16] Australian Energy Market Commission (AEMC). Distributed energy resources. `https://www.aemc.gov.au/energy-system/electricity/electricity-system/distributed-energy-resources`. (Accessed: June 2021).

[17] N. Hatziargyriou. *The Microgrids Concept*, chapter 1, pages 1–24. John Wiley & Sons, Ltd, 2014.

[18] Michiel Houwing, Austin N. Ajah, Petra W. Heijnen, Ivo Bouwmans, and Paulien M. Herder. Uncertainties in the design and operation of distributed energy resources: The case of micro-CHP systems. *Energy*, 33(10):1518–1536, 2008. PRES '07 10th Conference on Process Integration, Modelling and Optimisation for Energy Saving and Pollution Reduction.

[19] Robert H. Lasseter. Smart Distribution: Coupled Microgrids. *Proceedings of the IEEE*, 99(6):1074–1082, 2011.

[20] World Energy Council. World Energy Trilemma Index. In partnership with Oliver Wyman. *Report*, 2020.

[21] Janusz Bialek. What does the GB power outage on 9 August 2019 tell us about the current state of decarbonised power systems? *Energy Policy*, 146:111821, 2020.

[22] Josep M. Guerrero, Juan C. Vasquez, José Matas, Luis García de Vicuna, and Miguel Castilla. Hierarchical Control of Droop-Controlled AC and DC Microgrids—A General Approach Toward Standardization. *IEEE Transactions on Industrial Electronics*, 58(1):158–172, 2011.

[23] Vasileios A. Evangelopoulos, Pavlos S. Georgilakis, and Nikos D. Hatziargyriou. Optimal operation of smart distribution networks: A review of models, methods and future research. *Electric Power Systems Research*, 140:95–106, Nov. 2016.

[24] Office of Gas and Electricity Markets (Ofgem), U.K. Key enablers for DSO programme of work and the Long Term Development Statement Impacts, December 2019.

[25] H. E. Brown and S. Suryanarayanan. A survey seeking a definition of a smart distribution system. In *41st North American Power Symposium*, pages 1–7, 2009.

[26] S. Karagiannopoulos, J. Gallmann, M. G. Vayá, P. Aristidou, and G. Hug. Active Distribution Grids Offering Ancillary Services in Islanded and Grid-Connected Mode. *IEEE Transactions on Smart Grid*, 11(1):623–633, 2020.

[27] A. Khodaei. Resiliency-Oriented Microgrid Optimal Scheduling. *IEEE Transactions on Smart Grid*, 5(4):1584–1591, July 2014.

[28] A. Gholami, T. Shekari, and S. Grijalva. Proactive Management of Microgrids for Resiliency Enhancement: An Adaptive Robust Approach. *IEEE Transactions on Sustainable Energy*, 10(1):470–480, Jan. 2019.

[29] A. Hussain, V. Bui, and H. Kim. A Proactive and Survivability-Constrained Operation Strategy for Enhancing Resilience of Microgrids Using Energy Storage System. *IEEE Access*, 6:75495–75507, 2018.

[30] Y. Guo and C. Zhao. Islanding-Aware Robust Energy Management for Microgrids. *IEEE Transactions on Smart Grid*, 9(2):1301–1309, March 2018.

[31] Karthikeyan Balasubramaniam, Parimal Saraf, Ramtin Hadidi, and Elham B. Makram. Energy management system for enhanced resiliency of microgrids during islanded operation. *Electric Power Systems Research*, 137:133 – 141, 2016.

[32] Z. Li, M. Shahidehpour, F. Aminifar, A. Alabdulwahab, and Y. Al-Turki. Networked Microgrids for Enhancing the Power System Resilience. *Proceedings of the IEEE*, 105(7):1289–1310, July 2017.

[33] X. Liu, M. Shahidehpour, Z. Li, X. Liu, Y. Cao, and Z. Bie. Microgrids for enhancing the power grid resilience in extreme conditions. *IEEE Transactions on Smart Grid*, 8(2):589–597, 2017.

[34] Y. Zhang, J. Wang, and Z. Li. Uncertainty Modeling of Distributed Energy Resources: Techniques and Challenges. *Current Sustainable/Renewable Energy Reports*, 6(2):42–51, 2019.

[35] Carlos Adrian Correa-Florez, Andrea Michiorri, and Georges Kariniotakis. Robust optimization for day-ahead market participation of smart-home aggregators. *Applied Energy*, 229:433 – 445, 2018.

[36] Aharon Ben-tal and Arkadi Nemirovski. Robust solutions of Linear Programming problems contaminated with uncertain data. *Mathematical Programming*, 88:411–424, 2000.

[37] Zhenquan Yang, Yanjun Li, and Ji Xiang. Coordination Control Strategy for Power Management of Active Distribution Networks. *IEEE Transactions on Smart Grid*, 10(5):5524–5535, 2019.

[38] Alberto Borghetti, Mauro Bosetti, Samuele Grillo, Stefano Massucco, Carlo Alberto Nucci, Mario Paolone, and Federico Silvestro. Short-Term Scheduling and Control of Active Distribution Systems With High Penetration of Renewable Resources. *IEEE Systems Journal*, 4(3):313–322, 2010.

[39] Sultan S. AlKaabi, Vinod Khadkikar, and H. H. Zeineldin. Incorporating PV Inverter Control Schemes for Planning Active Distribution Networks. *IEEE Transactions on Sustainable Energy*, 6(4):1224–1233, 2015.

[40] Zechun Hu and Furong Li. Cost-Benefit Analyses of Active Distribution Network Management, Part II: Investment Reduction Analysis. *IEEE Transactions on Smart Grid*, 3(3):1075–1081, 2012.

[41] L. Igualada, C. Corchero, M. Cruz-Zambrano, and F. . J. Heredia. Optimal Energy Management for a Residential Microgrid Including a Vehicle-to-Grid System. *IEEE Transactions on Smart Grid*, 5(4):2163–2172, July 2014.

[42] S. Golshannavaz, S. Afsharnia, and F. Aminifar. Smart Distribution Grid: Optimal Day-Ahead Scheduling With Reconfigurable Topology. *IEEE Transactions on Smart Grid*, 5(5):2402–2411, Sept. 2014.

[43] Jia Tang, Dan Wang, Xuyang Wang, Hongjie Jia, Chengshan Wang, Renle Huang, Zhanyong Yang, and Menghua Fan. Study on day-ahead optimal economic operation of active distribution networks based on Kriging model assisted particle swarm optimization with constraint handling techniques. *Applied Energy*, 204:143 – 162, 2017.

[44] Xiaolong Jin, Yunfei Mu, Hongjie Jia, Jianzhong Wu, Xiandong Xu, and Xiaodan Yu. Optimal day-ahead scheduling of integrated urban energy systems. *Applied Energy*, 180:1 – 13, 2016.

[45] Juan S. Giraldo, Jhon A. Castrillon, Carlos A. Castro, and Federico Milano. Optimal Energy Management of Unbalanced Three-Phase Grid-Connected Microgrids. In *2019 IEEE Milan PowerTech*, pages 1–6, 2019.

[46] Long Fu, Ke Meng, Bin Liu, and Zhao Yang Dong. Mixed-integer second-order cone programming framework for optimal scheduling of microgrids considering power flow constraints. *IET Renewable Power Generation*, 13:2673–2683(10), October 2019.

[47] Zhaohong Bie, Yanling Lin, Gengfeng Li, and Furong Li. Battling the Extreme: A Study on the Power System Resilience. *Proceedings of the IEEE*, 105(7):1253–1266, 2017.

[48] Nikolaos C. Koutsoukis, Pavlos S. Georgilakis, and Nikos D. Hatziargyriou. Service restoration of active distribution systems with increasing penetration of renewable distributed generation. *IET Generation, Transmission & Distribution*, 13:3177–3187(10), July 2019.

[49] Juanxia Xiao, Yong Li, Yi Tan, Chun Chen, Yijia Cao, and Kwang Y. Lee. A Robust Mixed-Integer Second-Order Cone Programming for Service Restoration of Distribution Network. In *2018 IEEE Power Energy Society General Meeting (PESGM)*, pages 1–5, 2018.

[50] Nikolaos C. Koutsoukis, Dimitris O. Siagkas, Pavlos S. Georgilakis, and Nikos D. Hatziargyriou. Online Reconfiguration of Active Distribution Networks for Maximum Integration of Distributed Generation. *IEEE Transactions on Automation Science and Engineering*, 14(2):437–448, 2017.

[51] Tao Ding, Yanling Lin, Zhaohong Bie, and Chen Chen. A resilient microgrid formation strategy for load restoration considering master-slave distributed generators and topology reconfiguration. *Applied Energy*, 199:205–216, 2017.

[52] Z. Tian, W. Wu, B. Zhang, and A. Bose. Mixed-integer second-order cone programing model for VAR optimisation and network reconfiguration in active distribution networks. *IET Generation, Transmission Distribution*, 10(8):1938–1946, May 2016.

[53] Yinxiao Li, Yi Wang, and Qixin Chen. Optimal Dispatch With Transformer Dynamic Thermal Rating in ADNs Incorporating High PV Penetration. *IEEE Transactions on Smart Grid*, 12(3):1989–1999, 2021.

[54] Ehsan Hooshmand and Abbas Rabiee. Energy management in distribution systems, considering the impact of reconfiguration, RESs, ESSs and DR: A trade-off between cost and reliability. *Renewable Energy*, 139:346–358, 2019.

[55] Saeid Esmaeili, Amjad Anvari-Moghaddam, and Shahram Jadid. Retail market equilibrium and interactions among reconfigurable networked microgrids. *Sustainable Cities and Society*, 49:101628, 2019.

[56] Yi Zhao, Jilai Yu, Mingfei Ban, Yiqi Liu, and Zhiyi Li. Privacy-Preserving Economic Dispatch for An Active Distribution Network With Multiple Networked Microgrids. *IEEE Access*, 6:38802–38819, 2018.

[57] Jian Xu, Jing Wang, Siyang Liao, Yuanzhang Sun, Deping Ke, Xiong Li, Ji Liu, Yibo Jiang, Congying Wei, and Bowen Tang. Stochastic multi-objective optimization of photovoltaics integrated three-phase distribution network based on dynamic scenarios. *Applied Energy*, 231:985 – 996, 2018.

[58] Rana H. A. Zubo and Geev Mokryani. Active Distribution Network Operation: A Market-Based Approach. *IEEE Systems Journal*, 14(1):1405–1416, 2020.

[59] Juanxia Xiao, Yong Li, Xuebo Qiao, Yi Tan, Yijia Cao, and Lin Jiang. Enhancing Hosting Capacity of Uncertain and Correlated Wind Power in Distribution Network With ANM Strategies. *IEEE Access*, 8:189115–189128, 2020.

[60] Amir Naebi Toutounchi, Seyedjalal Seyedshenava, Javier Contreras, and Adel Akbarimajd. A Stochastic Bilevel Model to Manage Active Distribution Networks With Multi-Microgrids. *IEEE Systems Journal*, 13(4):4190–4199, 2019.

[61] Abouzar Samimi. Probabilistic day-ahead simultaneous active/reactive power management in active distribution systems. *Journal of Modern Power Systems and Clean Energy*, 7(6):1596–1607, 2019.

[62] Hesam Khazraj, Babak Yousefi Khanghah, Pramod Ghimire, Frank Martin, Mohammad Ghomi, Filipe Faria da Silva, and Claus Leth Bak. Optimal

operational scheduling and reconfiguration coordination in smart grids for extreme weather condition. *IET Generation, Transmission & Distribution*, 13:3455–3463(8), August 2019.

[63] Z. Bao, Q. Zhou, Z. Yang, Q. Yang, L. Xu, and T. Wu. A Multi Time-Scale and Multi Energy-Type Coordinated Microgrid Scheduling Solution—Part I: Model and Methodology. *IEEE Transactions on Power Systems*, 30(5):2257–2266, 2015.

[64] Ziwei Xiong, Yifan Huang, Wei Wang, Yumin Zhang, Xingming Xu, and Xia Sun. A Day-Ahead Chance Constrained Volt/Var Control Scheme With Renewable Energy Sources by Novel Scenario Generation Method in Active Distribution Networks. *IEEE Access*, 9:64033–64042, 2021.

[65] H. Gao, L. Wang, J. Liu, and Z. Wei. Integrated Day-Ahead Scheduling Considering Active Management in Future Smart Distribution System. *IEEE Transactions on Power Systems*, 33(6):6049–6061, 2018.

[66] Dongmei Zhao, Haoxiang Wang, and Ran Tao. Multi-time Scale Dispatch Approach for an AC/DC Hybrid Distribution System Considering the Response Uncertainty of Flexible Loads. *Electric Power Systems Research*, 199:107394, 2021.

[67] Jéssica Alice Alves da Silva, Juan Camilo López, Nataly Bañol Arias, Marcos Julio Rider, and Luiz Carlos Pereira da Silva. Security-Constrained Energy Management System for Microgrids Under Uncertainty. In *2020 IEEE PES Transmission Distribution Conference and Exhibition - Latin America (T D LA)*, pages 1–6, 2020.

[68] Hongjun Gao, Renjun Wang, Youbo Liu, Lingfeng Wang, Yingmeng Xiang, and Junyong Liu. Data-driven distributionally robust joint planning of distributed energy resources in active distribution network. *IET Generation, Transmission & Distribution*, 14:1653–1662(9), May 2020.

[69] Alireza Akbari-Dibavar, Mohammadreza Daneshvar, Behnam Mohammadi-ivatloo, Kazem Zare, and Amjad Anvari-Moghaddam. Optimal

Robust Energy Management of Microgrid with Fuel Cells, Hydrogen Energy Storage Units and Responsive Loads. In *2020 International Conference on Smart Energy Systems and Technologies (SEST)*, pages 1–6, 2020.

[70] Moein Borghei and Mona Ghassemi. Optimal planning of microgrids for resilient distribution networks. *International Journal of Electrical Power & Energy Systems*, 128:106682, 2021.

[71] Suyang Zhou, Yi Zhao, Wei Gu, Zhi Wu, Yunpeng Li, Zhonghao Qian, and Yu Ji. Robust Energy Management in Active Distribution Systems Considering Temporal and Spatial Correlation. *IEEE Access*, 7:153635–153649, 2019.

[72] Mohammad Salimi, Mohamad-Amin Nasr, Seyed Hossein Hosseinian, Gevork B. Gharehpetian, and Mohammad Shahidehpour. Information Gap Decision Theory-Based Active Distribution System Planning for Resilience Enhancement. *IEEE Transactions on Smart Grid*, 11(5):4390–4402, 2020.

[73] F. Garcia-Torres and C. Bordons. Optimal Economical Schedule of Hydrogen-Based Microgrids With Hybrid Storage Using Model Predictive Control. *IEEE Transactions on Industrial Electronics*, 62(8):5195–5207, Aug. 2015.

[74] Wanjun Lin, Junpeng Zhu, Yue Yuan, and Han Wu. Robust Optimization for Island Partition of Distribution System Considering Load Forecasting Error. *IEEE Access*, 7:64247–64255, 2019.

[75] Saman Nikkhah, Abbas Rabiee, Seyed Masoud Mohseni-Bonab, and Innocent Kamwa. Risk averse energy management strategy in the presence of distributed energy resources considering distribution network reconfiguration: an information gap decision theory approach. *IET Renewable Power Generation*, 14:305–312(7), February 2020.

[76] Tianyang Zhao, Jianhua Zhang, and Peng Wang. Flexible active distribution system management considering interaction with transmission networks using information-gap decision theory. *CSEE Journal of Power and Energy Systems*, 2(4):76–86, 2016.

[77] D. Bertsimas, E. Litvinov, X. A. Sun, J. Zhao, and T. Zheng. Adaptive Robust Optimization for the Security Constrained Unit Commitment Problem. *IEEE Transactions on Power Systems*, 28(1):52–63, 2013.

[78] A. Soroudi, P. Siano, and A. Keane. Optimal DR and ESS Scheduling for Distribution Losses Payments Minimization Under Electricity Price Uncertainty. *IEEE Transactions on Smart Grid*, 7(1):261–272, 2016.

[79] Bo Zeng and Long Zhao. Solving two-stage robust optimization problems using a column-and-constraint generation method. *Operations Research Letters*, 41(5):457–461, 2013.

[80] Mohammad Reza Ebrahimi and Nima Amjady. Adaptive robust optimization framework for day-ahead microgrid scheduling. *International Journal of Electrical Power & Energy Systems*, 107:213–223, 2019.

[81] Tao Ding, Shiyu Liu, Wei Yuan, Zhaohong Bie, and Bo Zeng. A Two-Stage Robust Reactive Power Optimization Considering Uncertain Wind Power Integration in Active Distribution Networks. *IEEE Transactions on Sustainable Energy*, 7(1):301–311, 2016.

[82] H. Gao, J. Liu, and L. Wang. Robust Coordinated Optimization of Active and Reactive Power in Active Distribution Systems. *IEEE Transactions on Smart Grid*, 9(5):4436–4447, 2018.

[83] Fernando Mancilla-David, Alejandro Angulo, and Alexandre Street. Power Management in Active Distribution Systems Penetrated by Photovoltaic Inverters: A Data-Driven Robust Approach. *IEEE Transactions on Smart Grid*, 11(3):2271–2280, 2020.

[84] J. S. Giraldo, J. A. Castrillon, J. C. López, M. J. Rider, and C. A. Castro. Microgrids Energy Management Using Robust Convex Programming. *IEEE Transactions on Smart Grid*, 10(4):4520–4530, 2019.

[85] M. Farivar and S. H. Low. Branch Flow Model: Relaxations and Convexification-Part I. *IEEE Transactions on Power Systems*, 28(3):2554–2564, Aug. 2013.

[86] M. Farivar, C. R. Clarke, S. H. Low, and K. M. Chandy. Inverter VAR control for distribution systems with renewables. In *2011 IEEE International Conference on Smart Grid Communications (SmartGridComm)*, pages 457–462, 2011.

[87] Dimitris Bertsimas and Melvyn Sim. The Price of Robustness. *Operations Research*, 52(1):35–53, 2004.

[88] S. Parhizi, H. Lotfi, A. Khodaei, and S. Bahramirad. State of the Art in Research on Microgrids: A Review. *IEEE Access*, 3:890–925, 2015.

[89] Aftab Ahmad Khan, Muhammad Naeem, Muhammad Iqbal, Saad Qaisar, and Alagan Anpalagan. A compendium of optimization objectives, constraints, tools and algorithms for energy management in microgrids. *Renewable and Sustainable Energy Reviews*, 58:1664 – 1683, 2016.

[90] Yi Wang, Anastasios Oulis Rousis, and Goran Strbac. On microgrids and resilience: A comprehensive review on modeling and operational strategies. *Renewable and Sustainable Energy Reviews*, 134:110313, 2020.

[91] M. Geidl and G. Andersson. Optimal Power Flow of Multiple Energy Carriers. *IEEE Transactions on Power Systems*, 22(1):145–155, 2007.

[92] Y. Wang, C. Chen, J. Wang, and R. Baldick. Research on Resilience of Power Systems Under Natural Disasters—A Review. *IEEE Transactions on Power Systems*, 31(2):1604–1613, March 2016.

[93] Alireza Soroudi and Mehdi Ehsan. IGDT Based Robust Decision Making Tool for DNOs in Load Procurement Under Severe Uncertainty. *IEEE Transactions on Smart Grid*, 4(2):886–895, 2013.

[94] Hongzhang Sheng, Chengfu Wang, Bowen Li, Jun Liang, Ming Yang, and Yunhui Dong. Multi-timescale Active Distribution Network Scheduling Considering Demand Response and User Comprehensive Satisfaction. *IEEE Transactions on Industry Applications*, 57(3):1995–2005, 2021.

[95] Benoît Martin, Emmanuel De Jaeger, and François Glineur. A robust convex optimization framework for autonomous network planning under load uncertainty. In *2017 IEEE Manchester PowerTech*, pages 1–6, 2017.

[96] Gaowa Saren, Zhebin Sun, Zhihai Yan, Tao Liang, Pengxuan Liu, and Mingjuan Wang. A Bi-level Robust Planning Method of Active Distribution Networks With Uncertain Renewable Energy Sources. In *2020 IEEE 4th Conference on Energy Internet and Energy System Integration (EI2)*, pages 1449–1454, 2020.

[97] F. Geth, R. D'Hulst, and D. Van Hertem. Convex power flow models for scalable electricity market modelling. *CIRED - Open Access Proceedings Journal*, 2017(1):989–993, 2017.

[98] Steven H. Low. Convex relaxation of optimal power flow: A tutorial. In *2013 IREP Symposium Bulk Power System Dynamics and Control - IX Optimization, Security and Control of the Emerging Power Grid*, pages 1–15, 2013.

[99] J. Carpentier. Contribution to the economic dispatch problem. (In French). *Bulletin de la Societe Francoise des Electriciens*, 3(28):431–447, 1962.

[100] M. Huneault and F.D. Galiana. A survey of the optimal power flow literature. *IEEE Transactions on Power Systems*, 6(2):762–770, 1991.

[101] R. A. Jabr. Radial distribution load flow using conic programming. *IEEE Transactions on Power Systems*, 21(3):1458–1459, 2006.

[102] Álvaro Lorca and Xu Andy Sun. The Adaptive Robust Multi-Period Alternating Current Optimal Power Flow Problem. *IEEE Transactions on Power Systems*, 33(2):1993–2003, 2018.

[103] Xuan Wu, Antonio J. Conejo, and Nima Amjady. Robust Security Constrained ACOPF via Conic Programming: Identifying the Worst Contingencies. *IEEE Transactions on Power Systems*, 33(6):5884–5891, 2018.

[104] Bose Subhonmesh, Steven H. Low, and K. Mani Chandy. Equivalence of branch flow and bus injection models. In *2012 50th Annual Allerton Conference on Communication, Control, and Computing (Allerton)*, pages 1893–1899, 2012.

[105] Dimitris Bertsimas, David B. Brown, and Constantine Caramanis. Theory and Applications of Robust Optimization. *SIAM Rev.*, 53(3):464–501, August 2011.

[106] A. L. Soyster. Technical Note—Convex Programming with Set-Inclusive Constraints and Applications to Inexact Linear Programming. *Operations Research*, 21(5):1154–1157, 1973.

[107] A. Ben-Tal and A. Nemirovski. Robust Solutions of Uncertain Linear Programs. *Oper. Res. Lett.*, 25(1):1–13, August 1999.

[108] A. Ben-Tal and A. Nemirovski. Robust Convex Optimization. *Mathematics of Operations Research*, 23(4):769–805, 1998.

[109] Stephen Boyd and Lieven Vandenberghe. *Convex Optimization*. Cambridge University Press, 2004.

[110] Jialiang Yi. Investigation of energy storage system and demand side response for distribution networks. (http://theses.ncl.ac.uk/jspui/handle/10443/3374), PhD Thesis, Newcastle University, UK, 2016.

[111] Rabih A. Jabr, Ravindra Singh, and Bikash C. Pal. Minimum Loss Network Reconfiguration Using Mixed-Integer Convex Programming. *IEEE Transactions on Power Systems*, 27(2):1106–1115, May 2012.

[112] Aharon Ben-Tal and Arkadi Nemirovski. On Polyhedral Approximations of the Second-Order Cone. *Math. Oper. Res.*, 26:193–205, 2001.

[113] M.R.M. Cruz, D.Z. Fitiwi, S.F. Santos, and J.P.S. Catalão. Influence of distributed storage systems and network switching/reinforcement on RES-based DG integration level. In *2016 13th International Conference on the European Energy Market (EEM)*, pages 1–5, 2016.

[114] MOSEK ApS. MOSEK Modeling Cookbook. Copenhagen, Denmark, 2019.

[115] P. A. Trodden, W. A. Bukhsh, A. Grothey, and K. I. M. McKinnon. Optimization-Based Islanding of Power Networks Using Piecewise Linear AC Power Flow. *IEEE Transactions on Power Systems*, 29(3):1212–1220, May 2014.

[116] Zeinab Ghofrani-Jahromi, Mostafa Kazemi, and Mehdi Ehsan. Distribution Switches Upgrade for Loss Reduction and Reliability Improvement. *IEEE Transactions on Power Delivery*, 30(2):684–692, 2015.

[117] David M. Greenwood, Neal S. Wade, Philip C. Taylor, Panagiotis Papadopoulos, and Nick Heyward. A Probabilistic Method Combining Electrical Energy Storage and Real-Time Thermal Ratings to Defer Network Reinforcement. *IEEE Transactions on Sustainable Energy*, 8(1):374–384, 2017.

[118] Ilias Sarantakos. Investigating the impact of asset condition on distribution network reconfiguration and its capacity value. (http://theses.ncl.ac.uk/jspui/handle/10443/4703), PhD Thesis, Newcastle University, UK, 2019.

[119] M.E. Baran and F.F. Wu. Optimal sizing of capacitors placed on a radial distribution system. *IEEE Trans. Power Del.; (United States)*, 4:1, Jan 1989.

[120] T. Ding, S. Liu, W. Yuan, Z. Bie, and B. Zeng. A two-stage robust reactive power optimization considering uncertain wind power integration in active distribution networks. *IEEE Transactions on Sustainable Energy*, 7(1):301–311, 2016.

[121] M. Farivar and S. H. Low. Branch Flow Model: Relaxations and Convexification—Part II. *IEEE Transactions on Power Systems*, 28(3):2565–2572, 2013.

[122] Eduardo A. Martínez Ceseña, Nicholas Good, Angeliki L.A. Syrri, and Pierluigi Mancarella. Techno-economic and business case assessment of multi-energy microgrids with co-optimization of energy, reserve and reliability services. *Applied Energy*, 210:896–913, 2018.

[123] Salman Mashayekh, Michael Stadler, Gonçalo Cardoso, and Miguel Heleno. A mixed integer linear programming approach for optimal DER portfolio, sizing, and placement in multi-energy microgrids. *Applied Energy*, 187:154–168, 2017.

[124] Alessandra Parisio, Carmen Del Vecchio, and Alfredo Vaccaro. A robust optimization approach to energy hub management. *International Journal of Electrical Power & Energy Systems*, 42(1):98–104, 2012.

[125] O.M. Babatunde, J.L. Munda, and Y. Hamam. Power system flexibility: A review. *Energy Reports*, 6:101–106, 2020. The 6th International Conference on Power and Energy Systems Engineering.

[126] Chenghua Zhang, Jianzhong Wu, Chao Long, and Meng Cheng. Review of Existing Peer-to-Peer Energy Trading Projects. *Energy Procedia*, 105:2563–2568, 2017. 8th International Conference on Applied Energy, ICAE2016, 8-11 October 2016, Beijing, China.